MEASURING AND MODELLING THERMAL AND MOISTURE REGIMES IN SEASONALLY FROZEN SOILS, WOLF CREEK, YUKON TERRITORY

MEASURING AND MODELLING THERMAL AND MOISTURE REGIMES IN SEASONALLY FROZEN SOILS, WOLF CREEK, YUKON TERRITORY

By HEATHER BONN, B.Sc

A Thesis Submitted to the School of Graduate Studies in Partial Fulfillment of the Requirements for the Degree Master of Science

MASTER OF SCIENCE (2019) McMaster University

(EARTH AND ENVIRONMENTAL SCIENCES) Hamilton, Ontario

TITLE: Measuring and modelling thermal and moisture regimes in seasonally frozen soils, Wolf Creek, Yukon Territory

AUTHOR: Heather J. Bonn

SUPERVISOR: Dr. Sean K. Carey

NUMBER OF PAGES: xii, 102

ABSTRACT

Frozen ground is an important consideration in cold regions hydrology because pore ice can impede the ability of water to infiltrate into and migrate within soils, thereby altering water flow paths and increasing surface runoff. High latitude regions are particularly susceptible to changes in climate, where increases in temperature and changing precipitation trends can alter soil freeze/thaw dynamics. However, there has been limited research on infiltration processes in subarctic alpine environments due to sparse historic data and difficulties with gathering direct measurements. In addition, few hydrological models consider the complexity of frozen soils in such environments. The objectives of this thesis are to assess the ability of the GeoStudio finite element modelling suite to simulate observed soil temperature and moisture data and to evaluate the sensitivity of the models to changing climate scenarios. GeoStudio's Multiphysics model integrates several models that allow it to simulate concurrent water flow and temperature dynamics in variably saturated environments experiencing soil freezing and thawing. Field data for this study are obtained from Wolf Creek Research Basin (WCRB) in southern Yukon, Canada. Data for quantifying snowmelt, soil moisture, soil temperature, and soil composition were collected at three sites in WCRB from April 2015 to August 2016, adding to the available historical data. Results of the GeoStudio models illustrate the dominance of snow in controlling freeze/thaw dynamics and simulate the study environment to reasonable accuracy with some discrepancies in timing and variability. In addition, GeoStudio is particularly sensitive to surface conditions affecting both coupled heat and water flow processes compared to independent changes of air temperature and precipitation, suggesting future climatic scenarios may have a notable impact on frozen soils. This research helps elucidate the complex heat transfer and water movement processes that control infiltration in northern environments and provides a quantitative assessment of their sensitivity to future climate warming.

ACKNOWLEDGMENTS

I would first and foremost like to thank my supervisor, Dr. Sean K. Carey, for all of his patience and support with completing my Masters degree. I am grateful for your unfailing encouragement and sense of humour that helped make everything more enjoyable. I greatly appreciate all of the unique and incredible educational opportunities over the last several years, particularly the invaluable experiences of working in exciting and remote locations.

I would also like to thank Dr. Barret Kurylyk, who provided extensive knowledge and insight into the world of modelling, which helped me find my footing for this thesis. I appreciate you consistently going above and beyond to help answer any of my questions and make the process as painless as possible. I am immensely grateful to Dr. Gord Drewitt for his assistance with MATLAB and willingness to help me tackle any challenge. I would also like to thank Dr. Scott Ketcheson for his support and advice for all things soil, whether it be in the field or in the lab.

The Yukon field crew, in particular Nadine Shatilla and Renee Lemmond, who were not only wonderful and enjoyable to work with, but extremely hard working and enthusiastic about field work and all research projects. I will greatly treasure all of the months that we had in Wolf Creek together. To both Dr. Mike Treberg and Ric Janowicz for their support in the field and extensive knowledge of Wolf Creek. In addition, the Yukon Government, who helped support our field crew and were always welcoming.

Thank you to the entire Watershed Hydrology Group for the camaraderie as well as to McMaster University for being my educational home for the past seven years.

Finally, a thank you to all of my friends and family for their unwavering support and encouragement over the years. I look forward to my future endeavours in hydrology and appreciate all of the opportunities for growth along the way.

TABLE OF CONTENTS

LIST OF TABLES

Chapter 3

Chapter 4

Chapter 5

LIST OF FIGURES

Chapter 2

Chapter 3

Chapter 4

Chapter 5

LIST OF ABBREVIATIONS AND SYMBOLS

FEM	Finite element model
GB	Granger Basin
GC	Granger Creek
HRU	Hydrological response unit
PDE	Partial differential equation
PLT	Plateau
PSD	Particle size distribution
NF	North Facing
NRCS	Natural Resources Conservation Service
RP	Riparian
SWE	Snow water equivalent
uwc/uvwc	Unfrozen water content (volumetric)
USCS	Unified Soil Classification System
USDA	United States Department of Agriculture
vlwc	Volumetric liquid water content
WCRB	Wolf Creek Research Basin

Q	Total discharge ($m^3\ s^{-1}$)
K	Hydraulic conductivity ($m\ s^{-1}$)
A	Area (m^2)
$\frac{dh}{dl}$	Hydraulic gradient
θ	Soil moisture (wfv)
$K(\theta)$	Unsaturated hydraulic conductivity ($m\ s^{-1}$)
∇	Gradient in three dimensions
t	Time (s)
q_h	Thermal flux ($W\ m^{-2}$)
κ	Thermal conductivity ($W\ m^{-1}\ K^{-1}$)
T	Temperature (°C)
C_T	Volumetric heat capacity ($J\ K^{-1}\ m^{-3}$)

C_s	Bulk volumetric heat capacity (J K^{-1} m^{-3})
C_w	Volumetric heat capacity of water (J K^{-1} m^{-3})
ρ_i	Density of ice (kg m^{-3})
H_f	Latent heat of fusion (J kg^{-1})
θ_i	Volumetric ice content (dimensionless)
λ	Bulk thermal conductivity (W m^{-1} K^{-1})
q_w	Vertical flux of liquid water (m s^{-1})
h	Hydraulic head
z	Elevation/depth (m)
$ø_g$	Gravitational potential
$ø_p$	Pressure potential
$ø_t$	Total potential

1. CHAPTER 1: Introduction

1.1 Motivation

Cold regions have a distinct hydrological regime that is dominated by the presence of snow and ice. These regions are typically defined by their air temperature, snow depth, ice cover, frost penetration, and tree limits (Koppen, 1936; Wilson, 1967; Woo, 2012). Based on this, cold regions make up a significant portion of the Northern Hemisphere, with almost all of the land mass north of 40°N being classified as a cold region (Bates and Bilello, 1966; Gerdel, 1969). With an extensive presence in northern and mountainous zones, the cold regions of the world are vital for supplying water to the large populations which rely on these systems (Harder et al., 2015). However, in recent years, an uncertain climate future has led to unprecedented global water related challenges (ACIA, 2005; Mortsch et al., 2015; Buttle et al., 2016). While exact changes will vary by region, greater surface warming rates at high latitudes and altitudes make cold regions more susceptible to altered hydrological processes (McBean et al., 2005; Zhang et al., 2008). Diminishing snowpacks, permafrost thaw, and extreme weather events are some of the changes impacting current hydrological regimes (ACIA, 2005; Hinzman et al., 2013). These changes have led to emerging global concerns over a wide range of issues, such as water security, impacting numerous sectors including agriculture, industry and government (Arnell, 1999). The rapidly growing need to adapt to these shifts has led to an increased research interest in cold regions.

To better address these global concerns, it is important to understand the complex hydrological processes that dominant these systems. The ability of water to move through soils is an important component of the hydrological cycle, with increasing complexity in cold regions where water exists more frequently in its frozen state as ice or snow. Whether the ice is seasonal or persist as permafrost, the influence of frozen water has a substantial impact on the storage and

movement both on and below the land surface (Woo, 2012). In particular, the partitioning of snowmelt to runoff and infiltration is an important control on managing flood risks and water resources. Pore ice can impede the ability of water to infiltrate into and migrate within soils, thereby altering water flow paths and the streamflow regime, in turn increasing surface runoff and impacting ecosystems (Granger et al., 1984; Gray et al., 1985; Buttle et al., 2016). Furthermore, soil freeze/thaw dynamics are crucial to the water balance and surface energy processes in cold regions (Woo and Marsh, 2005). As soil freezing and thawing dynamics are particularly susceptible to changes in climate, knowledge of the thermal and hydrological regimes is fundamental to understanding the future state of cold regions.

Although there is a significant dependence on these regions, there has been limited research on infiltration processes and soil thermal regimes in permafrost and alpine environments due to sparse historic data and difficulties with gathering direct measurements (Viviroli et al., 2011). This has resulted in a lack of data and baseline knowledge, with few long-term study sites. While there has been research on frozen soils, the majority of studies have been conducted in the agricultural sector, for example, the prairies in Canada (Granger et al., 1984; Gray et al., 1985; Johnsson and Lundin, 1991; Zhao and Gray, 1999; Hayashi et al., 2003). In general, modelling offers the potential to further study complex and remote environments at a reduced cost, making it an important tool for studying cold regions. However, few models currently include frozen ground and often generalize the intricate processes (Stähli et al., 1999; Zhao and Gray, 1999; Gray et al., 2001; Zhang et al., 2010; Kurylyk and Watanabe, 2013; Lundberg et al., 2016), thereby limiting the accuracy of such model's ability to simulate these environments and future scenarios.

Changes in alpine catchments and cold regions are having dramatic and rapid impacts on hydrological regimes, and projected trends indicate a need for adaptation (Middelkoop et al., 2001;

Hinzman et al., 2013; Walvoord and Kurylyk, 2016). With large portions of high latitude countries, including Canada, existing in cold regions, it is important to have a thorough understanding of the hydrological questions involving frozen soils and snow that may have both societal and scientific impacts (Marsh, 1999).

1.2 Research Objectives

Due to rapidly changing environments, the ability to measure and model hydrological processes has become increasingly important. Through field observations and numerical simulations, this study aims to advance our understanding of soil water and thermal dynamics in a headwater sub-catchment of the Wolf Creek Research Basin, Yukon, Canada. More specifically, soil and climate data will be used to 1) describe and explain the ground thermal and soil moisture regime patterns along an environmental gradient and 2) parameterize a GeoStudio multi-physics model. The GeoStudio finite element modelling suite is used to 3) simulate observed soil temperature and moisture data. In addition, the models are 4) tested for sensitivity to evaluate the potential impacts of climate change.

Results from this study will help elucidate the complex heat transfer and water movement processes that control infiltration and percolation in northern environments. As frozen soils along with soil freeze/thaw dynamics have significant influence on hydrological regimes in cold regions, improved understanding of these processes is important for effective water management and flood strategies under a changing climate.

2. CHAPTER 2: Background

2.1 Cold Regions Hydrology

The hydrology of cold regions is often defined by the dominance of snow and ice, influencing the ground thermal regimes and overall water movement (Marsh, 1999; Woo et al., 2000). Cold regions often include alpine and topographically complex areas, where soil heterogeneity and climatic variability can impact the timing and magnitude of hydrological processes. The sharp elevation transition creates variations in moisture content over small areas, causing precipitation patterns to be localized and variable events (Viviroli and Weingartner, 2004). Furthermore, the local relief of mountainous regions also creates significant temperature variability directly related to elevation aspect. As such, these regions typically experience extreme climates that exhibit strong seasonality consisting of a long winter, short snowmelt period, then a post-melt season, each with distinctive moisture and heat conditions (Woo, 2012).

These seasons with characteristic heat and moisture profiles affect processes both above and within the ground throughout the year. A long winter and temperatures consistently below 0°C results in long term water storage for a significant portion of the year in cold regions (Woo, 2012). As such, a large amount of the annual precipitation is only available for water storage or runoff during the brief snowmelt period, giving spring freshet an important hydrological role. Furthermore, with higher latitudes, snowmelt becomes increasingly important as the melt period typically shortens (Marsh, 1999). In regards to the ground thermal regime, snow cover acts as an insulator, moderating ground temperature from the extreme cold and weather events of northern winters (Goodrich, 1978; Bayard et al., 2005). Therefore, the quantity and spatial distribution of snow has important controls for the underlying soil temperature profile as well as for the delivery of meltwater in the spring (Bayard et al., 2005).

2.1.1 Frozen Soils

In general, throughout the winter, the soil moisture and temperature profiles are characterized by low or below freezing temperatures along with decreased unfrozen water content. As the shift from freezing to ground thaw begins, most available energy initially is used to increase the temperature of the snowpack (Goodrich, 1982; Bayard et al., 2005; Woo, 2012). Moisture fluxes will transition to a downward movement of the meltwater into frozen soils and soil temperatures strongly influenced by latent heat fluxes. During the post-melt season soil profiles will vary depending on permafrost or non-permafrost regions, but are nevertheless often characterized by higher ground temperatures as well as increased liquid water content (Woo, 2012).

2.2 Types of Frozen Ground

Cold regions are further categorized based on the types of frozen ground that can have different soil dynamics and hydrological impacts (Andersland and Ladanyi, 2013). This subdivision separates seasonally frozen ground from perennially frozen ground as well as continuous and discontinuous permafrost areas. It is important to note that frozen ground is not limited to permafrost regions and there are both similarities and differences in the hydrology of seasonally and perennially frozen ground (Woo, 2012; Andersland and Ladanyi, 2013).

2.2.1 Permafrost

Ground that has temperatures at or below 0°C for a minimum of two consecutive years is considered to be permafrost (Woo, 2012). Approximately 24% of the land surface in the northern hemisphere is underlain with permafrost (Brown et al., 1997). As noted, permafrost areas are commonly separated by whether the permafrost is continuous or discontinuous. Continuous permafrost is characterized as regions where 90% of the area or more is underlain by permafrost

whereas discontinuous permafrost regions have a more scattered distribution of permafrost. Discontinuous permafrost regions typically exist as a gradual transitional boundary between permafrost and non-permafrost zones.

Figure 2.1 summarizes the ground temperature profile and associated features of defining permafrost and frozen soils. In a permafrost area, the active layer is the top layer of ground which fluctuates between freeze and thaw and temperatures above and below 0°C (Harris et al., 1988). The permafrost zone extends vertically from the permafrost table (below the active layer) to the permafrost base and, depending on the conditions, may be on the order of tens to centimetres to several metres below the ground surface to the base of the permafrost several metres to 1000s of metres deep.

The occurrence, development and distribution of permafrost is influenced by numerous factors, including location, topography, vegetation, soils, snow cover, and water flow (Nicholson and Granberg, 1973; Zhang and Stamnes, 1998; Woo, 2012). These factors also affect the thickness of the active layer which in turn may affect certain hydrological characteristics. For example, the thickness of the active layer will have a direct influence on the thawing and recharge rates through the active layer thereby influencing the runoff regime. Vegetation directly impacts heat transfer to the ground by altering the albedo and can also modify snow distribution (Walker et al., 1993; Marsh et al., 2010). However, the influence of water in all its forms is typically considered the most significant factor in permafrost systems. More specifically, soil moisture content and snow distribution affect water inputs to and movement within the soil. Furthermore, snowmelt is usually a considerable portion of water inputs in permafrost dominated watersheds (Woo, 1986; McNamara et al., 1998; Carey and Woo, 1999).

The prolonged subfreezing temperatures in permafrost has long term impacts that can affect the hydrology and differentiates these regions from seasonally frozen soils. Most notably, permafrost acts as a semi-permanent aquitard, limiting permeability (Williams and van Everdingen, 1973; Dingman, 1975). Due to the impermeable nature of freezing front, infiltration and meltwater distribution are strongly controlled by soil thawing in the active layer (Metcalfe and Buttle, 1999; Carey and Woo, 1999; Quinton et al., 2005).

2.2.2 Seasonally Frozen Soils

Soils that are subject to seasonal freeze and thaw are similar to the active layer in permafrost zones and are usually considered to be equivalent in terms of most hydrologic behaviour. However, the active layer often implies the areas are underlain by permafrost, whereas seasonally frozen soils may also be used to refer to areas that are not underlain by permafrost (Harris et al., 1988). Nevertheless, it is in these seasonally frozen soils where most hydrological activities are confined, where freeze-thaw events impact the energy and water fluxes related to water storage and redistribution. Several similar hydrologic properties are observed in cold regions undergoing seasonal freeze-thaw, with or without permafrost. In these systems, moisture and heat fluxes are closely coupled and often interdependent. As the temperature falls further in frozen soils, the unfrozen water content drops (See Figure 2.2). In general, freezing will affect the physical properties of the soil including decreased hydraulic conductivity and specific heat capacity and increased thermal conductivity (Anderson and Morgenstern, 1973; Kane, 1980). Similar to permafrost acting as an aquitard, ground ice blocks pore space and makes the materials more impervious (Kane, 1980; Stähli et al., 2004). In addition, the hydrology of frozen soils is closely linked to snow hydrology, meaning the quantity and distribution of snow influences the hydrology.

The primary difference between permafrost and seasonally frozen soils is the duration of freezing. As mentioned, prolonged subfreezing temperatures have long term impacts on hydrological fluxes. When compared to seasonally frozen soils, the groundwater regimes in permafrost soils are affected by the presence of an aquitard in the active layer. While recharge may occur in frozen soils, the rate is significantly reduced compared to unfrozen conditions. As a result, the recharge rate in seasonally frozen soils is determined by the amount and duration of freezing and is typically greater than permafrost zones which are more likely to be perennially frozen thereby reducing recharge rates (Kane et al., 1978; Kane and Stein, 1983).

2.3 Frozen Soil Processes

Infiltration into frozen soils involves the combined heat and mass transfer processes as the soils experience phase changes. The following section outlines the governing physics that control how water moves through frozen soils, and importantly, the associated heat flow. The typical ground thermal regime of frozen soils that occurs in cold regions both with and without permafrost is also outlined.

2.3.1 Water Flow in Soils

The flows of water and heat through soils are closely coupled processes, with simultaneous temperature gradients and moisture gradients resulting in combined transport of heat and water (Hillel, 2004). While interconnected, particularly in frozen soils as a result of phase changes, there are physical controls of water flow independent of heat transfer which govern how water moves through soils.

The potential energy determines the state and movement of water in the soil where differences in potential energy drive the flow of water in the system. The total soil-water potential is the sum

of all the potential energies from different forces. Primarily, the dominant potential energies on soil water are the gravitational potential and pressure potential, as expressed by Equation 1.

$$\emptyset_t = \emptyset_g + \emptyset_p + \cdots \qquad (1)$$

Where $ø_t$ is the total potential, $ø_g$ is the gravitational potential, and $ø_p$ is the pressure potential, with other terms such as osmotic potentials important in certain circumstances. The gravitational potential energy is determined by the elevation of a point above some arbitrary reference datum. The pressure potential is determined relative to atmospheric pressure. When the hydrostatic pressure of soil water is lower than atmospheric, the pressure potential is considered negative, creating a suction or tension that is present in the pores of the soil that are not filled. This matric suction results from the interactive capillary and adsorptive forces between the water and soil matrix. Soil-water potential is most commonly expressed by units of hydraulic head, an energy per unit weight. The total potential head of soil water (hydraulic head) is the sum of the gravitational and pressure potential heads and controls the rate and direction of water movement from high hydraulic head to low hydraulic head. Hydraulic head is typically represented by the following equation:

$$h = z + \psi \qquad (2)$$

Where h is the hydraulic head, z is the elevation energy, and ψ is the pressure energy. The flow of water through a porous medium can be described quantitatively using Darcy's Law, which relates water flow velocity to hydraulic gradient under laminar flow conditions. For saturated conditions in one dimension:

$$Q = -KA\left(\frac{dh}{dl}\right) \qquad (3)$$

Where Q is the total discharge or volumetric flow rate, K is the hydraulic conductivity, A is the cross-sectional area through which flow occurs, and dh/dl is the hydraulic gradient, indicating change in head over a specific distance.

For unsaturated conditions:

$$Q = -K(\theta)\nabla h \qquad (4)$$

Where Q is the total discharge or volumetric flow rate, θ is the soil moisture, $K(\theta)$ represents the unsaturated hydraulic conductivity, and ∇h is the hydraulic gradient in all three coordinate directions indicated specifically by ∇.

From Darcy's Law, hydraulic conductivity, K, is the ratio of the flux to the potential gradient and is a measure of how easily water can flow through a porous medium. The degree of saturation will also influence how water moves through soils. In a saturated system, all of the pores are filled and highly conductive. Therefore, as a soil becomes desaturated and pores fill with air, the conductive area is reduced, decreasing the hydraulic conductivity. In addition, as suction develops, the first pores to empty are the large pores, limiting flow to the smaller pores and lowering hydraulic conductivity. Differences in hydraulic conductivities leads to preferential flow in a system, with water moving at a varying rate through the soil.

In frozen soils, hydraulic conductivity is significantly reduced as temperature decreases, with a rapid decrease between 0°C and -1°C. As temperatures decrease, free water freezes first, then bound (adsorbed) water, followed by soil cooling further without latent heat effects (Harlan, 1973; Walvoord and Kurylyk, 2016). It is important to note that frozen soils still have some permeability (Mackay, 1983; Granger et al., 1984; Stähli et al., 1996; Boike et al., 1998; Stadler et al., 2000; Scherler et al., 2010). While frozen soils are often considered to be similar to aquitards, the state of freezing and degree of saturation of a soil will inherently affect how water moves through the

soil to varying extents (Chamberlain and Gow, 1979; Walvoord et al., 2012). Frequently, unfrozen water can move through the unfrozen water film adsorbed to soil particles, which remains unfrozen at temperatures well below 0°C (Hoekstra, 1966; Anderson and Tice, 1972; Burt and Williams, 1976; Perfect and Williams, 1980). To estimate the hydraulic conductivity of frozen soils, Watanabe and Osada (2016) recommend using unfrozen water content rather than temperature.

As mentioned in Taylor and Luthin (1978), frozen soils impact these physical processes due to the interconnected nature of heat and mass transfer. The amount of liquid water in soil at sub-zero temperatures is important for physical, chemical, and mechanical properties of frozen soils. In addition, water accumulation and saturation will affect how the soil freezes, thereby influencing the water flow in the system. As a result, techniques for measuring the unfrozen water content are critical to the characterization of frozen soils (Jones and Holden, 1989).

2.3.2 Heat Flow in Soils

Soil temperature and its variation in time and space is critical in determining soil hydrological processes, particularly in frozen soils (de Vries, 1975; Campbell, 1977; Fuchs, 1986; Taylor and Jackson, 1986; Hanks, 1992; Evett, 2002; McInnes, 2002). Heat and water flow through soils are coupled processes with simultaneous temperature gradients and moisture gradients resulting in combined transport of heat and water. The primary modes of energy transfer in frozen soils include conduction and convection (advection). Similar to water flow in soils, there are physical controls on heat flow independent of water transfer that can govern the movement of heat. Energy transfer without mass transfer may occur by conduction, in where the propagation of heat is driven by a temperature gradient and is quantitatively represented by Fourier's Law:

$$q_h = -\kappa \nabla T \qquad (5)$$

Where q_h is the thermal flux, κ is the thermal conductivity, and ∇T is the temperature gradient in all three coordinate directions as indicated by ∇. Conduction is typically the principal method of heat transfer in porous media, governed by thermal properties of soils and the wetting and drying phase changes (Harlan, 1973; Zhao and Gray, 1999; Hillel, 2004). For seasonally frozen soils and particularly in the active layer, conduction and latent heat are central to heat and moisture flows. However, convective transfer processes with water and water vapour have been demonstrated as significant in some systems (Hinzman and Kane, 1992).

Whereas conduction is independent of mass transfer, convection is dependent on the transport of mass within a fluid system. Any analysis of convection needs to be a combination of fluid flow and heat transfer mechanisms with equations that are always coupled and cannot be solved independently. For simplification of the situation, convection problems are classified by free and forced convection. In forced convection, the flow is a result of an external force, such as an infiltration front or pump, whereas free convection the motion is driven by a density gradient which are related to the temperature variations. However, in most systems, free convection does not appear to be a dominant heat transfer mechanism (Kane et al., 2001).

Unlike conduction, there is no basic law of convection, but numerous approaches with differing degrees of complexity to represent and understand the processes. For a homogeneous system not undergoing phase change, the basic equation for transient heat flow can be written as:

$$K_T(\delta T/\delta z^2) = C_T(\delta T/\delta t) \qquad (6)$$

Where K_T is the thermal conductivity, C_T is the volumetric heat capacity, T is temperature, z is depth, and t is time.

As with water flow in soils, heat transfer processes undergo added complexity with phase changes, which are prominent in studying cold regions. The heat and water fluxes are commonly combined using some variation of the following vertical heat transport equation:

$$\frac{\partial(C_s T)}{\partial t} - \rho_i H_f \frac{\partial \theta_i}{\partial t} = \frac{\partial}{\partial z}\left(\lambda \frac{\partial T}{\partial z}\right) - C_w \frac{\partial(q_w T)}{\partial z} \qquad (7)$$

Where C_s is the bulk volumetric heat capacity, T is temperature, t is time, ρ_i is the density of ice, H_f represents the latent heat of fusion, θ_i is the dimensionless volumetric ice content, z is elevation, λ is the bulk thermal conductivity of the system, C_w is the volumetric heat capacity of water, and q_w is the vertical flux of liquid water. The first term on the left side of the equation represents the rate of change in sensible heat storage, whereas the second term (on the left) represents the latent energy released or absorbed during the phase change of pore water. The right side of the equation shows the divergence of heat fluxes, the first conductive and the second, advective. Both bulk thermal conductivity and bulk volumetric heat capacity are influenced by the liquid water, ice, and air content of the soil system. Furthermore, during phase change, the pore water available is dependent on water distribution.

While other methods of heat transfer are possible, conduction and convection (primarily through advection), dominate the soil system processes, along with latent heat exchanges through phase change.

2.3.2.1 Ground Thermal Regime of Frozen Soils

Changing meteorological conditions acting on the soil-atmosphere interface will cause continuous soil temperature variations. More specifically, soil temperatures typically follow diurnal and annual cycles in response to heat gains and losses at the ground surface and based on the meteorological regime of seasons and days and nights. However, the heat balance is highly variable with time and is affected by climatic conditions, terrain, vegetative cover, geographic

location, and human impacts as well as by the thermal soil properties. Irregular phenomena such as periods of drought and heavy rainstorms or snowstorms, can disturb the periodic pattern and such influence has long been recognized (Lachenbruch, 1959; Goodrich, 1982; Thorn et al., 2002). In addition to the external weather influences, changes to the soil properties occurs through wetting and drying and varies with depth further complicating the thermal regime of soils (Johnston, 1981). In regards to the ground thermal regime of soils, the important thermal soil properties to consider include thermal conductivity, heat capacity, and thermal diffusivity, all which have vertical and temporal variability within the soil profile (McGaw et al., 1978; Hinkel et al., 1990).

In cold regions, for seasonally frozen soils and the active layer, latent heat exchanges and conduction are fundamental to heat and moisture flows (Zhao et al., 1997; Zhao and Gray, 1999). Latent heat exchanges are particularly important for seasonally frozen soils due to phase changes that occur in these systems (Lunardini, 1981). The energy absorbed or released by a change in physical state without changing the temperature is known as latent heat. Although there is no direct temperature change with latent heat transfer, the phase change will impact the volume of water in the soil. As heat transfer occurs with snowmelt and latent heat is released from freezing, the thermal properties of the soil and subsequently impacted (Granger et al., 1984). Furthermore, the scale of freezing will later impact the thawing processes as the larger amount of frozen water will lead to a greater amount of latent heat being released during thaw.

During freezing, the effects of latent heat transfer create a period of time during which the soil temperature is a nearly constant temperature close to the freezing point, known as the zero-degree curtain. The zero-curtain effect is often a result of much of the heat in ice rich soils being consumed in converting ice to water and water to ice, thereby resulting in a lag in freeze/thaw in the active layer. Due to solutes in the water, the zero-curtain temperature is commonly lowered to -0.03 or -

0.02°C rather than exactly 0°C (Woo, 2012). This relationship can be seen in the soil freezing curve in Figure 2.3, depicting temperature over time in a porous media and is important for understanding heat and water transport in frozen soils (Spaans and Baker, 1996; Wang et al., 2017).

As mentioned, moisture is still able to move within frozen soil through the interconnected unfrozen water. Another mechanism that allows the movement of fluid is due to the heat transfer associated with phase change. Latent heat is released as the freezing front advances, resulting in accompanying moisture migration. The dissipation of latent heat will impact the rate of freezing in winter and reduces the progression of the freezing front. While ground freezing generally moves downwards from the surface, during the seasonal transition when surface heat inputs decline, upward freezing occurs from the permafrost table, resulting in two-sided freezing (Figure 2.4) (Mackay, 1983).

2.4 Modelling Frozen Soils

In recent years, modelling has become increasingly important to the advancement of water science (Riseborough et al., 2008). Models are becoming faster, more complex, and intensive with increased capabilities, allowing for rapid progress in this research area. There are several purposes as to why models are an important tool in hydrology. Models help to improve our understanding of the physics of certain processes. In addition, models can predict the outcome of processes through projections and forecasting, provided the model is first able to simulate the environments. However, few hydrological models consider the complexity of frozen soils in such environments and overall seasonally frozen soils are poorly represented in numerical methods, with large assumptions required for modelling simulations (Jarvis et al., 2016; Lundberg et al., 2016).

Thus far, models have been used to simulate certain climate change impacts in cryogenic soils such as active layer expansion (Quinton and Baltzer, 2013), permafrost degradation (Lawrence

and Slater, 2008; Bense et al., 2012; McKenzie and Voss, 2013), and changes in groundwater recharge and discharge (Kurylyk et al., 2014). Both analytical and numerical methods have been used for modelling soil freeze/thaw systems. For analytical solutions, Stefan's algorithm along with numerous modifications have been used extensively in permafrost and hydrological models (Carlson, 1952; Lunardini, 1981; Woo et al., 2004; Carey and Woo, 2005; Zhang et al., 2000). Numerical techniques have also been widely used to simulate frozen soils, including finite element (Goodrich, 1982; Romanovsky et al., 1997; Hinzman et al., 1998) and finite difference methods (Nakano and Brown, 1972; Goodrich, 1978; Taylor and Luthin, 1978; Luo et al., 2003; Ling and Zhang, 2004). Zhao and Gray (1997) developed a parametric expression from physically based numerical simulations to estimate infiltration into frozen soils. Goodrich (1982) used numerical model calculations to investigate the influence of snow cover on the ground thermal regime, however neglected latent heat effects and the changes to thermal properties related to freeze/thaw processes. While Ling and Zhang (2004), did consider latent heat effects for their surface energy balance and thermal regime numerical model, it was assumed that unfrozen water does not move within the frozen ground. Development of more encompassing and flexible models for cold regions and frozen soils include the Cold Regions Hydrological Model (Pomeroy et al., 2007) and SUTRA (Saturated-Unsaturated Transport Model) (Voss, 1984). Other applications of models and simulations for cold regions include contamination, cold regions infrastructure, and flood management.

Different models can test against existing analytical solutions or be developed from numerical problems. Comparisons and validation of models are typically done through the use of field and/or laboratory data (Taylor and Luthin, 1978; Hedstrom and Pomeroy, 1998). Hayhoe (1994) field tested a soil freeze/thaw simulation from the SHAW model and Cherkauer and Lettenmaier (1999)

revised a macroscale hydrological model using point data from various basins. Zhao et al. (2016) measured soil temperature and water profiles during freeze/thaw cycles to evaluate the freezing module and simulate further effects on frozen soil hydrological processes. Kurylyk et al. (2014) used numerical models to compare results to analytical solutions that consider heat exchange due to advection, conduction and pore water phase change. Models have progressed from primarily one dimensional to an increased demand for multi-dimensional water and energy transport models as well as two phase and multi-phase models.

2.4.1 Governing Equations

The existing algorithms and governing equations used to simulate ground freeze/thaw processes vary in the types of solutions, parameterizations, the use of latent energy during freezing and thawing, and the specific settings of model configurations. The different algorithms used to simulate frozen ground are divided by numerical or analytical solutions, along with the numerous parameterization methods.

Analytical algorithms are exact solutions for PDEs under certain assumptions and provide simpler solutions for approaching the dual heat and mass transfer problems. However, due to the nonlinearity of the phase change system, there are very few complete analytical solutions to frozen soil systems with concurrent heat and moisture flows (Lunardini, 1991). The most widely used analytical solution for seasonal soil freeze-thaw is the Stefan equation which is most applicable in saturated, homogenous soil conditions when using the original assumptions (Carlson, 1952; Lunardini, 1981), but has been modified to further its applicability. Kersten (1959) developed an approach for layered soils, Woo et al., (2004) included top and bottom forcing to improve the algorithm to simulate multiple freeze/thaw fronts in layered soil, and Hayashi et al., (2007) modified the Stefan algorithm to a permafrost site with layered peat soil. The Lunardini solution

(Lunardini, 1981) has accuracy that is proportional to the Stefan number and is a general approximate analytical solution used to estimate one dimensional soil thawing. The Lunardini solution accommodates advection, conduction, and pore water phase change, making it a useful option for an analytical method. While analytical solutions are simpler to use computationally and easier to parameterize, the extent of applicability requires strict evaluation of site conditions or may require modifications with less favourable systems.

Numerical solutions are approximate solutions to PDEs such as Equation (7) determined by finite element or finite difference analysis. While the exact combination of equations used for a numerical technique may vary, the important physical processes and interrelationships considered consistently include conduction, advection, latent heat, and transient Darcy flow. Examples of finite difference numerical methods include solutions using a Taylor series or the Crank-Nicholson equation (Jeppson, 1974; Zhang et al., 1995; Mikkola and Hartikainen, 2001; Grenier et al., 2018).

2.4.2 Current Modelling Limitations

Numerical representation of processes in seasonally frozen soils is poor compared with models that do not consider soil freezing, and is attributed to limitations from the complex processes involved, lack of intercode comparisons, limited data, and computational difficulties (Zhang et al., 2008; Grenier et al., 2018). While the specific limitations and assumptions will vary, there are general parallels consistent among most models.

At present, modelling frozen soils is primarily limited by computational difficulties arising from several factors. Predominantly, the freeze/thaw processes in frozen soils are inherently complex and interconnected, requiring involved equations that are computationally intensive. Accuracy and detail of some components of the model are often traded off for other components. For example, some complex surface processes may be sacrificed for increasing spatial scales in the model.

Including all complex processes at a large spatial scale can be too computationally difficult and therefore unfeasible. As a result, models are still limited by current processing capabilities of software and hardware. In addition, insufficient field data in cold regions prevents thorough evaluation of freeze/thaw simulations and the parameterization techniques. While typically limited due to logistical obstacles, ample field data would improve model validation and help further development in cold regions research.

Due to the current limitations of modelling frozen soils, models will often make assumptions for simplification purposes. Whether a result of computational difficulties or spatial and temporal limitations, there are assumptions consistent for most freeze/thaw simulations, but also those that are situation specific. The assumption that is present among all models is that concerning spatial and temporal limitations, more specifically the mesh size and time interval discretization. As it is impractical to run simulations at infinitesimally fine mesh sizes and time intervals, an informed hypothesis is made when setting up a simulation and usually will be tested. In addition, the modeller needs to decide on the extent of the domain of a simulation, which is ultimately an assumption and may need to be adjusted. In regards to situation specific assumptions, boundary conditions, parameterization, as well as the inclusion or exclusion of certain processes are model specific. For example, a unit gradient hydraulic boundary condition assumes that the negative pore-water pressure is constant with depth or a land-climate boundary condition including snow may assume snowmelt only occurs when the average air temperature is greater than 0°C. Furthermore, since conduction is typically recognized as the dominant heat transfer process, many models make this assumption and do not often consider the influence of advection. However, given the current understanding of soil freeze/thaw processes, this is a fair assumption (Nixon, 1975; Hinkel and Outcalt, 1994; Carey and Woo, 2005; Hayashi et al., 2007; Zhang et al., 2016). Other studies

suggest including advective processes for certain environments and scenarios, but acknowledge the importance of conduction as a heat transport mechanism (Kane et al., 2001; Kurylyk and Watanabe, 2013).

While most modelling limitations are a result of the current modelling landscape, there are some levels of uncertainty that may be too difficult or impractical to fully eliminate. Analytical solutions are limited to 1D and homogeneous systems, and while simpler, are better for idealized situations. While numerical methods are more complex and offer the opportunity to fully capture the ability to simulate more involved processes, such simulations will likely always lack precision in a practical context and be limited by spatial variability to some extent. In addition, high levels of uncertainty can be a result of parameter values which are often calibrated and difficult to constrain due to measurement precision and spatial variability (Grenier et al., 2018).

In regards to progressing frozen soil models, a particular hindrance stems from a lack of intercode comparisons, which allow for reducing uncertainties and validate models. Rühaak et al. (2015) provides a benchmark comparison of numerical freeze/thaw models in attempts to reduce this current limitation. In addition, heat transportation and subsurface flow models have numerous inconsistencies in governing equations and numerical solution methods (Kurylyk and Watanabe, 2013), providing further motivation for code comparison and validation. Diverse research backgrounds can lead to certain inconsistencies in studying soil freeze/thaw processes and associated modelling, as assumptions and focus can vary among disciplines. For example, an engineering perspective with design considerations for construction with ground freezing may be more concerned with the overall mechanical properties of frozen soils and less concerned with fine temperature data as long as it is within a reasonable range, whereas a biologist may require finer temperature and moisture data when considering sensitive species. These study biases may lead to

differences in model designs that will occur as a result of the intended applications of each model. In attempts to reduce model uncertainty and validate freeze/thaw systems with heat and mass transfer, both Zhang et al. (2008) and Grenier et al. (2018) offer tangible guidelines and recommendations for future model developers.

2.4.3 GeoStudio Modelling Suite

The GeoStudio finite element modelling suite integrates several models (e.g. TEMP/W and SEEP/W) that allow it to simulate concurrent water flow and temperature dynamics in variably saturated environments experiencing soil freezing and thawing (GEOSLOPE International Ltd., 2017). A commercial software used for solving geotechnical and geoscience problems and generally used by engineers, GeoStudio allows for an integrated, multi-physics model by combining multiple analyses. Both one dimensional and multi-dimensional analyses are supported by the software, with the same formulation and finite element processes. The finite element method implemented in GeoStudio is a numerical approach which uses partial differential equations (PDEs) to provide a mathematical description of the physical process. A full derivation of the governing PDEs can be found in the GeoStudio heat and mass transfer manual (GEOSLOPE International Ltd., 2017), where the formulations are derived from the requirement for mass or energy conservation.

In GeoStudio, mass transfer is modelled using SEEP/W, which simulates the movement of water through saturated and unsaturated porous media. Both the movement of liquid water and water vapour can be simulated using SEEP/W. This may include transient or steady-state groundwater flow through different systems. SEEP/W uses PDEs with numerous storage and flow processes to model mass transfer. More specifically, for mass transfer, the governing equations are derived from Darcy's Law, Fick's Law, and the conservation of mass. By default, flow processes

are pressure and gravity driven, however, can be driven by density variations due to temperature if coupled with TEMP/W. Changes in storage are due to the compressibility of water and soil as well as changes in matric suction, but also due to thermal expansion and contraction in a coupled system. Furthermore, as will all models, in SEEP/W the model needs to be parameterized with material properties and boundary conditions, with estimations available for certain processes.

Heat transfer in GeoStudio is modelled using TEMP/W, which simulates the movement of thermal energy through porous media and can be coupled with SEEP/W for coupled heat and water transfer processes. When coupled, the change in a state variable governing one process changes the state variable governing another. With a SEEP/W and TEMP/W coupled model, the difference in densities created by temperature variations affects the water flow of the system. The governing equations for heat transfer in TEMP/W are based on the first law of thermodynamics, the law of energy conservation, and Fourier's Law. Similarly to SEEP/W, the PDE includes heat storage and heat flow processes. The default flow process in TEMP/W is conductive heat transfer, however, can be driven by sensible heat advection with water transfer with options for both forced and free convection. Changes in stored sensible energy and latent heat of fusion through freeze/thaw processes control the storage physical processes in TEMP/W. As with SEEP/W and the other GeoStudio products, parameterization of the model for material properties, boundary conditions, and selective processes can be customized.

3. CHAPTER 3: Site Description and Methodology

3.1 Characteristics of the Wolf Creek Research Basin

The research area is focused in the Wolf Creek Research Basin (WCRB), located in southern Yukon (60°31'40" N, 135°31'14" W). The study site catchment area is approximately 176 km^2 with an elevation range from roughly 800 m to 2080 m and a median elevation at 1325 m (Janowicz, 1992; Granger, 1998). WCRB is also defined by discontinuous permafrost (Brown, 1977), which influences the hydrological regime. Lewkowicz and Ednie (2004), estimate 70-80% of the basin is underlain with permafrost. The study sites are more specifically located in the sub catchment of Granger Basin (Figure 3.1).

As a subarctic alpine region, Wolf Creek is characterized by highly variable precipitation and temperature typical of a subarctic continental climate. The mean annual temperature is approximately -3°C with a mean summer temperature range between 5°C to 15°C and winter temperatures ranging between -10°C to -20°C on average. Extreme summer and winter temperatures have been recorded in the past of 25°C and -40°C respectively, and are not unusual. Mean annual precipitation varies between 300 mm to 400 mm with approximately 40% of the precipitation occurring as snow (Janowicz, 1992). However, since alpine environments have variable precipitation, the elevation and location of an area within Wolf Creek will influence the precipitation and temperature trends (Janowicz, 1986).

As a subarctic alpine environment, vegetation is variable in the Wolf Creek Research Basin, typically at different elevations. While WCRB is comprised primarily of subalpine taiga, the lower elevations consist of dense boreal forest, with the treeline located at approximately 1300 m. Furthermore, alpine tundra dominates the highest elevations where perennial snow drifts on leeward slopes are common.

The geologic composition of Wolf Creek is mainly sedimentary consisting of sandstone, limestone, siltstone, and conglomerate along with some volcanic materials. A mantle of glacial till from depths of several centimetres to one to two metres overlays the basin, with deposits consisting of glacial, glaciolacustrine, and glaciofluvial origins. More specifically, the upland soils are primarily classified as Orthic Eutric Brunisols, with a texture ranging from sandy loam to a gravelly sandy loam. Lower forest soils have a variable texture ranging from gravel to clay, whereas upper elevations tend to have shallow soils of poorly sorted variable texture with exposed bedrock. Heterogeneous mineral soils with a thin organic topsoil layer are characteristic of Wolf Creek. Organic layers are typically 5 cm to 15 cm thick over either sandy or clayey mineral soils. In addition, the basin is underlain with a 2 cm layer of volcanic ash, present around 10 cm below the ground surface (Rostad et al., 1977). The soil profiles of each site vary slightly throughout the basin in layer thickness and grain size, and soils are moderately well drained.

3.2 Site Description

Three sites were used as a study area in WCRB, Riparian (RP), North Facing (NF), and Plateau (PLT) (Figures 3.1 and 3.2). Each site is located in a unique hydrological response unit (HRU), selected based on properties of snow accumulation, vegetation, aspect, and elevation. In terms of elevation, RP is the lower site, NF is the middle site, and PLT is the upper site. The headwater stream of Granger Creek (GC) defines the sub catchment of Granger Basin as well as the HRUs and the site properties based on proximity to the stream.

3.2.1 Riparian

Riparian (RP) is located in Granger Basin adjacent to GC, downslope from NF in the base of the valley (Figure 3.2a). RP does not have a gradient and is located on level ground surface. The

properties of soils at RP are more variable among the layers than the other sites, with a greater soil texture change in each layer. The soil textures of RP from shallowest to deepest are loamy fine sand, sandy loam, and loam (Table 3.1). RP soil texture decreases in sand percentage with depth, however, increases in both silt and clay. RP soils have a bulk density of 1.3 g/cm^3 and 1.98 g/cm^3 with corresponding porosities of 0.51 and 0.25 (Table 3.1). Bulk density increases with depth and porosity decreases with depth. The highest bulk density and lowest porosity of all the sites is found at RP (RP_2). Classified as sandy loam soil texture, the bulk density value at RP_2 of 1.98 g/cm^3 is a notably high bulk density. RP soils have saturated hydraulic conductivities in the range of 10^{-5} to 10^{-9} m/s, measured with both KSAT and HYPROP devices (as specified in Section 3.3.2), typical of fine-grained sand to silty clay (Table 3.2). Furthermore, the conductivity values classify soils from a range of permeable to very weakly permeable.

3.2.2 North Facing

Within Granger Basin, the North Facing (NF) site is located upslope from RP and below PLT (Figure 3.2b). Located on the leeward side of an alpine slope, this site is dominated by snow coverage that remains well into late spring. Instrumentation on the NF site is approximately midpoint for the slope at 60 m along a 150 m gradient, with a grade of 17.5 degrees. NF soils are typically loam in texture. The shallow layers are defined as silt loam and loam whereas the deeper layers are all classified as sandy loam (Table 3.1). NF soils had overall higher percentages of clay than the other sites. For NF, soil grain size increases with depth, with higher sand percentage, and lower percentages of silt and clay with deeper soil layers. Similar to RP, the bulk density increases with depth and porosity decreases with depth, with bulk density values of 0.82 g/cm^3, 1.56 g/cm^3 and 1.9 g/cm^3, and porosity values of 0.69, 0.41 and 0.28 respectively (Table 3.1). Higher bulk density values occur in soils with higher sand percentage, evident at NF. The lowest bulk density

and highest porosity of all the sites is found at the uppermost layer of NF (NF_1). Classified as sandy loam soil texture, NF_3 has a notably high bulk density of 1.9 g/cm^3. The values of bulk density, porosity, and saturated hydraulic conductivity reflect the soil texture at each layer. The saturated hydraulic conductivity of NF soils, depending on the measurement, ranges from highly permeable to permeable with values of 10^{-3} to 10^{-6} m/s (Table 3.2). The conductivities reflect soil textures of medium grained sand, fine grained sand, and silty sand.

3.2.3 Plateau

Also located in Granger Basin is the Plateau (PLT) site, located upland from NF on level ground surface (Figure 3.2c). PLT soil layers are less variable between layers when compared to the other sites. While the soil texture varies slightly, each distinct layer at PLT has a similar grain size breakdown. The soil textures of PLT from shallowest to deepest are sandy loam, loamy fine sand, and fine sand (Table 3.1). PLT soils have a bulk density of 1.63 g/cm^3 and 1.7 g/cm^3 with corresponding porosities of 0.38 and 0.36 (Table 3.1). Likewise to other soils in Granger Basin, with increasing depth bulk density increases and porosity decreases. PLT soils have fairly consistent saturated hydraulic conductivities with varying values at 10^{-6} m/s, typical of silty sand (Table 3.2). Furthermore, the conductivity values classify soils from as either permeable or slightly permeable.

3.3 Methods

3.3.1 Instrumentation and Field Data

Wolf Creek has been instrumented at numerous different sites since 1992 (Rasouli et al., 2019). Instrumentation details are provided in Table 3.3.

3.3.1.1 Meteorological Data

Meteorological data for Granger Basin was measured at PLT (Figures 3.1 and 3.2c). Air temperature, net radiation, relative humidity, and wind speed were measured at an interval of 30 minutes. Data was primarily used from PLT, however, due to discontinuities, some data from nearby sites were used for data correction. Precipitation values were measured at 30-minute intervals using Geonor and Pluvio rain gauges. Daily total precipitation values were obtained as an average from the two gauges.

3.3.1.2 Soil Sensors

Soil moisture and soil temperature data were measured using Steven's Water HydraProbe Soil Sensors (Campbell Scientific, 2017). HydraProbe is a dielectric constant sensor which measures the liquid volumetric water content of the soil to obtain soil moisture values. Due to the low inter-sensor variability, direct comparisons along the soil column are possible without sensor specific calibrations. The soil moisture sensors were set for 30-minute intervals at varying depths from 5 cm to 60 cm. Measurement depths at RP and NF were 5 cm, 15 cm, 30 cm, 45 cm, and 60 cm. Data at RP and NF were collected beginning in August 2014 when the sites were instrumented, with some gaps, most notably between December 2015 to April 2016. Measurement depths at PLT were 5 cm, 15 cm, and 30 cm, with continuous data available for 2015 and 2016, the exception being missing data in November and December 2015.

3.3.1.3 Snow Surveys

Manual snow surveys, based on Woo (1997), measuring snow depth and density were conducted for quantifying snowmelt at all three sites in Granger Basin using an avalanche probe and the modified Mount Rose snow sampler, which includes a barrel corer, spring balance, and

weighing scale. Measurements were taken throughout the months from April to June in 2016 at a frequency of twice per week until the snow had melted entirely. Snow depth measurements were taken at 5 m intervals along established 30 point (150 m) transects. Snow density was measured every 25 m along the transect by using the Mount Rose barrel corer and weighed using the calibrated SWE scale. Snow pit measurements for SWE and snow density were collected at all sites corresponding to each snow survey. Additional snow depth measurements were available from tower data at the PLT site.

3.3.1.4 Soil Sampling

Soil texture was evaluated both qualitatively in the field and quantitatively in the laboratory. During the snow surveys, several soil samples were taken to observe examples of frozen soils at each site with ice impeding pore space (Figure 3.3). To characterize and determine soil composition for parameterizing the model, soil samples were collected in June and July 2016, once the soil had completely thawed. A soil pit was dug at each site (RP, NF, PLT) to an attainable depth or until the water table was reached (Figure 3.4). Each soil pit was characterized by both qualitative and quantitative observations on site based on standard soil classification (USDA soil taxonomy and USCS). A sample was collected from each unique layer for particle size distribution analysis to further quantify the soils. 250 mL soil sampling rings were used to collect an in-situ sample for the KSAT and HYPROP devices at distinct layers in each soil pit (Figure 3.5). Three rings were sampled for NF, while RP and PLT had two ring samples each.

3.3.2 Laboratory Methodology

3.3.2.1 KSAT

Using the METER KSAT device, saturated hydraulic conductivity was measured for 7 soil samples from RP, NF, and PLT. The measurement principle of the KSAT device is based on the

Darcy equation (See Equation (3)) (METER, 2017). After soil samples were collected at the selected field sites, each sample was first fully saturated (approximately 24 hours) in degassed water to minimize air trapped within the sample. Using either the mesh plate for consolidated materials or the porous plate for non-consolidated materials, a soil sample was mounted on the KSAT device (Figure 3.6). The device was configured with the appropriate plate resistance and followed the standard measuring procedure for the falling head technique. Each sample was run a minimum of three times and the results were averaged to achieve a mean saturated hydraulic conductivity value.

3.3.2.2 HYPROP

The UMS HYPROP automated measuring and evaluation system was used to determine the hydraulic properties of soil samples for the 7 soil samples from RP, NF and PLT. The evaporation measuring technique is based on Schindler's method and is outlined in detail in the HYPROP manual (UMS, 2015). HYPROP measures the water tension at two different levels of a soil sample using two tensiometers to measure tension as water evaporates from the soil (Figure 3.7). The water content for the water retention curve is calculated based on the weight loss of the sample. Each soil sample was first fully saturated as specified in the KSAT methodology (See Section 3.3.2.1). The tensiometers were then filled with degassed water and the full set up was placed on a tared scale to measure the weight loss as evaporation occurs. The entire process of running the HYPROP varied between one day and two weeks. After running each sample on the HYPROP, samples were analysed for bulk density following standard methods (Freeze and Cherry, 1979; Klute, 1986).

3.3.2.3 Particle Size Distribution

Soil particle size distribution (PSD) analysis was conducted for the field collected soil samples from RP, NF, and PLT at each distinct layer to further classify soil texture based on grain size. Three samples were run for RP, five for NF, and four for PLT following the methodology of Beierle et al. (2002) using the Beckman-Coulter LS 13 320 Laser Diffraction Particle Size Analyzer. Samples were pre-treated by weighing the dry samples and sieving out grains >2 mm, followed by a treatment with 30% hydrogen peroxide to react with organic material. Each sample run length was 60 seconds with 3 runs per sample. Particle size analysis results were translated to soil texture using GRADISTAT macros and USDA/NRCS classification.

3.3.3 GeoStudio Modelling

GeoStudio v9 beta model integrates multiple physical processes (e.g. water transfer, heat transfer) that allow it to simulate concurrent water flow and temperature dynamics in variably saturated environments experiencing soil freezing and thawing. Analyses in GeoStudio were defined by the physical processes of water transfer as free convection and heat transfer as forced convection with water transfer to simulate the concurrent processes. The analysis type was defined as transient with initial temperature and heat conditions as the parent process. Time increments of 30 minutes were used, with steps increasing linearly to reflect the time step of the field data. The maximum number of iterations allowed was 500, with under-relaxation criteria set to the default values. To simply the problem, a 1D model was used for the model domain.

3.3.3.1 Model Parameterization

Model parameterization for the 1D model included materials, boundary conditions, and measured thermo-hydraulic conditions. Numerous parameterizations exist for the soil and water

properties of the system, however there are several approaches commonly used that were selected for parameterizing the GeoStudio model.

Initial conditions for water and heat were required to further define the analyses. For water transfer, the initial head/pore water pressure conditions from a generated spatial function were used and a pressure head function was created. The Thiesen Formula function, provided by GeoStudio, was selected as the water density function for the model. Physical constants of the unit weight of water and bulk modulus of pore-fluid were defined according to standard values of 9.807 kN/m^3 and 2.15 x 10^{-9} Pa respectively. For heat transfer, initial temperatures from a spatial function generated using field data was selected. The physical constants of latent heat of water as 3.34 x 10^{-8} J/m^3 and phase change temperature of 0°C were also defined.

To begin creating the model, a 1D model was used for the domain, with each individual soil layer defined using laboratory data as outlined in Section 3.3.2 for material properties of the model and points which correspond to the depths of soil sensors mentioned in Section 3.3.1.2 for direct result comparison. The material properties were defined for both thermal and hydraulic functions, each with a material model option and specific parameters. For the thermal material properties, the material model chosen was coupled convective thermal. This material model required several functions to be defined including a thermal conductivity vs. volumetric water content function, a volumetric specific heat function, and an unfrozen volumetric water content function. The functional relationship between thermal conductivity and volumetric water content for unfrozen soil was estimated by Johansen (1975) and the specific heat functions for each soil type was estimated using de Vries (1975). The unfrozen volumetric water content function for each soil layer was estimated using GeoStudio's provided normalized sample functions based on the soil particle size and using the Clausius-Clapeyron equation. For the hydraulic material properties, the

material model selected was saturated/unsaturated. The functions required for this model include a volumetric water content function and a hydraulic conductivity function. To define the volumetric water content function and parameterize the model for water content and water pressure, a van Genuchten (1980) function was selected. The values used to determine the van Genuchten function were derived from the HYPROP analysis as mentioned in section 3.3.2.2 (Table 3.4). The hydraulic conductivity functions for each soil layer were estimated in GeoStudio using the van Genuchten approach with the previously defined volumetric water content. In addition, the option to reduce conductivity in frozen ground was selected for each material property.

Hydraulic and thermal boundary conditions were specified for both the initial and transient settings at the upper and lower boundaries. For the initial conditions, the upper hydraulic boundary was defined as a land-climate interaction including climate and snow data. The lower or bottom boundary hydraulic conditions was set as zero pressure head to allow for initial hydrostatic conditions. For the transient seepage model, the upper hydraulic boundary condition chosen was also the land-climate interaction and the bottom hydraulic boundary condition used a unit gradient to allow for drainage. Both the initial and transient thermal boundary condition was a surface balance for the upper boundary.

4. CHAPTER 4: Results

Results from this study include data collected during 2015 and 2016 with a focus on two time periods, the 2015 freezing period (September to December) and the 2016 thawing period (April to July).

4.1 Climate

4.1.1 Annual Climate

Average air temperature and precipitation for Whitehorse, Yukon from 2015 - 2016 are summarized in Table 4.1. Average annual air temperature was 1.4°C in 2015 and slightly warmer at 2.4°C in 2016. Relative to the 30-year annual climate normal of -0.1°C, both years were marginally warmer. Annual total precipitation for 2015 was 252.5 mm with an average of 21.0 mm per month, whereas 2016 had more precipitation with a total of 317.8 mm and an average of 26.5 m per month. With the monthly climate normal average of 21.9 mm, 2015 was slightly drier and 2016 was a wetter year. In addition, 2015 was overall drier and 2016 was wetter than the annual climate normal of 262.4 mm.

When considering the two distinct time periods, the freezing period and the thawing period, there were more notable variations from the climate normals. From September to December 2015, the average air temperature was slightly cooler than the climate normal of -3.6°C. Total precipitation during the freezing period in 2015 was 86.7 mm, which was similar to the climate normal of 92.9 mm. In the thawing period from April to July 2016, average air temperature exceeded the normal of 8.7°C, with an average of 11.2°C. Total precipitation was also greater than the climate normal of 93.8 mm in 2016, with a value of 142.2 mm, making the thaw period warmer and wetter than the climate normals and 2015.

4.1.2 Freezing Period

The freezing period occurred throughout the months of September to December in WCRB and is reported with meteorological data measured at PLT. During this time, there was missing data for net radiation for the months of November and December 2015. Nevertheless, average daily air temperature and average daily net radiation both showed decreasing trends over the freezing period (Figures 4.1-4.3). Air temperature ranged between -22°C and 8°C and net radiation ranged from approximately 0 W m^{-2} to 70 W m^{-2}. During October, air temperature fluctuated around 0°C, with below freezing temperatures beginning around late October to early November and dropped steadily onwards throughout the freezing period. The lowest air temperature of the freezing period occurred in mid-November at -22°C followed by a rapid increase to around -3°C over several days, while still decreasing over time. Early in the freezing period in September, net radiation ranged between 25 W m^{-2} and 70 W m^{-2}. A drop close to 0 W m^{-2} occurred early October and again in late October, remaining between 0 W m^{-2} and approximately 15 W m^{-2} for later part of the freezing period. Snow depth in September to mid-October ranged in depths between 0.15 m and 0.2 m, fluctuating slightly, but gradually increased over the freezing period. A sudden increase in snow depth to 0.25 m followed by a quick drop to 0.15 m occurred in late October, as well as again at the beginning of December with a snow event bringing depth to 0.28 m before dropping to around 0.2 m towards mid-December. With the exception of the two notable events, snow depth averaged around 0.2 m for November and December with some variability.

4.1.3 Thawing Period

During the thawing period of April to July at PLT, there was a gradual overall increase in average daily air temperature from approximately -2°C in late April to 15°C by the end of July (Figures 4.4-4.6). Two spikes of temperature occurred mid-May to 10°C and steep increases in

temperature to approximately 12°C also occurred in mid-June. In general, temperatures over the thawing period in WCRB increased steadily with the expected variation. Average daily net radiation gradually increased from April to July, however, with only a slight overall change. Net radiation values over the thawing period ranged from approximately 50 W m^{-2} to 250 W m^{-2}, with typical oscillations of 50 W m^{-2} to 100 W m^{-2} over several days. Snow depth decreased over time at all three sites, with significant melting occurring during the rapid onset of positive temperatures at the end of April into May. For RP, snow depth at the start of the measured thaw period was 0.5 m and decreased steadily to 0 in mid-May (Figure 4.4). NF follows a similar snow melting pattern, but with more snow and therefore an extended melt period, fully clearing at the end of May from a depth of around 0.68 m at the end of April (Figure 4.5). The upper site, PLT, had a lower average snow depth at the start of the thaw period with a value of 0.32 m and was snow free by mid-May, a few days before RP (Figure 4.6).

4.2 Ground Thermal and Soil Moisture Regime

4.2.1 Freezing Period

Figures 4.7 and 4.8 show soil temperature and volumetric liquid water content (vlwc) during the freezing period from September to December 2015 at RP, NF, and PLT. During this time, there was incomplete soil temperature and vlwc data at PLT for the end of November and December 2015. Soil temperature at RP from September to December, ranged between 4°C and -1°C (Figures 4.7a and 4.1). Colder temperatures initially started at the shallower depths and move downwards in the soil over time. At RP, there was a steady trend of cooling throughout the freezing period, with shallower depths becoming colder faster than the deeper layers. Temperatures of 0°C began at 0 - 10 cm early in October, migrating deeper to 30 cm around November and reaching 60 - 70 cm depth later in the period in December. Below freezing temperatures of -0.5°C were present at

the shallow depths beginning in late October and continued throughout the freezing period. One significant temperature spike occurred at the beginning of October to 6°C at 5 cm depth. At NF, soil temperatures typically ranged between 2°C and -2°C during the same freezing period, with 2°C occurring only briefly at 0 - 10 cm in late September (Figures 4.7b and 4.2). Soil temperatures at NF hovered around 0°C for the duration of the freezing period at depths of approximately 15 cm and below. Soils at 0 - 10 cm had freezing temperatures between -0.5°C and -2°C briefly in early October and then consistently at the end of October for the remaining duration. Similarly, soil temperature increased with depth, the colder temperatures between -1.5°C and -2°C were at shallower depths than temperatures of -0.5°C. A notable point in soil temperature occurred at 5 cm depth with a 5°C peak in early October, followed by a rapid drop in temperature to around -3°C over the next ten days (Figure 4.2). PLT soil temperature throughout September at all soil depths, ranged from approximately 0°C to 3°C, then steadily decreased later in the month, with the shallower depths temperature dropping more rapidly than deeper soils (Figures 4.7c and 4.3). With the exception of a spike early October, the soil temperature plateaus and hovered at 0°C at all depths until November. At this time, soil temperature at 30 cm remained at 0°C, whereas temperatures at 5 cm and 15 cm both decreased steadily to approximately -2°C, with 5 cm depth slightly colder than 15 cm during this time. Towards the end of the freezing period, soil temperature for 30 cm also began to decrease below 0°C.

Volumetric liquid water content during the freezing period ranged from close to 0 to 0.45 at RP (Figures 4.8a and 4.1). Between 0 - 10 cm depth, the soil moisture value decreased significantly over time, with sudden changes occurring late in October dropping to liquid water content of 0.2 and below. These values extended deeper into the soil later in the freezing period, approximately mid-November. Soil moisture around 50 cm and deeper was approximately 0.2 and 0.3 for the

duration of the freezing period, with some slight variations. A prominent feature of the soil moisture in RP was the close to full saturation value of 0.4 between 10 - 45 cm that is persistent from September to December. Towards the end of November, early December, vlwc at this depth decreased its range to approximately 25 - 30 cm, with lower soil moisture migrating both upwards and downwards. Soil moisture at NF ranged from approximately 0.05 to 0.4 during the freezing period (Figures 4.8b and 4.2), with significant changes only occurring in the first 30 cm. With depths of 30 cm and greater, vlwc was fairly consistent between 0.2 and 0.3 for the entire freezing period. The most notable changes in vlwc occurred in approximately the first 15 cm of the soil profile at NF. Values decreased over time and extended deeper into the soil ranging between an interpolated 0 value to 0.2 as the soil froze. Moving upslope to PLT, vlwc ranged between 0.05 and 0.35 (Figures 4.8c and 4.3). Soil moisture values at 5 cm and 15 cm similarly vary in early September, around 0.3 to 0.35, gradually decreasing later in the month (Figures 4.8c and 4.3). At 30 cm, soil moisture fluctuated minimally in the early freezing period, then hovered around 0.1, decreasing minutely throughout the later months. Throughout October, vlwc decreased, with 5 cm depth consistently lower than at 15 cm depth. During this time, there were several sharp increases in vlwc, however, the overall trend decreased over time. Soil moisture values fell sharply in early November and slowly decreased for the remainder of the freezing period, with 5 cm around 0.1 and 15 cm slightly greater at approximately 0.11.

4.2.2 Thawing Period

Figures 4.9 and 4.10 illustrate soil temperature and vlwc during the thawing period from April to July 2016 at RP, NF, and PLT at various depths. Soil temperature at RP ranged from approximately 0°C to 18°C and gradually warmed at all depths over time (Figures 4.9a and 4.4). Positive temperatures began in the shallower soil depths in early May and migrated downwards,

with strong warming occurring in early June. From April to May, soils at 10 cm and deeper remained around 0°C. In early June, there was a sudden increase in soil temperatures at all depths as temperatures jumped to 1°C, then steadily increased throughout the thawing period to higher temperatures. At NF, soil temperatures ranged from -0.5°C to 16°C (Figures 4.9b and 4.5). The thawing period extended well into July, particularly at the lower depths where soil temperatures still remained close to 0°C. Soil temperature at all depths in late April to early May ranged between -0.5°C and 0°C, with higher temperatures beginning in mid-May between 0 - 10 cm and migrated into deeper soils as time progressed. Temperatures at 10 cm and deeper hovered around 0°C until early June when the soil temperature gradually increased over time, with shallower soils experiencing the temperature changes before the deeper soils. At the end of the thawing period in July, positive temperatures reached all soil depths, with 0 - 15 cm soils ranging from 3°C to 16°C, 15 - 45 cm ranging from 2°C to 3°C, and 45 - 70 cm ranging between 0.5°C to 2°C. For the ground thermal regime at the upper site of PLT, the soil temperature hovered around 0°C at all depths until late April and early May, when there was a rapid increase of soil temperature for each depth (Figures 4.9c and 4.6). Soil temperature increased the quickest for 5 cm towards 14°C and slowest for 30 cm depth, which reached ~ 8°C. Soil temperature at 15 cm increased steadily to 10°C.

Volumetric liquid water content at RP during the thawing period ranged between 0.1 and 0.5, approximately full saturation (Figures 4.10a and 4.4). Water content values of 0.3 and 0.4 occurred early in the thawing period, specifically at depths of 0 - 5 cm and 60 - 70 cm, while the soils between 5 - 60 cm remained consistent at a value around 0.2. Following this early high soil moisture between 0 - 5 cm, soil moisture values dropped in mid-May to 0.1 and 0.2 while higher saturation occurred deeper in the soil profile. In mid-May, between 10 cm and 40 cm, soil moisture was close to full saturation at 0.3 - 0.4, and persisted for the remainder of the thawing period. Soil

moisture between 50 to 60 cm hovered consistently around 0.3. At NF, vlwc ranged from 0.05 to 0.5, with greater saturation typically occurring later in the thawing period (Figures 4.10b and 4.5). From April to early May at all depths, soil moisture was around 0.1, and increased slightly to 0.2 in early May, beginning at 0 - 10 cm. The most significant changes in vlwc occurred in approximately the first 20 cm of the soil profile at NF, with rapid change from 0.3 to 0.5 occurring in mid-May between 0 - 10 cm. This extended to 10 - 20 cm around late May, early June in the thawing period while the soil moisture decreased slightly at 0 - 10 cm. Overall, vlwc increased gradually over time and extended deeper into the soil ranging in values of 0.1 to 0.3. At PLT, vlwc hovered around 0.1 for each depth throughout most of April, with slightly lower soil moisture for 30 cm depth, and slightly higher for 15 cm depth (Figures 4.10c and 4.6). Water content at the shallowest layer of 5 cm increased rapidly towards 0.5 near the end of April, followed by 15 cm at 0.45, then 30 cm to a value of approximately 0.15. The vlwc for each layer peaked around mid-May, dipped and then plateaued for the remainder of the thawing season with some drainage oscillations. During this time, soil moisture at 5 cm dropped the furthest and fell below the soil moisture value at 15 cm.

4.3 Modelling

Three distinct models were created, one for each site, NF, RP and PLT and run from September 2015 until July 2016, to capture both the freezing period (September to December), and the thawing period (April to July) with results yielding soil temperature and unfrozen volumetric water (uwc) content values over time. The freezing period and thawing period used field data from the corresponding time frame to reflect the appropriate conditions during the period and drive the model. However, the material properties and boundary condition types remained consistent among each site over the simulation.

4.3.1 Freezing Period

Figures 4.11-4.13 show the full model results for soil temperature and unfrozen volumetric water content for NF, RP, and PLT. During the freezing period at NF, soil temperature ranged from approximately 0.5°C to -6°C, with the temperature fluctuating around 0°C at all depths until early December (Figure 4.11a). Temperature then decreased rapidly for soil layers at 5 cm, 15 cm, and 30 cm, with greater drops in temperature the shallower the soil. At 5 cm, soil temperature decreased to approximately -6°C in mid-December, followed by a brief increase to around -1.5°C, then varying between -3°C to -5°C for the remainder of the freezing period. At 15 cm, temperatures began to lower in approximately mid-December, overall decreasing throughout the month from -0.5°C to -2°C with some daily variation. For the soil at 30 cm, the model began to produce negative temperatures late in December with a slight decrease to -1°C. Results from 45 cm and 60 cm show soil temperature remained around 0°C during the freezing period, however, experienced below freezing temperatures later in the winter in mid-January for 45 cm and March for 60 cm. Unfrozen volumetric water content at NF varied at each depth throughout the freezing period, with a range between almost 0 and 0.57 (Figure 4.11b). Similarly to soil temperature patterns, there was a dampening with depth, as unfrozen water content approached 0 at the soils closer to the surface sooner than the deeper soils. Soils at 5 cm and 15 cm began with an uwc value around 0.5 at the beginning of the freezing period and fluctuated between 0.45 and 0.5 in mid-October, with 5 cm slightly lower than 15 cm. Towards the end of October, uwc at 5 cm dropped suddenly to 0.3, slowly decreasing to 0.25 until mid-December where it rapidly drops towards 0, fluctuating near 0 for the remainder of the freezing period. At 15 cm, there was a slight decrease from 0.5 to 0.4 from mid-October to mid-December, where the unfrozen water content fell rapidly to around 0.075, increasingly slightly and fluctuating around 0 for the rest of the freezing period. Unfrozen

water content for 30 cm followed a similar pattern to the shallower soils, but with lower values, starting at 0.24 in mid-September and dropped to around 0.2 in mid-October. This was followed by a steady decrease to 0.15 before dropping to almost 0 in the end of December. Soils at 45 cm and 60 cm varied slightly between 0.2 and 0.24 throughout most of the freezing period, with 45 cm decreasing to 0 in late December and early January and 60 cm steadily lowering towards 0 from mid-January to mid-March.

At RP during the freezing period, soil temperature ranged from 3°C to -10°C, with temperatures dropping sooner for the shallower soil depths (Figure 4.12a). At the beginning of the modelled period, all soils at RP were between 2°C and 3°C, ranging from the shallowest soil as the coldest and the deepest soil as the warmest. By the middle of October, all soil temperatures were at 0°C, with minimal differences in timing. At 5 cm depth, the soil temperature began at 2°C, fluctuating slightly towards 0°C with a zero-degree curtain until the end of October. Negative soil temperatures began early November and large drops in temperature occurred in December going from -4°C to over -10°C with diurnal variations. At 15 cm, the pattern was similar to 5 cm, but with negative temperatures only starting in early December and soil temperatures just below -6°C. Results from 30 cm, 45 cm and 60 cm followed a similar pattern, decreasing to 0°C in mid-October and remaining at that temperature for the selected freezing period. The full modelled soil freeze/thaw simulation showed these deeper soils decreasing below the zero-degree curtain at the end of December. Unfrozen volumetric water content at RP during the freezing period had a range between close to 0 and 0.45 (Figure 4.12b). Soils at 5 cm and 15 cm began with an uwc value around 0.45 at the start of the freezing period and fluctuated around this value until the end of October, with 5 cm slightly lower than 15 cm. At the end of October, uwc at 5 cm dropped steeply to 0.05, then fluctuating and progressively decreasing until levelling out in mid-December. At 15

cm, uwc steadily decreased towards 0 over November, and plateaued in mid-December for the remainder of the freezing period. Unfrozen water content for soils at 30 cm, 45 cm and 60 cm remained at 0.15 throughout most of the freezing period, with 30 cm approaching 0 in mid-December, 45 cm decreasing to 0 in late December, and 60 cm steadily lowering towards 0 in late December and early January.

At the upper site, PLT, model results over the freezing period showed soil temperatures ranging from approximately 1°C to -8°C (Figure 4.13a). Similar to NF and RP, soil temperatures at the shallower depths had colder temperatures sooner than the deeper soil layers. At 5 cm, soil temperature starts at 0.75°C then quickly approached the zero-degree curtain, with a small half degree spike in temperature late in September. Soil temperatures remained at 0°C until mid-December, when the soil temperature dropped to -2.5°C. Overall soil temperature lowered for the remainder of the month, with a minimum temperature of just over -8°C by the end of the freezing period. Soil temperature for 15 cm and 30 cm both start just over 1°C and quickly fall to 0°C by mid-October. Negative temperatures began in mid-December for 15 cm and mid-January for 30 cm depth, with 15 cm following a similar pattern to shallower soils, however, only dampened and reaching a temperature -4.5°C within the same time frame. Unfrozen volumetric water content at PLT followed similar trends with slight variations at each depth throughout the freezing period, with a range between 0.01 and 0.29 (Figure 4.13b). The simulation for the shallower depths, 5 cm and 15 cm, started the freezing period with an uwc of 0.32 and 0.31, respectively. Water content at both points decreased throughout September, with a spike in early October, more notably for the shallower soil. In mid-October, uwc at 5 cm dropped from 0.24 to 0.17, falling to lower uwc than the 15 cm level. The water content hovered around 0.2 for rest of the month before gradually lowering towards 0 in mid-December. At 15 cm, uwc varied around 0.24 in October and steadily

decreased until sharply dropping near 0 in mid-December, slightly later in the shallower points. Unfrozen water content for 30 cm followed a similar pattern to the shallower soils, but with dampened values and timing, starting at 0.27 for the freezing period and slowly declining to 0.18 until late December when the rate of the downtrend increased significantly.

4.3.2 Thawing Period

Over the thawing period from April to July, GeoStudio results for soil temperature at NF showed an overall increase for every point with a dampening effect with depth (Figure 4.11a). During the thawing period simulation for NF, soil temperature initially remained close to 0°C for all depths with little to no fluctuation until the end of May. Around the end of May and beginning of June, soil temperatures at 5 cm, 15 cm, and 30 cm, suddenly increased to positive temperatures with a strong diurnal fluctuation and steadily increased over the season. At 5 cm, the maximum temperature reached is approximately 24°C, with the daily average around 15°C in June and July. Soil at 15 cm had less daily variation than 5 cm and steadily increased from 5°C to 15°C over June and July, reaching a maximum temperature just over 17°C. For 30 cm, soil temperature increased in early June and gradually increased to a maximum temperature of 16°C by the end of the season, with temperatures always less than 15 cm. The soils at 45 cm and 60 cm began to experience positive temperatures in mid-June and late June respectively. At these deeper soils, there was little to no diurnal patterns present, with 45 cm increasing to around 2.5°C in mid-June, plateauing, then steadily increasing towards 15.5°C for the remainder of the thawing period. At 60 cm, soil temperatures hovered around 0°C until late June and then gradually increased to approximately 15°C, following a similar trend to 45 cm, just slightly cooler. Each soil depth at NF followed a similar trend for unfrozen volumetric water content over the thawing period, with sudden increases corresponding to timing of thaw (Figure 4.11b). As the thawing period commenced, uwc at 5 cm

increased steadily from 0.15 in April to 0.26 by June. At the start of June, water content at 5 cm jumped suddenly to 0.57 before dipping back down to 0.47 and fluctuating there for the rest of the modelled period. The modelled 15 cm point followed the same pattern, but increased at a slower rate than 5 cm. Unfrozen water content at 15 cm spiked several days after 5 cm, from 0.13 to 0.55, dropping to around 0.5 where the value varied for the remainder of the thawing period. The deeper points, 30 cm, 45 cm, and 60 cm, unfrozen volumetric water content held at 0.01 until early to mid-June, where each value rose rapidly to 0.27 in order of depth. After the jump, modelled water content at 30 cm dropped below the deeper soil values and the three points fluctuated between 0.2 to 0.27 until the end of the model simulation.

At the lower site of RP during the thawing period, soil temperature ranged from 0°C to 29°C, with temperatures increasing sooner for the shallower soil depths (Figure 4.12a). Soil temperature initially held near 0°C for all depths with little to no fluctuation until mid-May. The thawing process began near the surface and migrated downwards as changes in soil temperature occurred in order of depth. Around the end of May and beginning of June, soil temperatures at 5 cm and 15 cm suddenly increased to positive temperatures with a strong diurnal fluctuation and steadily rose over the thawing season. At 5 cm, the maximum temperature reached is approximately 29°C, with the daily average around 18°C to 20°C in June and July. Soil at 15 cm has less significant daily variation than 5 cm and steadily increased from May to July, reaching a maximum temperature around 23°C, with soil temperature always less than 5 cm. The soils at 30 cm, 45 cm and 60 cm began to experience positive temperatures in mid to late May. At these deeper soils, there was significant dampening with little to no oscillations present. Soil temperatures at 30 cm, 45 cm and 60 cm increased steadily to around 15°C in June, dipping several degrees over a week, then overall continuing to rise over the modelled period, peaking at 20°C. All results over the thawing period

at these three points were highly similar, with 30 cm experiencing diurnal changes to a greater degree and slightly earlier than 45 cm and 60 cm. There was approximately a half day lag between 45 cm and 60 cm which otherwise are very similar. Unfrozen volumetric water content at RP during the thawing period had a range between close to 0 and 0.45 (Figure 4.12b). Soils at 5 cm and 15 cm began with an uwc value around 0.06 and 0.025 respectively at the start of the thawing period, gradually increasing until a spike in mid-May. Unfrozen water content at 5 cm jumped to 0.45, slightly fluctuating over the thawing period. At 15 cm, uwc surged a couple days later than 5 cm to 0.45, hovering around the same values for the remainder of the modelled simulation. Unfrozen volumetric water content for soils at 30 cm, 45 cm and 60 cm began around 0.01, holding until mid to late May, then increased to 0.08 with a slight lag between each point. This value remained for the rest of the simulated thawing period.

At the upper site, PLT, model results over the thawing period showed soil temperatures ranging from approximately 0°C to 30°C (Figure 4.13a). Similarly to NF and RP, soil temperatures at the shallower depths had warmer temperatures sooner than the deeper soil layers. All points held at 0°C from the beginning of the modelled thawing period, until mid to late May, when positive temperatures rapidly occurred and soils fully thawed. Soil temperatures at 5 cm and 15 cm followed a close pattern, with the shallower points with a greater degree of diurnal oscillations and 15 cm being less sensitive to the surface changes. In mid-May, soil temperatures at 5 cm and 15 cm both increased quickly and continued to rise over the thawing period. The temperature increased to over 20°C at 5 cm during a period of several days after the initial thaw, whereas the soil temperature at 15 cm is approximately half during the same time. At 5 cm, the maximum temperature reached approximately 30°C, with the daily average around 18°C to 20°C in June and July. Soil at 15 cm had less significant daily variation than 5 cm and steadily increased from May

to July, reaching a maximum temperature around 23°C, with soil temperature always less than 5 cm. For 30 cm, a rise in soil temperature from 0°C began in late May, increasing to 16°C over 10 days with some variation. The temperature then dipped by several degrees followed by a gradual rise in average temperature for the remainder of the model simulation, peaking at just over 20°C. Similar to the freezing period at PLT for unfrozen volumetric water content, the pattern during the thawing period was very similar at each depth, with dampening of values and timing. Over this time, the shallower soils uwc were greater than those deeper with one exception of 15 cm peaking above 5 cm in mid-May. At 5 cm, uwc increased at a steady rate from 0.035 to 0.075 then jumped up to 0.34 in early May. Water content then decreased over the next month and a half with strong variation before plateauing in early to mid-June around 0.27. The modelled point of 15 cm followed a similar trend, increasing suddenly in mid-May to 0.34 then dropping to 0.25 over the month before evening out in June. The deeper layer at 30 cm had a slight rise in uwc prior to a rapid rise to 0.24 in mid to late May. Unfrozen volumetric water content plateaued at 0.26 for 15 cm and 0.23 for 30 cm.

5. CHAPTER 5: Discussion

5.1 Soil Freeze Thaw Systems in Cold Regions

The three sites measured and simulated in Granger Basin are unique hydrological units with differing elevation, aspect, snow accumulation, vegetation, and proximity to streams. These characteristics influence the ground thermal and soil moisture regimes, which further define the environmental gradient. The patterns of the soil temperature reflect patterns in the soil moisture, the snow regime and surface energy balance. Dampening with depth occurs as shallower soils experience diurnal changes more than deeper soils at all sites and are more sensitive to changes in climate at the surface.

5.1.1 Freezing Period

When comparing ground thermal and soil moisture regimes at each site, soil freezing moves downwards along the elevation gradient with the upper site freezing first, followed by the middle site, then the lower site. The lower site, RP was considerably warmer and wetter than NF and PLT (Figures 4.7 and 4.8). Over the freezing period, RP had few temperatures below 0°C and had higher vlwc than the other sites. Compared to the mid and upper sites, RP depicts an overall higher soil moisture content with shallower depths, with rapidly diminishing liquid water content later into the winter (Figure 4.8a). Due to the greater moisture content at RP, the soils have a higher heat capacity and therefore freeze more slowly. Moving upslope, NF had consistently colder temperatures and lower soil moisture values, particularly at shallower depths, with earlier freezing than RP (Figures 4.7 and 4.8). At the upper PLT site, soil freezing occurred first when comparing the soil temperature and volumetric liquid water content for the same depths (Figures 4.7 and 4.8). Soils froze deeper and faster at PLT as a result of being drier and having less snow coverage. However, these differences are less pronounced between PLT and NF than PLT and RP.

Comparatively, the timing of freezing is more similar for the shallowest soils at all sites and the time differences are amplified with depth, likely due to moisture content.

5.1.2 Thawing Period

During the thawing period, the ground thermal and soil moisture regimes varied from the freezing period. As derived from the soil temperature and volumetric liquid water content, the upper site thawed first, followed by the lower site, then finally the middle NF site. Rather than the relatively simple downslope trend that occurred for freezing, the soil thawing process at the middle site is significantly longer than the upper and lower sites. At PLT, the soil became warmer and wetter quicker than the other two sites as snow melted here first, but experienced greater drainage later in the season and became comparatively dry (Figures 4.9a-c and 4.10a-c). In addition, thawing at PLT happens over a quicker period of time than the lower sites. Moving downslope to the lower site, RP had positive soil temperatures around the same time as PLT, yet took longer to propagate downwards into the soil due to greater moisture content (Figures 4.9a-c and 4.10a-c). The middle NF site had colder temperatures and less volumetric liquid water content over the thawing period with deeper soils remaining frozen well into the thawing period (Figures 4.9a-c and 4.10a-c). The aspect at NF results in more persistent snow coverage and a longer snowmelt period than the other sites, insulating the surface and keeping the soils frozen for longer. In addition, it receives less energy than the other two sites because of its aspect. Similar to the freezing period, the timing of thawing is more comparable among sites for soils closer to the surface and diverge with depth.

5.2 Model Ability to Simulate Environment

GeoStudio results for soil temperature and unfrozen volumetric water content are compared to observed field data for soil temperature and volumetric liquid water content at each corresponding

site over the specified freezing and thawing periods. While soil temperature and unfrozen volumetric water content vary from observed values depending on the site and soil depth, these properties are simulated reasonably, within realistic value ranges and capture the expected overall patterns of freezing and thawing. It is important to note that the models were not calibrated, and that parameters were set from field values and boundary conditions chosen as to those which best represented the soil.

5.2.1 Freezing Period

Over the freezing period, observed soil temperatures at NF show shallower soils freezing sooner and a prolonged zero-degree curtain for the deeper soils, also present in the modelled results (Figure 5.1a,b). While all the soils do eventually freeze in the GeoStudio simulation, there is a significant lag of one to two months from the observed results at 5 cm depth. This lag is also present when comparing the observed volumetric liquid water content to the modelled unfrozen water content, particularly at 5 cm and 15 cm, with a time lag of around one month (Figure 5.1c,d). Furthermore, the model estimates lower unfrozen water content for depths 30 cm and below and overestimates the water content for soils closer to the surface. However, the deeper soil layers are reasonably well represented based on the data presented for both soil temperature and unfrozen volumetric water content, indicating that the dampening with depth is successfully modelled during soil freezing. Ultimately, deeper soils are modelled to greater accuracy over the freezing period than shallower soils, which has a larger margin of error and major lag. As the shallower soils are more sensitive to changes at the surface, the parameterization of the surface boundary conditions influences the timing of freezing. In particular, the presence or depth of snow at the surface has the most impact on the shallowest soils and its thermal effects are dampened with depth. As the snow data used for the model during the freezing period is not sampled at the exact

location of the observed data, any discrepancies from the actual timing and depth of snow would consequentially impact the accuracy of modelled soil freezing.

Downslope at RP, the freezing period was modelled with similar inaccuracies as NF with respect to timing discrepancies and value ranges (Figure 5.2). While the zero-degree curtain is reached fairly quickly in the GeoStudio simulation, observed soil temperature data depict a more gradual freezing, yet also experience temperatures below zero earlier than the modelled results. In addition, the soil temperature at RP is much lower later in the freezing period than the observed values, with a modelled temperature of -10°C at 5 cm that is simultaneously observed around -1°C. This is likely because GeoStudio freezes all soil water in the near-surface layers prior to this actually being the case, allowing the model to overcome the latent heat limitations and lowering soil temperatures. Conversely, the soil temperatures at the beginning of the freezing period are comparable to the measured data, but with shallower soils in the simulation demonstrating less temperature variation. For RP, GeoStudio modelled certain points along the soil profile considerably better than others for unfrozen water content. For the two deepest points, the pattern over the freezing period was similar, but the model underestimated the amount of volumetric liquid water content in the soil. Conversely, the shallower soils are overestimated for water content and the timing for freezing is slightly delayed.

Observed soil temperatures at PLT follow a similar trend for each soil depth, however, within a different range of values (Figure 5.3a,b). Similar to the modelled data, shallower soils responded to atmospheric forcing sooner than the deeper soils, with 5 cm becoming colder earlier in the freezing period than 15 cm and 30 cm. Soil temperatures for the modelled results at 5 cm and 15 cm did not exceed the zero curtain until early December, whereas the observed data for the same depths showed negative temperatures occurring in late October and early November. While the

full data set into December was not available for the observed values, 30 cm also began to decrease below the zero curtain in mid-November, while this does not occur until well into January for the modelled data. In addition, there is a notable 3°C temperature spike in late September, which only slightly appears in the modelled results for 5 cm. While the observed data at PLT does appear to show variation based on climate, the modelled results were affected more suddenly and directly with exaggerated results. For the unfrozen water content, there was more inconsistency between the observed and modelled data, particularly for the deeper soils (Figure 5.3c,d). Similar to NF and RP, there was a lag in freezing present in the unfrozen water content for the simulation as well as discrepancies in the amount of liquid water in the soil, particularly underestimating water content for the deeper soils.

Considering all site simulations, GeoStudio freezes soils later than observed with wider ranges in values and greater rates of change. In addition, the unfrozen volumetric water content predicts values closer to 0 than the measured results, as liquid water is still present even in frozen soils (Bouyoucos, 1920; Miller, 1966; Gray and Granger, 1986; Newman and Wilson, 1997; Watanabe and Mizoguchi, 2002; Tian et al., 2014). These differences in modelled versus observed results are a product of how heat is treated and controlled in the model and the coupling with water flow. With respect to the remaining water content in frozen soils, this is governed by an estimated function of unfrozen water content in GeoStudio based on grain size and the volumetric water content function. Volumetric liquid water content is also better simulated during the freezing period, as freezing happens over a shorter period of time than thawing based on the observed data, likely due to the rate of air temperature change over each period. Both freeze and thaw occur rapidly in the GeoStudio simulation, resulting in freezing being consequently more accurate. As previously mentioned, the snow algorithm in GeoStudio is an important factor in the soil freezing

process. Any discrepancies between actual vs. modelled parameterization in terms of amount of snow or timing of snow consequentially influences the timing and rate of soil freezing. In addition, the thermal parameterizations of the soil material properties also impact how heat, and therefore freezing, is handled in the model. Using the coupled convective thermal model, the thermal properties can vary throughout the modelling domain with changes in volumetric water content. These thermal parameters were estimated in GeoStudio based on various soil properties. The interconnected nature of the coupled convective thermal model results in any over or underestimation being exacerbated in a following step in the model.

5.2.2 Thawing Period

Analogous to the freezing period, the thawing period modelled results yield discrepancies against the observed results with respect to timing, value ranges, and variability. At NF, soil temperature is simulated with reasonable accuracy for the trend and variability, with the expected dampening with depth (Figure 5.4a,b). However, the modelled soil temperature began thaw several weeks later than the measured data, likely due to the presence of snow remaining at the surface, but quickly surpassed the observed temperatures at all depths. Modelled unfrozen volumetric water content was less variable than observed data and thawed at a greater rate (Figure 5.4c,d). As with soil temperature, the timing and estimations of water content differ from observations, with the shallower points increasing later than observed and deeper points increasing earlier. In addition, there was limited drainage at the shallower soils later in the season as evident by modelled points hovering around the same value over time.

Downslope at RP, soil temperature during thaw was simulated moderately well whereas volumetric liquid water content was not accurately represented (Figure 5.5). Modelled soil temperature exhibited similar accuracy and deviations as the NF simulation, however, the timing

is slightly better represented. While the modelled unfrozen water content increased over the thawing period, therefore simulating appropriate thawing, the results lack variability and were highly over simplified compared to observed results. The ability of the model to capture the nature of volumetric liquid water content at RP was a result of the limited discretization of soil layers and large differences between the thermal and hydraulic properties of the layers. More specifically, only two layers were used to create the RP 1D model and a distinct change in saturated hydraulic conductivity impacted the water movement over freeze and thaw periods at this site.

For PLT, modelled soil thaw temperature data followed a close pattern to the observed data, including the dampening effect with depth and diurnal fluctuations (Figure 5.6a,b). However, similarly to the other modelled sites, the soil temperatures were comparatively greater and increased more rapidly. Model results for unfrozen water content captured the overall processes for thaw, but did not include several key elements. In particular, after the soils have thawed fully in the model, there was no indication of drainage later in the season that is present in the observed results (Figure 5.6c,d). While a bottom unit gradient boundary condition allows for drainage, this expected result was not seen in the PLT simulation. In addition, although GeoStudio incorporates ET through the selected upper land-climate interaction boundary condition, there appears to be limited drainage at the surface layers with the model underestimating any drainage. The model makes further underestimations with the observed water content peaking at a notably higher value in the shallower soils than the modelled results.

In GeoStudio, the onset of thaw happened more quickly and suddenly than in reality. The observed rate of thaw appears to be much less at both NF and RP, whereas PLT is more comparable as the measured data also exhibited a fairly rapid thaw. The timing of soil thaw in the model was controlled by the melting of snow at the surface. When the snow is fully melted at each site, a

sudden increase in temperature and volumetric liquid water content occurs. Discrepancies between the timing of thaw onset between modelled and observed data may be a direct result of the presence of snow on the surface. Snow depth used for model simulations was an average of the site transect and thereby did not directly reflect the occurrence of snow at the exact location for the observed data. Reducing conductivity in frozen soils in GeoStudio removes some fluctuation from the thawing period for unfrozen water content, suggesting that the rate of water movement alters the soil sensitivity to sudden surface changes and restricts how heat moves through the soil. Overall, soil temperatures were modelled more accurately than unfrozen water content during the thawing period. Thawing was slower than freezing and the models were less compatible during thaw for volumetric water content, but more so for soil temperature. Furthermore, GeoStudio failed to simulate the drainage patterns for soil moisture while using an appropriate drainage boundary condition. The position along the soil profile for the measured points as well as the layer discretization ultimately influences the soil moisture content and soil temperature results.

5.2.3 Model Sensitivity

The sensitivity of GeoStudio SEEP/W and TEMP/W freeze/thaw simulations to changing environmental conditions was tested for each site over the freezing period and thawing period. Temperature and precipitation data were adjusted to simulate warmer and colder conditions as well as wetter and drier seasons and tested on the model simulations from NF, which had the best results of the three sites (Table 5.1). Air temperature was decreased by 1°C to simulate a colder climate scenario, and increased by 0.5°C, 1°C, and 2°C, in the more likely future warming scenario in a changing climate. Total precipitation was increased by 25% and decreased by 25% as well several combinations of warmer and wetter (+2°C and +25%) and colder and drier (-1°C and -25%)

simulations. Through additional testing of each model, further conclusions were derived regarding GeoStudio model sensitivity.

Soil temperature and unfrozen water content were both sensitive to changes in air temperature, most importantly during times of freeze and thaw. As air temperature changed, the timing and extent of freezing and thawing was subsequently impacted. In a warmer climate, the average soil temperature increased along with the air temperature, with the most significant changes occurring with higher temperatures (Figure 5.7a-d). During the winter, colder soil temperatures did not migrate as far into the deeper soils, reducing the extent of freezing. As a result, soil thaw occurred earlier at deeper soils with increased air temperature leading to overall higher soil temperatures later in the season. Similarly, frozen water content was lessened with a warmer environment, particularly during winter (Figure 5.8a-d). In a colder environment, soil temperatures over the winter were notably colder and the timing of the thawing period was extended, particularly for deeper soils which remain frozen for an extended period of time (Figure 5.7e). In addition, the overall unfrozen water content decreased with a colder environment, especially in the shallower soils for the freezing period. Overall, shallower soils as well as soils near freeze or thaw boundaries appeared to be the most sensitive to climatic changes in the GeoStudio simulations.

Changes to precipitation also influenced the soil temperature and soil moisture regimes of the modelled simulations. However, compared to changes in air temperature, the impact appeared to be less pronounced. With an increase in precipitation, soil temperature was slightly warmer, most apparent in the shallowest soils during the winter months and the beginning on the thawing period (Figure 5.9b). Conversely, towards the end of the modelled period, soil temperature and the deeper soils were slightly cooler with increased precipitation than the original simulation. The unfrozen water content with this climatic change scenario increased during the freezing and thawing period

at soils near the surface (Figure 5.9e). With less precipitation, soil temperatures were overall somewhat cooler with the shallow soils during the winter months again experiencing the most change (Figure 5.9c). Surface soils in this simulation showed less unfrozen water content over the freezing and thawing period (Figure 5.9f). Overall, increases or decreases in precipitation impact both the modelled soil temperature and the unfrozen water content, however the model was less sensitive to these climatic changes.

By changing both air temperature and precipitation simultaneously, soil temperature and unfrozen water content experienced large changes over the entire simulation (Figure 5.10a-f). In a warmer and wetter climate scenario, both the overall soil temperature and unfrozen water content increase, the extent of freezing is reduced, and slight freeze/thaw timing shifts (Figure 5.9b,e). Conversely, a colder and drier scenario resulted in overall lower soil temperatures, less unfrozen water content, and more substantial freezing over the winter (Figure 5.9c,f). When the soils are drier, colder temperatures are able to propagate into the soil more rapidly and latent heat effects are less substantial. The dominance of latent heat also impacts the timing of freeze/thaw as soil freezing releases heat and soil thawing absorbs heat, meaning higher soil moisture content results in a larger zero-degree curtain. Furthermore, as previously mentioned, the timing of soil thaw was controlled by and sensitive to the surface conditions, particularly snow, however, with climatic changes, there was a slight timing shift for deeper soils. Adjusting additional model parameters such as the thermal and hydraulic properties of the soil also reveals model sensitivity to the coupled heat and water flow. When the hydraulic properties of the soil were adjusted, soil temperature was directly impacted. Considering soil temperature and unfrozen water content changes to climatic shifts, GeoStudio models are more sensitive to surface conditions affecting both coupled heat and water flow processes compared to independent changes of air temperature and precipitation.

Furthermore, the modelled results indicate that cold regions are susceptible to changes in the climate, most significantly impacting the timing of soil freeze/thaw as well as the extent of freezing.

5.3 Limitations and Recommendations in GeoStudio

Based on the ability to GeoStudio to simulate freeze/thaw processes and the model sensitivity, several limitations are recognized and recommendations provided for future studies. While GeoStudio provides a fairly straightforward user interface and allows for the simulation of complicated concurrent problems including heat and mass transfer, there are still challenges and limitations in the software. Some past limitations are remedied by the current updates of the GeoStudio software, including a combined multi-physics model which simplifies concurrent simulations, such as temperature and seepage. If there is inadequate or missing parameter data, both TEMP/W and SEEP/W have built in equations to estimate the required functions. However, while these approximations are useful when data is unavailable, the GeoStudio functions are not extensive and can be limited by the assumptions and applicability. In TEMP/W, material properties have several options for creating thermal functions depending on the material model. However, some of these functions have minimal customization or are estimated by only one soil property, thereby restricting control on how heat is handled in the model. This minimal customization particularly applies if attempting to include organic soils in a SEEP/W or TEMP/W simulation. Organic soil may be included through surface vegetation inputs or would need to be added similarly to mineral soils. The latter option becomes limited when using GeoStudio's function estimates which are based on mineral soils. Another limitation that still remains in the current version of GeoStudio is the minimal customization ability for results. Nevertheless, this is easily managed by exporting selected results and working with the data outside of GeoStudio.

For simulating freeze/thaw systems and frozen soils, the following recommendations are provided for future studies to improve the model outcome.

1. Fine layer discretization and detailed data on soil properties.
2. Accurate and thorough heat data for each material property.
3. Accurate and complete climate data, with particular emphasis on snow depth measurements.
4. Incorporation of organic soils in model simulations.

Overall, it is important when studying complex environments to attain as detailed data as possible to accurately discretize the model and drive the simulations. Finer layer discretization allows for each point modelled along a soil profile to more accurately reflect the simulated environment as transitions between material properties can create significant differences in how a soil freezes and thaws. When using GeoStudio, it is especially crucial for thermal functions and heat data as how the model handles heat notably influences the outcome of both soil temperature and soil moisture. This extends to all soil properties as heat and water are closely coupled and errors in one property will perpetuate throughout the model. Furthermore, shallower soils are highly sensitive to thermal and hydraulic boundary conditions, meaning emphasis on accurate and complete climate data is also key to correctly simulate freeze/thaw timing and reduce over and under estimations of soil temperature and unfrozen volumetric water content. In addition, as organic soils are important for storage and water flow, inclusion in simulations may be necessary for accurately representing soil freeze/thaw systems.

6. CHAPTER 6: Summary and Conclusions

As greater surface warming rates at high latitudes and altitudes make cold regions more susceptible to altered hydrological processes, investigations of frozen soils are important for understanding and forecasting changes of such environments. However, few hydrological models consider the complexity of frozen soils and there is limited research on soil freeze/thaw processes. This study analyzes soil freeze/thaw in WCRB from September 2015 to July 2016 through observed and modelled data. The objectives of this research are to assess the ability of the GeoStudio finite element modelling suite to simulate observed soil temperature and moisture data and to apply the models to evaluate the sensitivity of the environment to future climate change scenarios.

Based on the results of this study, the key findings and conclusions are:

1. Freezing in WCRB occurs first at the upper site, followed by the middle site, then the lower site with the shallower soils at each site have similar timing of freezing and the time differences are amplified with depth.
2. Observed thawing of soils in WCRB occurs less steadily than freezing and is considerably influenced by snowmelt and persistence of snow coverage. The timing of thawing is more comparable among sites for soils closer to the surface and diverge with depth.
3. GeoStudio freezes soils later than observed with wider ranges in values and greater rates of change. Deeper soils are modelled to greater accuracy over the freezing period than shallower soils, which has a larger margin of error and major lag.
4. The thawing period modelled results yield discrepancies against the observed results with respect to timing, value ranges, and variability, with the onset of thaw

happening more quickly and suddenly than in reality. The timing of thaw is particularly controlled by the melting of snow at the surface.

5. Soil temperature and unfrozen water content were both sensitive to changes in air temperature and slightly less sensitive to changes in precipitation.
6. GeoStudio models are more sensitive to surface conditions affecting both coupled heat and water flow processes compared to independent changes of air temperature and precipitation.

Results of both the observed and modelled data illustrate the dominance of snow in controlling freeze/thaw processes. Overall, GeoStudio can be a useful tool for simulating freeze/thaw systems in cold regions, with some limitations. Both SEEP/W and TEMP/W would benefit from complete climate driving data and detailed geometry information, particularly for finer discretization and accurate heat data (e.g. material properties), as well as incorporation of organic soils. The complex heat transfer and water movement processes that control infiltration in northern environments are a challenging and increasingly important area of research with the current predictions of future climate. This quantitative assessment of WCRB soils and their sensitivity to future climate warming provide some insight into utilizing GeoStudio for future studies. Although there were some timing and value discrepancies between the observed and modelled results, GeoStudio is one of the few hydrological models considering frozen soils and has potential to help elucidate soil freeze/thaw process as well as deliver valuable predictive simulations.

REFERENCES

ACIA, E. (2005). Arctic climate impact assessment. *Scientific Report*.

Andersland, O. B., & Ladanyi, B. (2013). *An introduction to frozen ground engineering*. Springer Science & Business Media.

Anderson, D. M., & Tice, A. R. (1972). Predicting unfrozen water contents in frozen soils from surface area measurements. *Highway research record*, (393).

Anderson, D. M., & Morgenstern, N. R. (1973, July). Physics, chemistry and mechanics of frozen ground: A review. In *Proceedings 2nd International Conference on Permafrost, Yakutsk, USSR*. (pp. 257-288).

Arnell, N. W. (1999). Climate change and global water resources. *Global environmental change*, *9*, S31-S49.

Bates, R. E., & Bilello, M. A. (1966). Defining the Cold Regions of the Northern Hemisphere (No. TR-178). Cold Regions Research and Engineering Lab Hanover NH.

Bayard, D., Stähli, M., Parriaux, A., & Flühler, H. (2005). The influence of seasonally frozen soil on the snowmelt runoff at two Alpine sites in southern Switzerland. *Journal of Hydrology*, *309*(1–4), 66–84. https://doi.org/10.1016/j.jhydrol.2004.11.012

Beierle, B. D., Lamoureux, S. F., Cockburn, J. M., & Spooner, I. (2002). A new method for visualizing sediment particle size distributions. *Journal of Paleolimnology*, *27*(2), 279-283.

Bense, V. F., Kooi, H., Ferguson, G., & Read, T. (2012). Permafrost degradation as a control on hydrogeological regime shifts in a warming climate. *Journal of Geophysical Research: Earth Surface*, *117*(F3).

Boike, J., Roth, K., & Overduin, P. P. (1998). Thermal and hydrologic dynamics of the active layer at a continuous permafrost site (Taymyr Peninsula, Siberia). *Water Resources Research*, *34*(3), 355-363.

Brown, R.J.E. (1977). Permafrost in Canada. Map compiled by R.J.E. Brown, lit Hydrological Atlas of Canada. Environment Canada. Ottawa

Brown, J., Ferrians Jr, O. J., Heginbottom, J. A., & Melnikov, E. S. (1997). *Circum-Arctic map of permafrost and ground-ice conditions* (p. 45). Reston: US Geological Survey.

Burt, T. P., & Williams, P. J. (1976). Hydraulic conductivity in frozen soils. *Earth Surface Processes*, *1*(4), 349-360.

Buttle, J. M., Allen, D. M., Caissie, D., Davison, B., Hayashi, M., Peters, D. L., ... & Whitfield, P. H. (2016). Flood processes in Canada: regional and special aspects. *Canadian Water Resources Journal/Revue canadienne des ressources hydriques*, *41*(1-2), 7-30.

Campbell Scientific – HydraProbe Steven's Water Soil Sensor Instruction Manual. (2017). CAMPBELL SCIENTIFIC (CANADA) CORP., 14532 131 Avenue NW, Edmonton, Alberta, Canada.

Carey, S. K., & Woo, M. K. (1999). Hydrology of two slopes in subarctic Yukon, Canada. *Hydrological Processes*, *13*(16 SPEC. ISS.), 2549–2562. https://doi.org/10.1002/(SICI)1099-1085(199911)13:16<2549::AID-HYP938>3.0.CO;2-H

Carey, S. K., & Woo, M. (2005). Freezing of Subarctic Hillslopes, Wolf Creek Basin, Yukon, Canada. *Arctic, Antarctic, and Alpine Research*, *37*(1), 1–10. https://doi.org/10.1657/1523-0430(2005)037[0001:FOSHWC]2.0.CO;2

Carlson, H. (1952). Calculation of depth of thaw in frozen ground. *Highway Research Board Special Report*, (2).

Chamberlain, E. J., & Gow, A. J. (1979). Effect of freezing and thawing on the permeability and structure of soils. *Developments in Geotechnical Engineering*, *26*(C), 73–92. https://doi.org/10.1016/B978-0-444-41782-4.50012-9

Cherkauer, K. a., & Lettenmaier, D. P. (1999). Hydrologic effects of frozen soils in the upper Mississippi River basin. *Journal of Geophysical Research*, *104*(D16), 19599. https://doi.org/10.1029/1999JD900337

de Vries, D. A. (1975). Heat transfer in soils, Heat and Mass Transfer in the Biosphere. *Advances in Thermal Engineerings*, *3*.

Dingman, S. L. (1975). *Hydrologic effects of frozen ground: Literature review and synthesis*. DUBOIS AND KING INC RANDOLPH VT.

Freeze, R. A., & Cherry, J. A. (1979). Groundwater. Englewood Cliffs, NJ: Prentice Hall.

GEOSLOPE International Ltd. (2017). Heat and mass transfer modeling with GeoStudio 2018 (Second Edition). Calgary, Alberta, Canada.

Gerdel, R. W. (1969). *Characteristics of the cold regions* (Vol. 1). Corps of Engineers, US Army, Cold Regions Research and Engineering Laboratory.

Goodrich, L. E. (1978). Efficient numerical technique for one-dimensional thermal problems with phase change. *International Journal of Heat and Mass Transfer*, *21*(5), 615-621.

Goodrich, L. E. (1982). The influence of snow cover on the ground thermal regime. *Canadian Geotechnical Journal*, *19*(4), 421–432. https://doi.org/10.1139/t82-047

Granger, R. J., Gray, D. M., & Dyck, G. E. (1984). Snowmelt infiltration to frozen Prairie soils. *Canadian Journal of Earth Sciences*, *21*(6), 669–677. https://doi.org/10.1139/e84-073

Granger, R. J. (1998). Partitioning of energy during the snow-free season at the Wolf Creek Research Basin. *Wolf Creek Research Basin: Hydrology, Ecology, Environment*, 33–44.

Gray, D. M., Landine, P. G., & Granger, R. J. (1985). Simulating infiltration into frozen prairie soils in streamflow models. *Canadian Journal of Earth Sciences*, *22*(3), 464-472.

Gray, D. M., Toth, B., Zhao, L., Pomeroy, J. W., & Granger, R. J. (2001). Estimating areal snowmelt infiltration into frozen soils. *Hydrological Processes*, *15*(16), 3095–3111. https://doi.org/10.1002/hyp.320

Grenier, C., Anbergen, H., Bense, V., Chanzy, Q., Coon, E., Collier, N., ... & Gonçalvès, J. (2018). Groundwater flow and heat transport for systems undergoing freeze-thaw: Intercomparison of numerical simulators for 2D test cases. *Advances in Water Resources*, *114*, 196-218.

Harder, P., Pomeroy, J. W., & Westbrook, C. J. (2015). Hydrological resilience of a Canadian Rockies headwaters basin subject to changing climate, extreme weather, and forest management. *Hydrological Processes*, *29*(18), 3905-3924.

Harlan, R. L. (1973). Analysis of coupled heat-fluid transport in partially frozen soil. *Water Resources Research*, *9*(5), 1314-1323.

Harris, S. A. (1988). Observations on the redistribution of moisture in the active layer and permafrost. In *Proceedings, Fifth International Conference on Permafrost* (Vol. 2, pp. 364-369). Trondheim, Norway: Tapir Publishers.

Hayashi, M., Van Der Kamp, G., & Schmidt, R. (2003). Focused infiltration of snowmelt water in partially frozen soil under small depressions. *Journal of Hydrology*, *270*, 214–229. https://doi.org/10.1016/S0022-1694(02)00287-1

Hayashi, M., Goeller, N., Quinton, W. L., & Wright, N. (2007). A simple heat-conduction method for simulating the frost-table depth in hydrological models. *Hydrological Processes: An International Journal*, *21*(19), 2610-2622.

Hayhoe, H. N. (1994). Field testing of simulated soil freezing and thawing by the SHAW model. *Canadian Agricultural Engineering*, *36*(4), 279–285.

Hedstrom, N. R., & Pomeroy, J. W. (1998). Measurements and modelling of snow interception in the boreal forest. *Hydrological Processes*, *12*(10-11), 1611-1625.

Hillel, D. (2004). *Introduction to environmental soil physics*. Elsevier.

Hinkel, K. M., Outcalt, S. I., & Nelson, F. E. (1990). Temperature variation and apparent thermal diffusivity in the refreezing active layer, Toolik Lake, Alaska. *Permafrost and Periglacial Processes*, *1*(3-4), 265-274.

Hinkel, K. M., & Outcalt, S. I. (1994). Identification of heat-transfer processes during soil cooling, freezing, and thaw in central alaska. *Permafrost and Periglacial Processes*, *5*(4), 217-235.

Hinzman, L. D., & Kane, D. L. (1992). Potential response of an Arctic watershed during a period of global warming. *Journal of Geophysical Research: Atmospheres*, *97*(D3), 2811-2820.

Hinzman, L. D., Goering, D. J., & Kane, D. L. (1998). A distributed thermal model for calculating soil temperature profiles and depth of thaw in permafrost regions. *Journal of Geophysical Research: Atmospheres*, *103*(D22), 28975-28991.

Hinzman, L. D., Deal, C. J., McGuire, A. D., Mernild, S. H., Polyakov, I. V., & Walsh, J. E. (2013). Trajectory of the Arctic as an integrated system. *Ecological Applications*, *23*(8), 1837-1868.

Hoekstra, P. (1966). Moisture movement in soils under temperature gradients with the cold-side temperature below freezing. *Water Resources Research*, *2*(2), 241-250.

Janowicz, J. R. (1986). Methodology for Estimating Design Peak Flows for Yukon Territory. In *Proceedings of the Symposium: Cold Regions Hydrology. University of Alaska-Fairbanks, Fairbanks, Alaska. American Water Resources Association, Bethesda Maryland. 1986. p 313-320.*

Janowicz, J. R. (1992). Wolf Creek Research Basin - Overview, 121–130.

Jeppson, R. W. (1974). Axisymmetric infiltration in soils, I. Numerical techniques for solution. *Journal of Hydrology*, *23*(1-2), 111-130.

Johansen, O. (1975). *Thermal conductivity of soils* (No. CRREL-TL-637). Cold Regions Research and Engineering Lab Hanover NH.

Johnsson, H., & Lundin, L. C. (1991). Surface runoff and soil water percolation as affected by snow and soil frost. *Journal of Hydrology*, *122*(1–4), 141–159. https://doi.org/10.1016/0022-1694(91)90177-J

Johnston, G. H. (1981). *Permafrost: engineering design and construction*. J. Wiley.

Jones, R. H., & Holden, J. T. (Eds.). (1989). *Ground Freezing 88*. AA Balkema.

Kane, D. L., Seifert, R. D., & Taylor, G. S. (1978). *Hydrologic properties of subarctic organic soils*. University of Alaska, Institute of Water Resources.

Kane, D. L. (1980). Snowmelt infiltration into seasonally frozen soils. *Cold Regions Science and Technology*, *3*(2–3), 153–161. https://doi.org/10.1016/0165-232X(80)90020-8

Kane, D. L., & Stein, J. (1983). Water movement into seasonally frozen soils. *Water Resources Research*, *19*(6), 1547-1557.

Kane, D. L., Hinkel, K. M., Goering, D. J., Hinzman, L. D., & Outcalt, S. I. (2001). Non-conductive heat transfer associated with frozen soils. *Global and Planetary Change*, *29*(3–4), 275–292. https://doi.org/10.1016/S0921-8181(01)00095-9

Kersten, M. S. (1959). Frost penetration: Relationship to air temperatures and other factors. *Highway Research Board Bulletin*, (225).

Klute, A. (Ed.), 1986. Methods of Soil Analysis: Part 1 - Physical and Mineralogical Methods (Second Edition). American Society of Agronomy, Inc., Madison, Wisconsin.

Koppen, W. (1936). Das geographische system der klimat. *Handbuch der klimatologie*, 46.

Kurylyk, B. L., MacQuarrie, K. T. B., & McKenzie, J. M. (2014). Climate change impacts on groundwater and soil temperatures in cold and temperate regions: Implications, mathematical theory, and emerging simulation tools. *Earth-Science Reviews*, *138*, 313–334.

Kurylyk, B. L., McKenzie, J. M., MacQuarrie, K. T. B., & Voss, C. I. (2014). Analytical solutions for benchmarking cold regions subsurface water flow and energy transport models: One-dimensional soil thaw with conduction and advection. *Advances in Water Resources*, *70*, 172–184. https://doi.org/10.1016/j.advwatres.2014.05.005

Kurylyk, B. L., & Watanabe, K. (2013). The mathematical representation of freezing and thawing processes in variably-saturated, non-deformable soils. *Advances in Water Resources*, *60*, 160–177. https://doi.org/10.1016/j.advwatres.2013.07.016

Lachenbruch, A. H. (1959). *Periodic Heat Flow in a Stratified Medium, with Application to Permafrost Problems* (No. 1083). US Government Printing Office.

Lawrence, D. M., Slater, A. G., Romanovsky, V. E., & Nicolsky, D. J. (2008). Sensitivity of a model projection of near-surface permafrost degradation to soil column depth and representation of soil organic matter. *Journal of Geophysical Research: Earth Surface*, *113*(F2).

Lewkowicz, A. G., & Ednie, M. (2004). Probability mapping of mountain permafrost using the BTS method, Wolf Creek, Yukon Territory, Canada. *Permafrost and Periglacial Processes*, *15*(1), 67-80.

Ling, F., & Zhang, T. (2004). A numerical model for surface energy balance and thermal regime of the active layer and permafrost containing unfrozen water. *Cold Regions Science and Technology*, *38*(1), 1-15.

Lunardini, V. J. (1981). *Heat transfer in cold climates*. Van Nostrand Reinhold Company.

Lunardini, V. J. (1991). *Heat transfer with freezing and thawing*(Vol. 65). Elsevier.

Lundberg, A., Ala-Aho, P., Eklo, O., Klöve, B., Kværner, J., & Stumpp, C. (2016). Snow and frost: Implications for spatiotemporal infiltration patterns - a review. *Hydrological Processes*, *30*(8), 1230–1250. https://doi.org/10.1002/hyp.10703

Luo, L., Robock, A., Vinnikov, K. Y., Schlosser, C. A., Slater, A. G., Boone, A., ... & Cox, P. (2003). Effects of frozen soil on soil temperature, spring infiltration, and runoff: Results from the PILPS 2 (d) experiment at Valdai, Russia. *Journal of Hydrometeorology*, *4*(2), 334-351.

Mackay, J. R. (1983). Downward water movement into frozen ground, western arctic coast, Canada. *Canadian Journal of Earth Sciences*, *20*(1), 120-134.

Marsh, P. (1999). Snowcover formation and melt: recent advances and future prospects. *Hydrological Processes*, *13*(14-15), 2117-2134.

Marsh, P., Endrizzi, S., Derksen, C., Russell, M., Onclin, C., Wilson, H., ... & Marsh, C. (2010, December). Factors controlling the spatial variability in end of winter snowcover and spring melt at an arctic tundra site.

McBean, G., Alekseev, G., Chen, D., Foerland, E., Fyfe, J., Groisman, P. Y., ... & Whitfield, P. H. (2005). Chapter 2: Arctic Climate: past and present. *Arctic Climate Impact Assessment.[np]*.

McGaw, R. W., Outcalt, S. I., & Ng, E. (1978, July). Thermal properties of wet tundra soils at Barrow, Alaska. In *Proceedings of 3rd International Conference on Permafrost*(Vol. 1, pp. 47-53).

McKenzie, J. M., & Voss, C. I. (2013). Permafrost thaw in a nested groundwater-flow system. *Hydrogeology Journal*, *21*(1), 299-316.

McNamara, J. P., Kane, D. L., & Hinzman, L. D. (1998). An analysis of streamflow hydrology in the Kuparuk River Basin, Arctic Alaska: a nested watershed approach. *Journal of Hydrology*, *206*(1-2), 39-57.

Metcalfe, R. A., & Buttle, J. M. (1999). Semi-distributed water balance dynamics in a small boreal forest basin. *Journal of Hydrology*, *226*(1), 66-87.

METER KSAT-Operation Manual. (2017). METER Group AG, Mettlacher Staße 8, 81379 Munich, Germany.

Middelkoop, H., Daamen, K., Gellens, D., Grabs, W., Kwadijk, J. C., Lang, H., ... & Wilke, K. (2001). Impact of climate change on hydrological regimes and water resources management in the Rhine basin. *Climatic change*, *49*(1-2), 105-128.

Mikkola, M., & Hartikainen, J. (2001). Mathematical model of soil freezing and its numerical implementation. *International Journal for Numerical Methods in Engineering*, *52*(5-6), 543-557.

Mortsch, L., Cohen, S., & Koshida, G. (2015). Climate and water availability indicators in Canada: Challenges and a way forward. Part II–Historic trends. *Canadian Water Resources Journal/Revue canadienne des ressources hydriques*, *40*(2), 146-159.

Nakano, Y., & Brown, J. (1972). Mathematical modeling and validation of the thermal regimes in tundra soils, Barrow, Alaska. *Arctic and Alpine Research*, *4*(1), 19-38.

Newman, G. P., & Wilson, G. W. (1997). Heat and mass transfer in unsaturated soils during freezing. *Canadian Geotechnical Journal*, *34*(1), 63–70. https://doi.org/10.1139/cgj-34-1-63

Nicholson, F. H., & Granberg, H. B. (1973, July). Permafrost and snowcover relationships near Schefferville. In *Permafrost: North American Contribution [to the] Second International Conference, Natl. Acad. Press, Washington, D. C* (pp. 151-158).

Nixon, J. F. (1975). The role of convective heat transport in the thawing of frozen soils. *Canadian Geotechnical Journal*, *12*(3), 425-429.

Perfect, E., & Williams, P. J. (1980). Thermally induced water migration in frozen soils. *Cold Regions Science and Technology*, *3*(2-3), 101-109.

Pomeroy, J. W., Gray, D. M., Brown, T., Hedstrom, N. R., Quinton, W. L., Granger, R. J., & Carey, S. K. (2007). The cold regions hydrological model: a platform for basing process representation and model structure on physical evidence. *Hydrological Processes: An International Journal*, *21*(19), 2650-2667.

Quinton, W. L., Shirazi, T., Carey, S. K., & Pomeroy, J. W. (2005). Soil water storage and active-layer development in a sub-alpine Tundra hillslope, southern Yukon Territory, Canada. *Permafrost and Periglacial Processes*, *16*(4), 369–382.

Quinton, W. L., & Baltzer, J. L. (2013). The active-layer hydrology of a peat plateau with thawing permafrost (Scotty Creek, Canada). *Hydrogeology Journal*, *21*(1), 201-220.

Rasouli, K., Pomeroy, J. W., Janowicz, J. R., Williams, T. J., & Carey, S. K. (2019). A long-term hydrometeorological dataset (1993–2014) of a northern mountain basin: Wolf Creek Research Basin, Yukon Territory, Canada. *Earth System Science Data*, *11*(1), 89-100.

Riseborough, D., Shiklomanov, N., Etzelmüller, B., Gruber, S., & Marchenko, S. (2008). Recent advances in permafrost modelling. *Permafrost and Periglacial Processes*, *19*(2), 137-156.

Romanovsky, V. E., Osterkamp, T. E., & Duxbury, N. S. (1997). An evaluation of three numerical models used in simulations of the active layer and permafrost temperature regimes. *Cold Regions Science and Technology*, *26*(3), 195-203.

Rostad. H.P.W., L.M. Kozak and D.F. Acton. (1977). Soil Survey and Land Evaluation of the Yukon Territory. Saskatchewan Institute of Pedology. Publication 5174. 495pp.

Rühaak, W., Anbergen, H., Grenier, C., McKenzie, J., Kurylyk, B. L., Molson, J., … Sass, I. (2015). Benchmarking Numerical Freeze/Thaw Models. *Energy Procedia*, *76*, 301–310. https://doi.org/10.1016/j.egypro.2015.07.866

Scherler, M., Hauck, C., Hoelzle, M., Stähli, M., & Völksch, I. (2010). Meltwater infiltration into the frozen active layer at an alpine permafrost site. *Permafrost and Periglacial Processes*, *21*(4), 325–334. https://doi.org/10.1002/ppp.694

Spaans, E. J. A., & Baker, J. M. (1996). The soil freezing characteristic: Its measurement and similarity to the soil moisture characteristic. *Soil Science Society of America Journal*. https://doi.org/10.2136/sssaj1996.03615995006000010005x

Stadler, D., & Aeby, P. (2000). Dye tracing and image analysis for quantifying water infiltration into frozen soils.

Stähli, M., Jansson, P. E., & Lundin, L. C. (1996). Preferential water flow in a frozen soil—a two-domain model approach. *Hydrological processes*, *10*(10), 1305-1316.

Stähli, M., Jansson, P. E., & Lundin, L. C. (1999). Soil moisture redistribution and infiltration in frozen sandy soils. *Water Resources Research*, *35*(1), 95–103. https://doi.org/10.1029/1998WR900045

Stähli, M., Bayard, D., Wydler, H., & Flühler, H. (2004). Snowmelt Infiltration into Alpine Soils Visualized by Dye Tracer Technique. *Arctic, Antarctic, and Alpine Research*, *36*(1), 128–135. https://doi.org/10.1657/1523-0430(2004)036[0128:SIIASV]2.0.CO;2

Taylor, S., & Luthin, N. (1978). A model for coupled heat and moisture transfer during soil freezing, *16*(2), 1978–1979.

Thorn, C. E., Darmody, R. G., Allen, C. E., & Dixon, J. C. (2002). Near-surface ground temperature regime variability in selected microenvironments, Kärkevagge, Swedish Lapland. *Geografiska Annaler: Series A, Physical Geography*, *84*(3–4), 289–300. https://doi.org/10.1111/j.0435-3676.2002.00183.x

UMS HYPROP-User Manual. (2015). UMS GmBH, Gmun- der Str. 37, 81379 Munchen, Germany.

Van Genuchten, M. T. (1980). A closed-form equation for predicting the hydraulic conductivity of unsaturated soils 1. *Soil science society of America journal*, *44*(5), 892-898.

Viviroli, D., & Weingartner, R. (2004). The hydrological significance of mountains: from regional to global scale. *Hydrology and Earth System Sciences Discussions*, *8*(6), 1017-1030.

Viviroli, D., Archer, D. R., Buytaert, W., Fowler, H. J., Greenwood, G., Hamlet, A. F., ... & Lorentz, S. (2011). Climate change and mountain water resources: overview and recommendations for research, management and policy. *Hydrology and Earth System Sciences*, *15*(2), 471-504.

Voss, C. I., & Provost, A. M. (1984). Sutra. *US Geological Survey Water Resources Investigation Reports*, 84-4369.

Walker, D. A., Halfpenny, J. C., Walker, M. D., & Wessman, C. A. (1993). Long-term studies of snow-vegetation interactions. *BioScience*, *43*(5), 287-301.

Walvoord, M. A., Voss, C. I., & Wellman, T. P. (2012). Influence of permafrost distribution on groundwater flow in the context of climate-driven permafrost thaw: Example from Yukon Flats Basin, Alaska, United States. *Water Resources Research*, *48*(7).

Walvoord, M. A., & Kurylyk, B. L. (2016). Hydrologic Impacts of Thawing Permafrost—A Review. *Vadose Zone Journal*, *15*(6), 0. https://doi.org/10.2136/vzj2016.01.0010

Wang, C., Lai, Y., & Zhang, M. (2017). Estimating soil freezing characteristic curve based on pore-size distribution. *Applied Thermal Engineering*, *124*, 1049–1060. https://doi.org/10.1016/j.applthermaleng.2017.06.006

Watanabe, K., & Mizoguchi, M. (2002). Amount of unfrozen water in frozen porous media saturated with solution. *Cold Regions Science and Technology*, *34*(2), 103-110.

Watanabe, K., & Osada, Y. (2016). Comparison of Hydraulic Conductivity in Frozen Saturated and Unfrozen Unsaturated Soils. *Vadose Zone Journal*, *15*(5), 0. https://doi.org/10.2136/vzj2015.11.0154

Williams, J. R., & Van Everdingen, R. O. (1973, July). Groundwater investigations in permafrost regions of North America: a review. In *Permafrost: North American Contribution to the Second International Conference* (pp. 435-446). Washington: National Academy of Sciences.

Wilson, C. V. (1967). *Climatology of the cold regions*. US Army Corps of Engineers, Cold Regions Research and Engineering Laboratory.

Woo, M. K. (1986). Permafrost hydrology in North America. *Atmosphere-Ocean*, *24*(3), 201-234.

Woo, M. (1997). A Guide for Ground Based Measurement of the Arctic Snow Cover, (December).

Woo, M. K., Marsh, P., & Pomeroy, J. W. (2000). Snow, frozen soils and permafrost hydrology in Canada, 1995-1998. *Hydrological Processes*, *14*(9), 1591–1611.

Woo, M. K., Arain, M. A., Mollinga, M., & Yi, S. (2004). A two-directional freeze and thaw algorithm for hydrologic and land surface modelling. *Geophysical Research Letters*, *31*(12).

Woo, M. K. (2012). *Permafrost hydrology*. Springer Science & Business Media.

Zhang, T., & Osterkamp, T. E. (1995). Considerations in determining thermal diffusivity from temperature time series using finite difference methods. *Cold Regions Science and Technology*, *23*(4), 333-341.

Zhang, T., & Stamnes, K. (1998). Impact of climatic factors on the active layer and permafrost at Barrow, Alaska. *Permafrost and Periglacial Processes*, *9*(3), 229-246.

Zhang, Z., Kane, D. L., & Hinzman, L. D. (2000). Development and application of a spatial-distributed Arctic hydrological and thermal process model. *Hydrol. Process*, *14*, 1591-1611.

Zhang, Y., Carey, S. K., & Quinton, W. L. (2008). Evaluation of the algorithms and parameterizations for ground thawing and freezing simulation in permafrost regions. *Journal of Geophysical Research Atmospheres*, *113*(17), 1–17. https://doi.org/10.1029/2007JD009343

Zhang, Y., Carey, S. K., Quinton, W. L., Janowicz, J. R., Pomeroy, J. W., & Flerchinger, G. N. (2010). Comparison of algorithms and parameterisations for infiltration into organic-covered permafrost soils. *Hydrology and Earth System Sciences*, *14*(5), 729–750. https://doi.org/10.5194/hess-14-729-2010

Zhang, M., Wen, Z., Xue, K., Chen, L., & Li, D. (2016). A coupled model for liquid water, water vapor and heat transport of saturated–unsaturated soil in cold regions: model formulation and verification. *Environmental Earth Sciences*, *75*(8), 1–19. https://doi.org/10.1007/s12665-016-5499-3

Zhao, L., & Gray, D. (1997). A parametric expression for estimating infiltration into frozen soils. *Hydrological Processes*, *11*, 1761–1775. https://doi.org/10.1002/(SICI)1099-1085(19971030)11:13<1761::AID-HYP604>3.0.CO;2-O

Zhao, L., & Gray, D. M. (1999). Estimating snowmelt infiltration into frozen soils, *1842*(May 1998), 1827–1842.

Zhao, Y., Si, B., He, H., Xu, J., Peth, S., & Horn, R. (2016). Modeling of Coupled Water and Heat Transfer in Freezing and Thawing Soils, Inner Mongolia. *Water*, *8*(10), 424. https://doi.org/10.3390/w8100424

TABLES

Table 3.1: Summary of soil properties for NF, PLT, and RP at respective depths.

Site	Depth	Bulk Density (g/cm3)	Porosity	%>2mm	%<2mm				Soil Texture
					Total	%Sand	%Silt	%Clay	
NF_1	6-11	0.82	0.69	17.1	82.9	31.8	55.2	13.0	Silt loam
NF_2	11-16	1.56	0.41	11.4	88.6	38.5	49.6	11.9	Loam
NF_3	41-46	1.9	0.28	72.0	28.0	54.9	31.8	13.3	Sandy loam
NF_4	66-71	-	-	53.4	46.6	63.1	27.2	9.7	Sandy loam
NF_5	86-91	-	-	43.3	56.7	69.5	19.8	10.7	Sandy loam
PLT_1	8-13	1.63	0.38	31.3	68.7	73.4	19.9	6.7	Sandy loam
PLT_2	24-30	1.7	0.36	36.0	64.0	64.7	28.3	7.0	Sandy loam
PLT_3	47-52	-	-	54.0	46.0	78.0	16.0	6.0	Loamy fine sand
PLT_4	73-76	-	-	57.2	42.8	87.3	10.2	2.5	Fine sand
RP_1	21-26	1.3	0.51	30.2	69.8	82.0	13.7	4.3	Loamy fine sand
RP_2	31-41	1.98	0.25	1.7	98.3	69.6	23.8	6.6	Sandy loam
RP_3	51-61	-	-	67.6	32.4	35.9	48.6	15.5	Loam

Table 3.2: Saturated hydraulic conductivity for each site measured using KSAT and HYPROP devices.

Site	Depth	KSAT		HYPROP	
		(cm/d)	(m/s)	(cm/d)	(m/s)
NF_1	6-11	3470.00	4.04×10^{-4}	30.60	3.54×10^{-6}
NF_2	11-16	10838.33	1.26 x 10-3	117.60	1.36×10^{-5}
NF_3	41-46	17.00	1.95 x 10-6	47.80	5.53×10^{-6}
PLT_1	8-13	49.00	5.72×10^{-6}	14.30	1.66×10^{-6}
PLT_2	24-30	44.67	5.18×10^{-6}	17.90	2.07×10^{-6}
RP_1	21-26	88.75	1.04×10^{-5}	14.40	1.67×10^{-6}
RP_2	31-41	2.33	2.93×10^{-7}	0.0708	8.19×10^{-9}

Table 3.3: Instrumentation specifications and details at PLT, NF and RP for data sampling in 2015-2016.

Site	Instrument	Manufacturer	Data Output	Depth/Height
PLT	CR3000 Datalogger	Campbell Scientific		
	LI-7500A	LI-COR	Eddy stuff	340 – 40 cm
	R3-50 3D Sonic Anemometer	Gill Instruments	Wind, eddy stuff	340 cm
	FW3 Type E Fine-Wire Thermocouple	Campbell Scientific	Air temperature	340 – 23 cm
	HC2S3	Rotronic (distributed by Campbell Scientific)	Air temperature, humidity	198 cm
	05103 Wind Monitor	R.M. Young (distributed by Campbell Scientific)	Wind speed, wind direction	206 cm
	CNR4 Net Radiometer	Kipp & Zonen (distributed by Campbell Scientific)	Shortwave, longwave, net radiation	240 cm
	SR50A snow depth sensor	Campbell Scientific	Snow depth	161 cm
	HydraProbe	Stevens	Soil temperature, soil moisture, soil conductivity	5, 15, 30 cm
NF	CR1000 Datalogger HydraProbe	Campbell Scientific Stevens	Soil temperature, soil moisture, soil conductivity	5, 15, 30, 45, 60 cm
RP	CR1000 Datalogger HydraProbe	Campbell Scientific Stevens	Soil temperature, soil moisture, soil conductivity	5, 15, 30, 45, 60 cm

Table 3.4: Summary of van Genuchten modelling parameters from HYPROP FIT.

Site	Depth	alpha (1/cm)	n	Res wc (cm3/cm3)	Sat wc (cm3/cm3)	Initial wc (Vol%)
NF_R1	6-11	0.0371	1.353	0	0.579	60.2
NF_R2	11-16	0.1286	1.635	0.096	0.321	32.0
NF_R3	41-46	0.0374	1.241	0.053	0.282	28.2
PLT_R1	8-13	0.0431	1.376	0.084	0.34	34.2
PLT_R2	24-30	0.0217	1.678	0.111	0.296	30.8
RP_R1	21-26	0.00648	2.748	0.101	0.458	47.0
RP_R2	31-41	0.00001	8.602	0.087	0.149	29.9

Table 4.1: Monthly climatic averages in Whitehorse for air temperature and total precipitation for 2015 and 2016 reported by Environment Canada.

Month	Air Temperature (°C)			Precipitation (mm)		
	2015	2016	CN	2015	2016	CN
January	-11.9	-8.7	-15.2 ± 6.5	26.7	25.1	17.8
February	-12.4	-5.7	-12.7 ± 4.7	3.4	33.7	11.8
March	-3.7	-1.7	-6.3 ± 3.5	11.9	23.1	10.3
April	2.9	5.1	1.0 ± 2.3	2.9	29.7	7.0
May	11.8	9.9	7.3 ± 1.5	5.1	43.6	16.3
June	13.8	14.0	12.3 ± 1.3	16.0	46.5	32.4
July	14.5	15.6	14.3 ± 0.9	35.2	22.4	38.1
August	12.1	14.4	12.6 ± 1.4	64.6	31.6	35.8
September	6.9	8.4	7.2 ± 1.6	21.1	27.5	33.3
October	2.9	-1.5	0.5 ± 1.8	18.7	10.9	23.2
November	-7.3	-5.2	-9.4 ± 4.8	34.0	13.7	20.1
December	-12.6	-16.1	-12.5 ± 4.7	12.9	10.0	16.3

Table 5.1: Summary of model sensitivity tests for changing climate scenarios.

Simulation	Climate Scenario (From Initial Model)	Parameter Adjustment	
		Air Temperature (°C)	Total Precipitation (%)
Soil temperature, unfrozen water content	Warmer	+0.5	-
	Warmer	+1	-
	Warmer	+2	-
	Colder	-1	-
	Wetter	-	+25
	Drier	-	-25
	Warmer, wetter	+2	+25
	Colder, drier	-1	-25

FIGURES

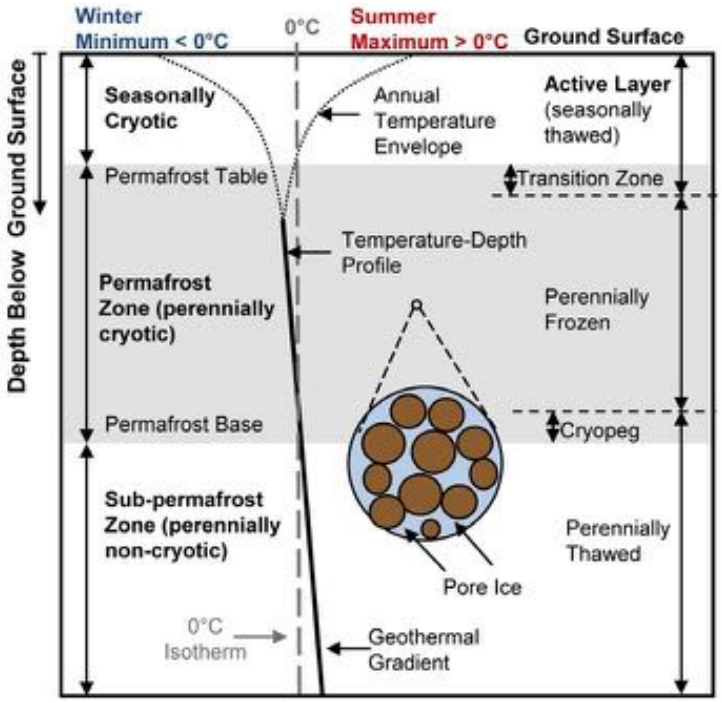

Figure 2.1: Representation of the ground temperature profile variation relative to depth of permafrost with associated permafrost descriptors (Walvoord and Kurylyk, 2016).

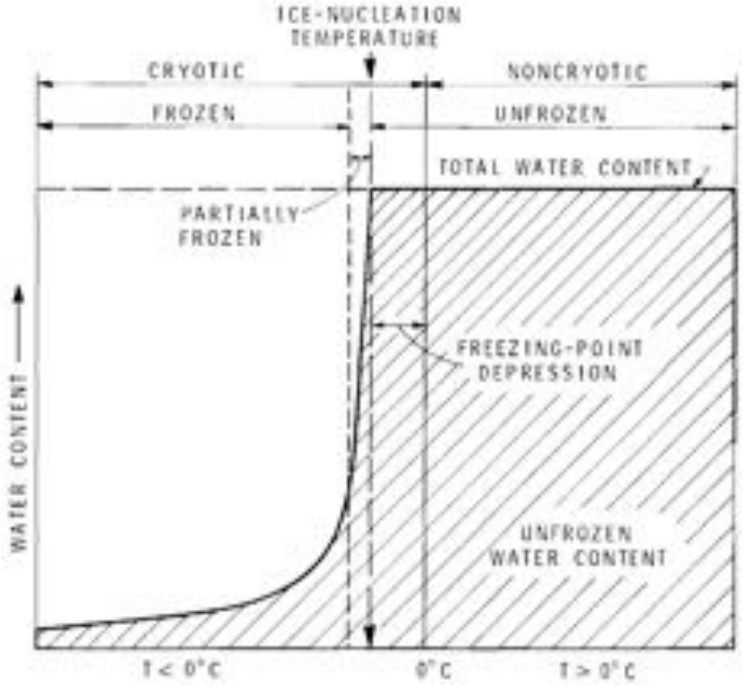

Figure 2.2: The relationship of terms to describe the state of water relative to ground temperature.

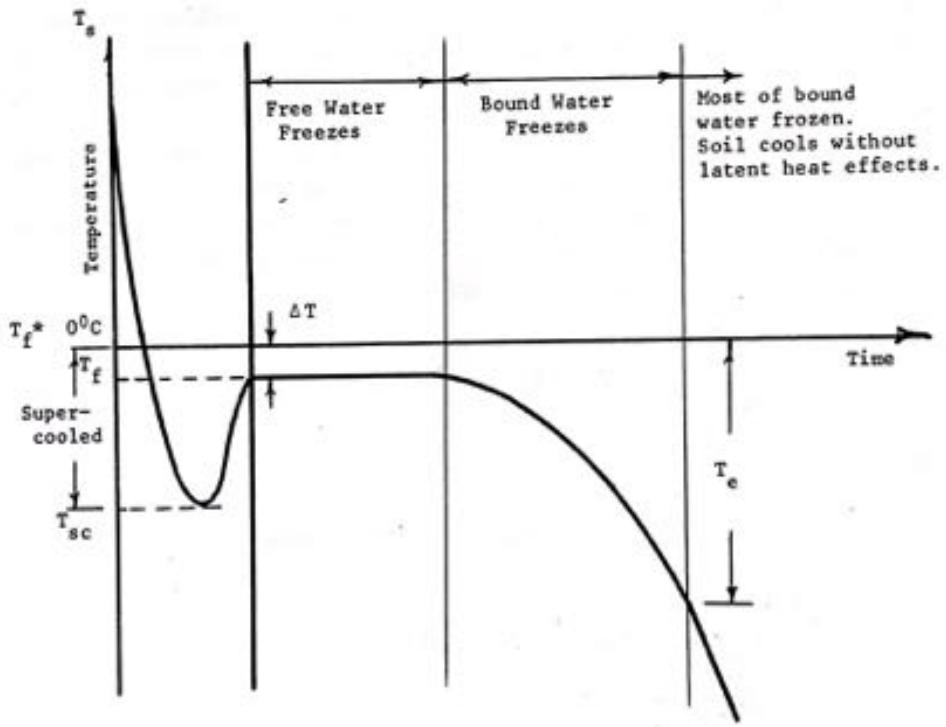

Figure 2.3: Typical soil water freezing curve (Lunardini, 1981).

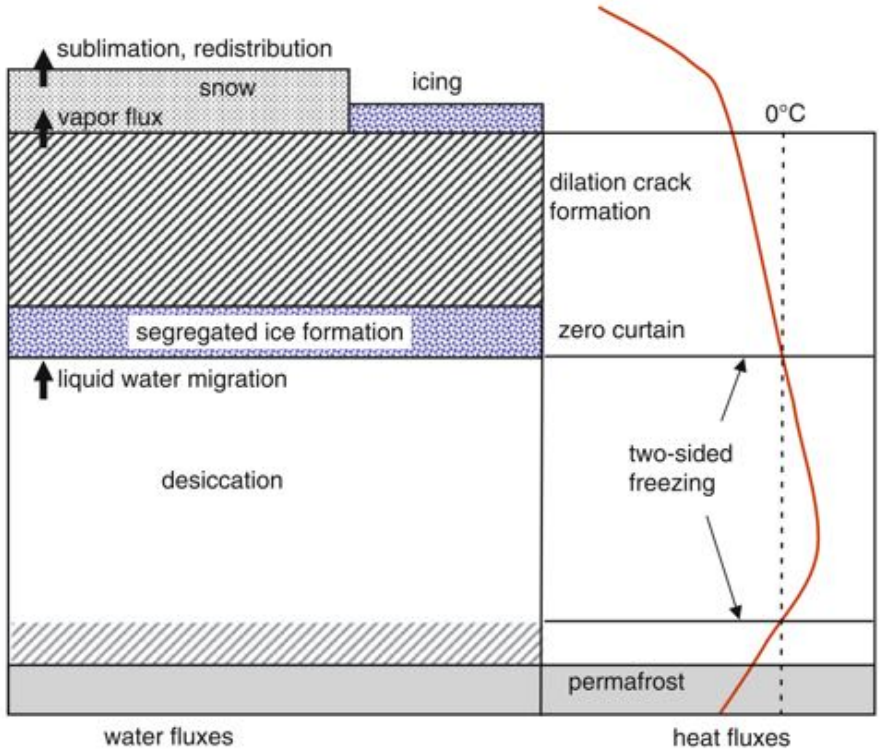

Figure 2.4: Thermal and hydrological conditions during freeze-back in the active layer/seasonally frozen soils (Woo, 2012).

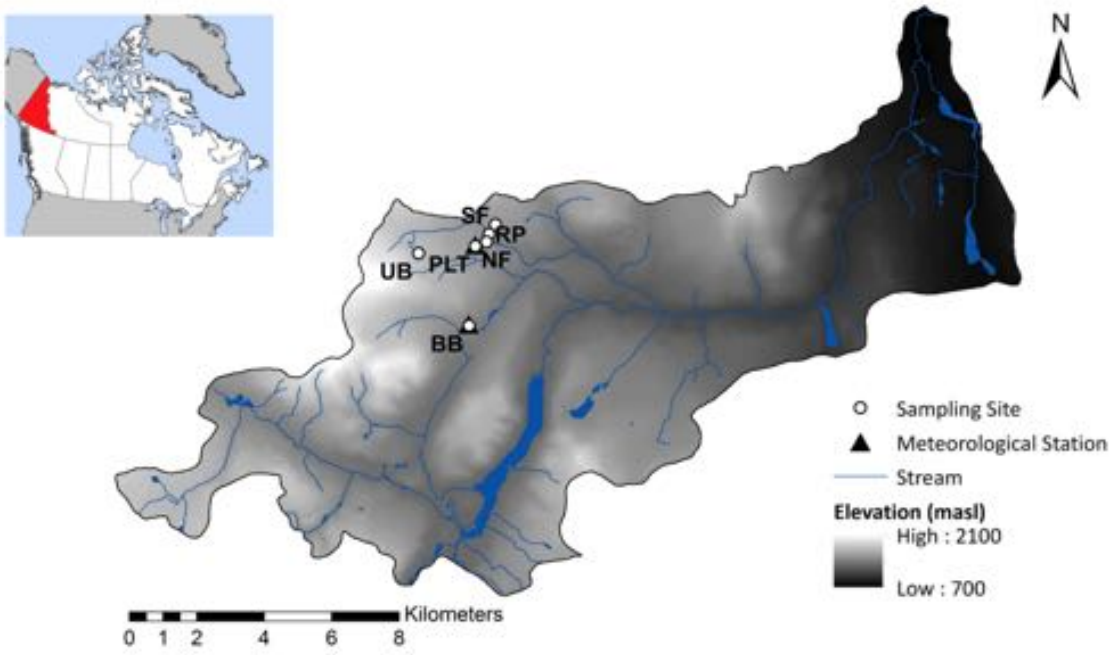

Figure 3.1: Map of research sites in Wolf Creek Research Basin.

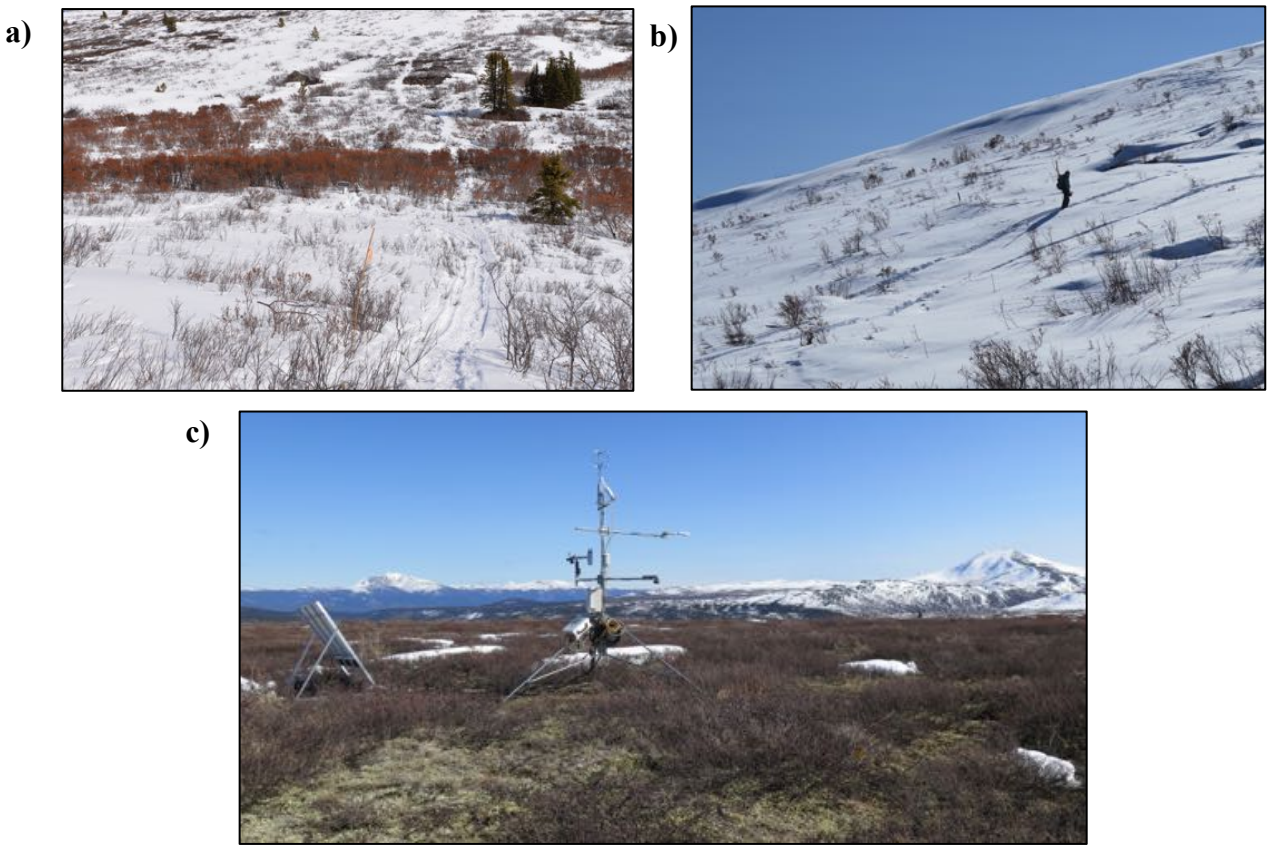

Figure 3.2: Study sites in WCRB at a) RP, b) NF, and c) PLT.

Figure 3.3a-c: Examples of frozen soils with ice impeding pore space at the sampled sites.

Figure 3.4: Example of soil pit for qualitative and quantitative analysis with surface organic layer.

Figure 3.5: UMS HYPROP 250 mL soil ring sample in field.

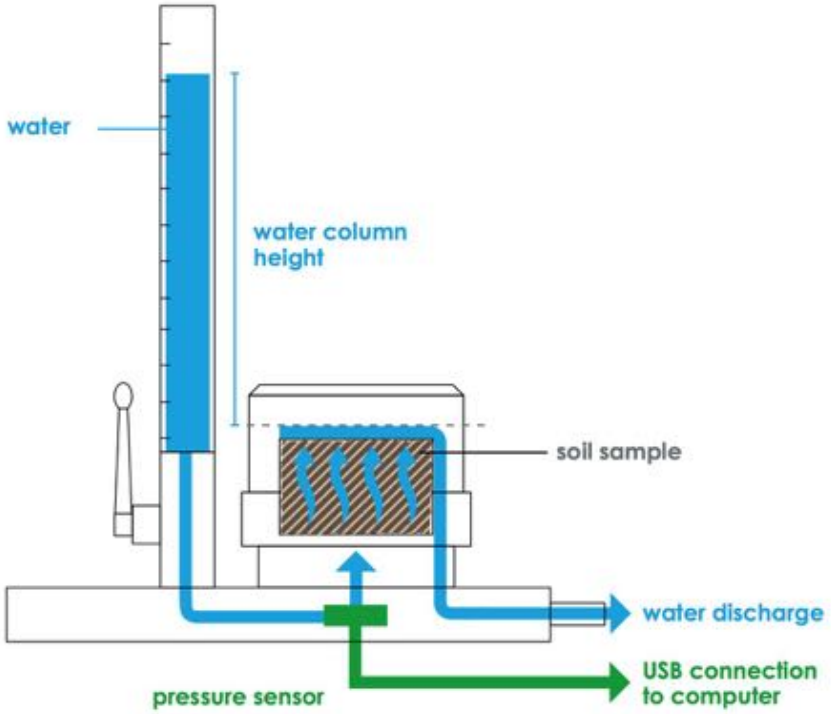

Figure 3.6: Summary of KSAT set up and methodology (METER, 2017).

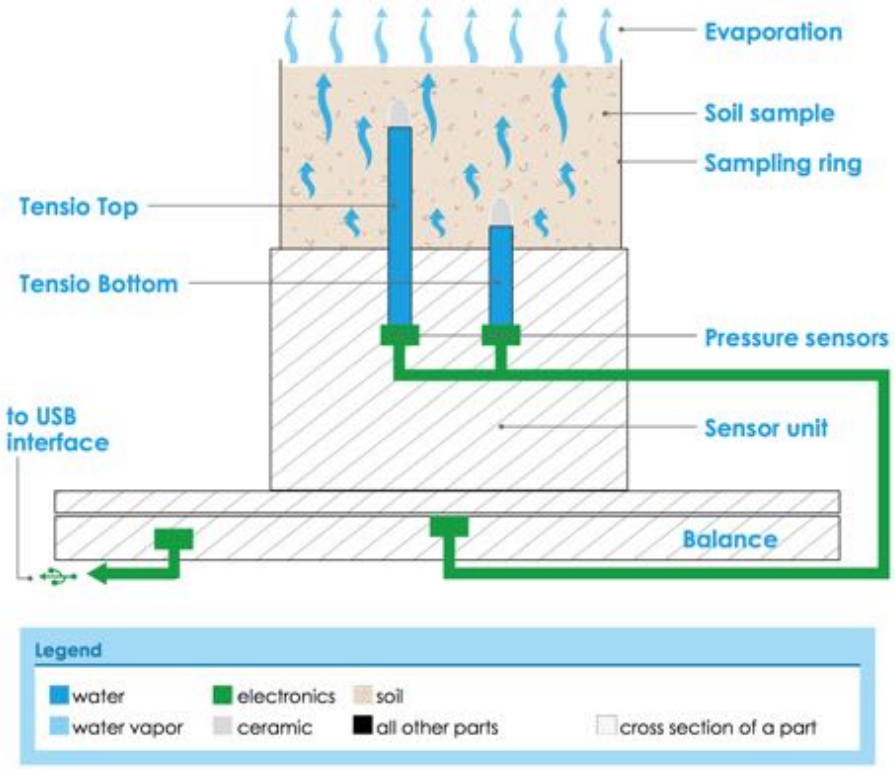

Figure 3.7: Summary of HYPROP set up and methodology (UMS, 2015).

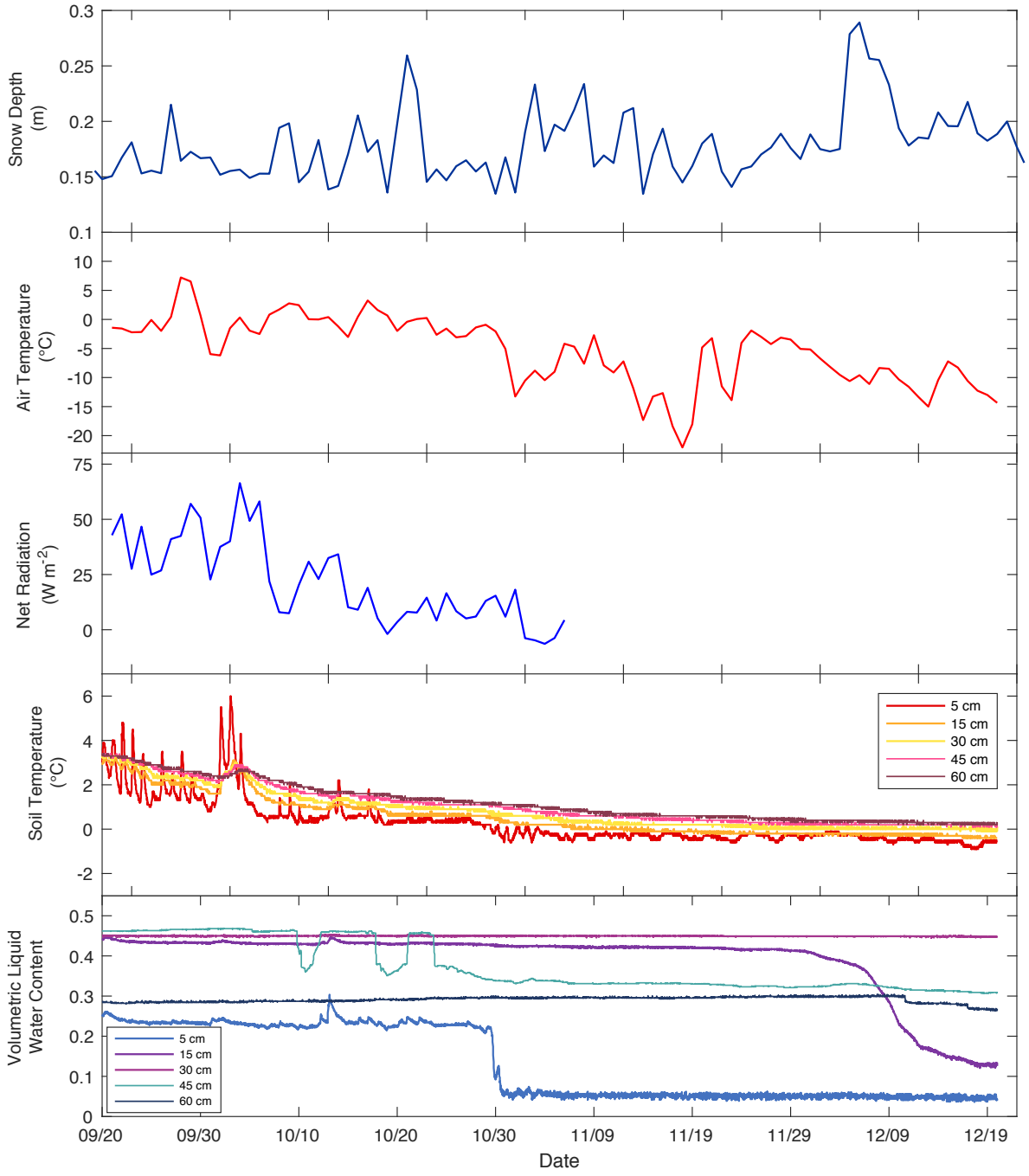

Figure 4.1: Climate data with soil temperature and volumetric liquid water content at RP during the freezing period.

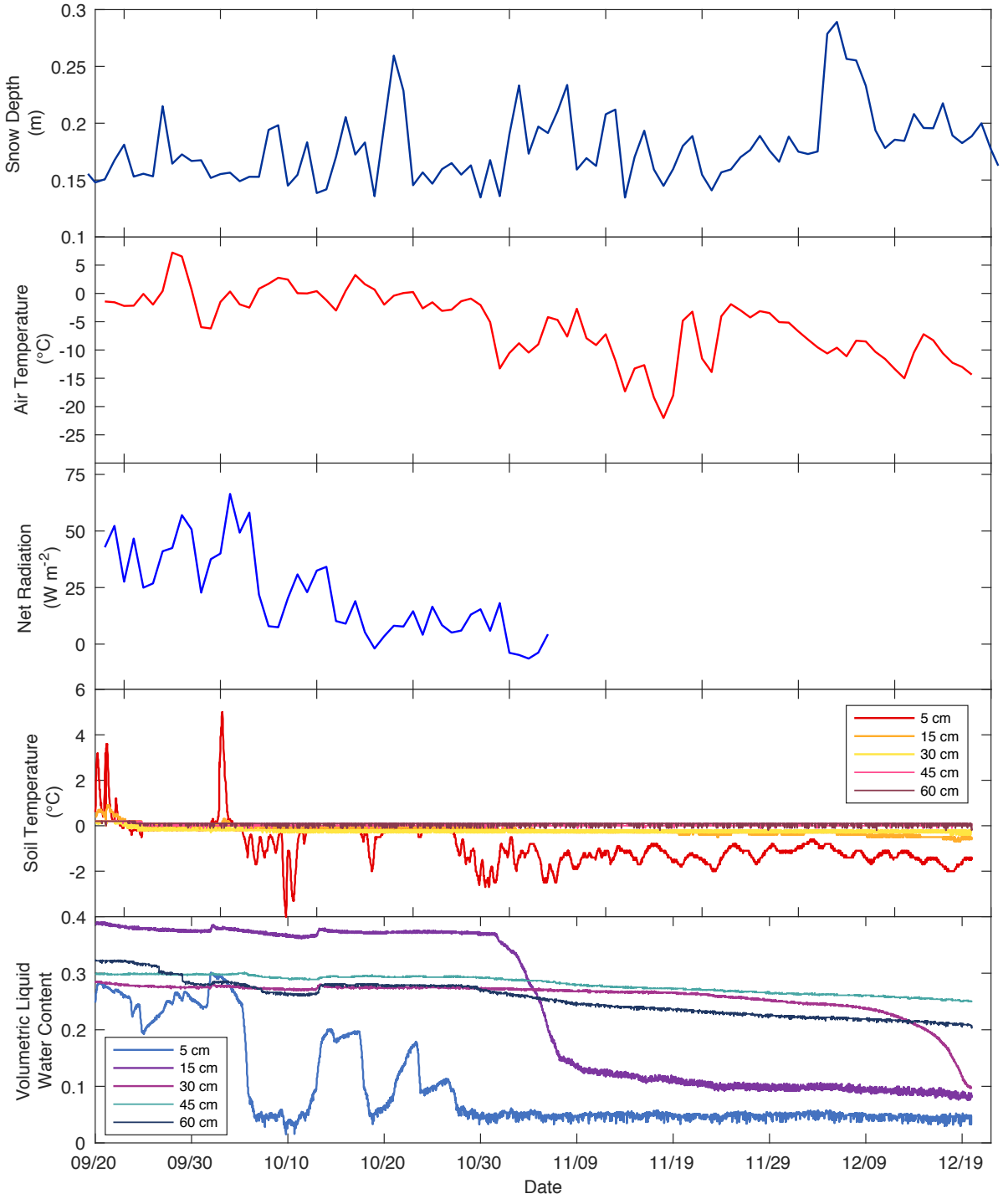

Figure 4.2: Climate data with soil temperature and volumetric liquid water content at NF during the freezing period.

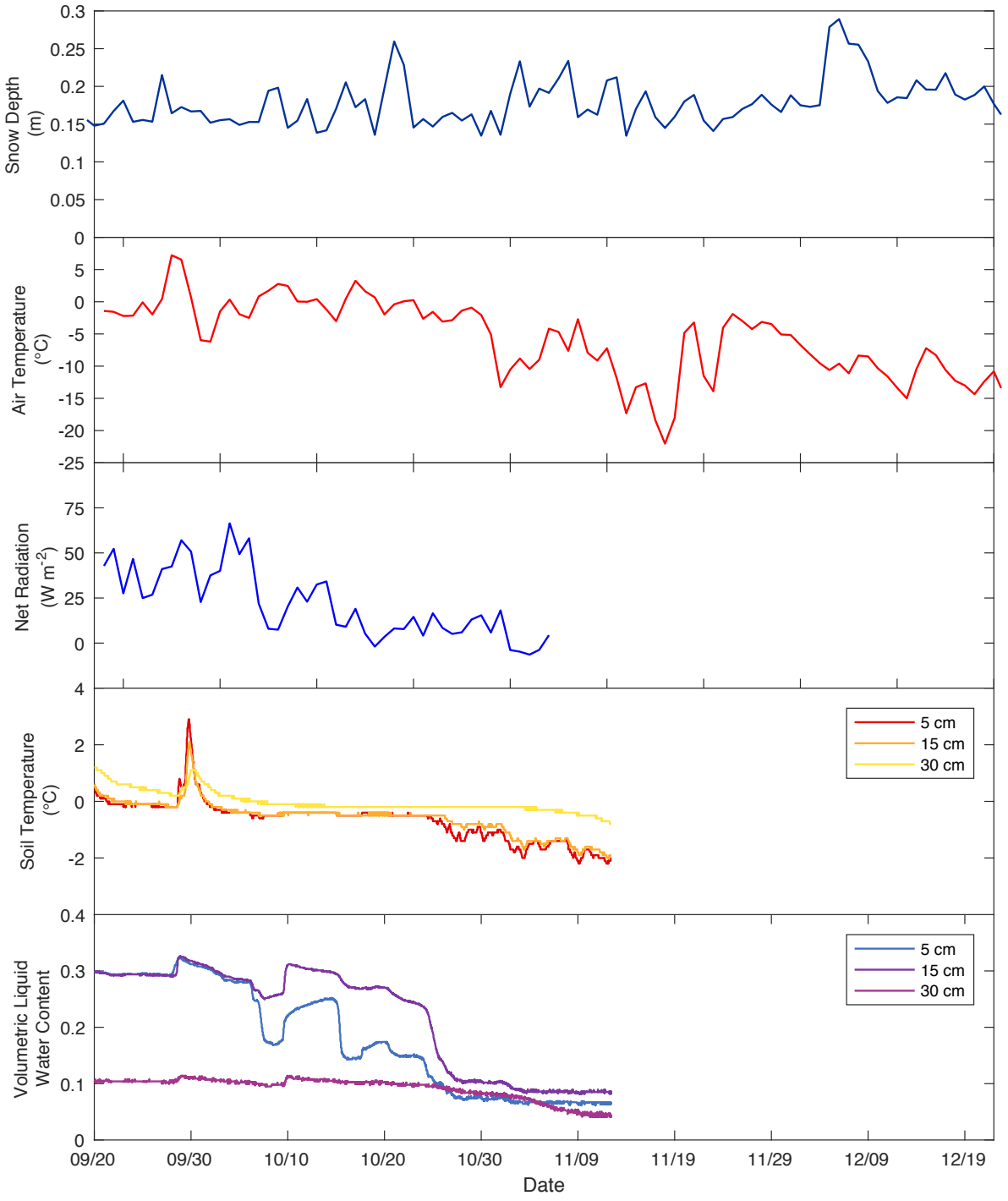

Figure 4.3: Climate data with soil temperature and volumetric liquid water content at PLT during the freezing period.

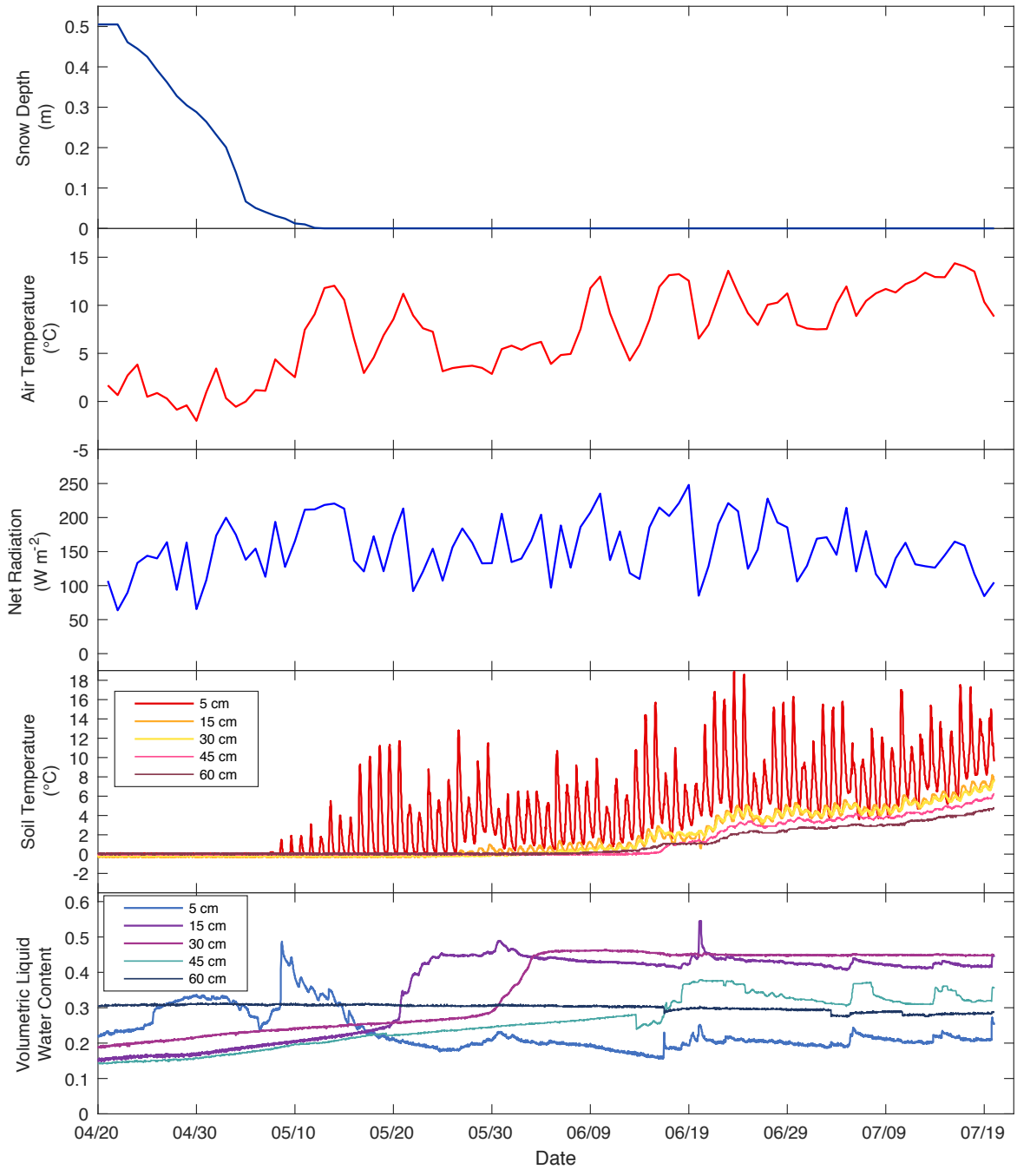

Figure 4.4: Climate data with soil temperature and volumetric liquid water content at RP during the thawing period.

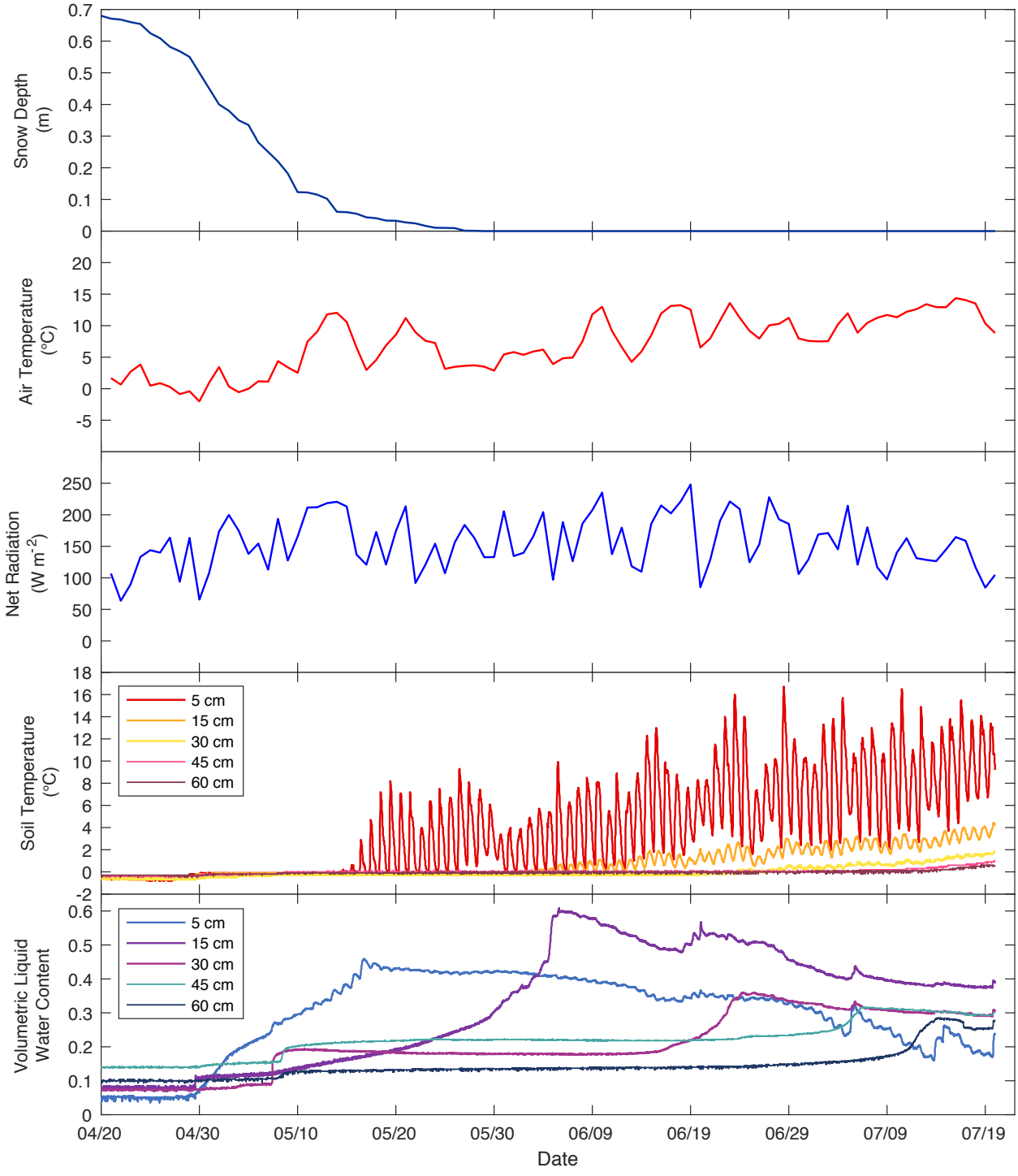

Figure 4.5: Climate data with soil temperature and volumetric liquid water content at NF during the thawing period.

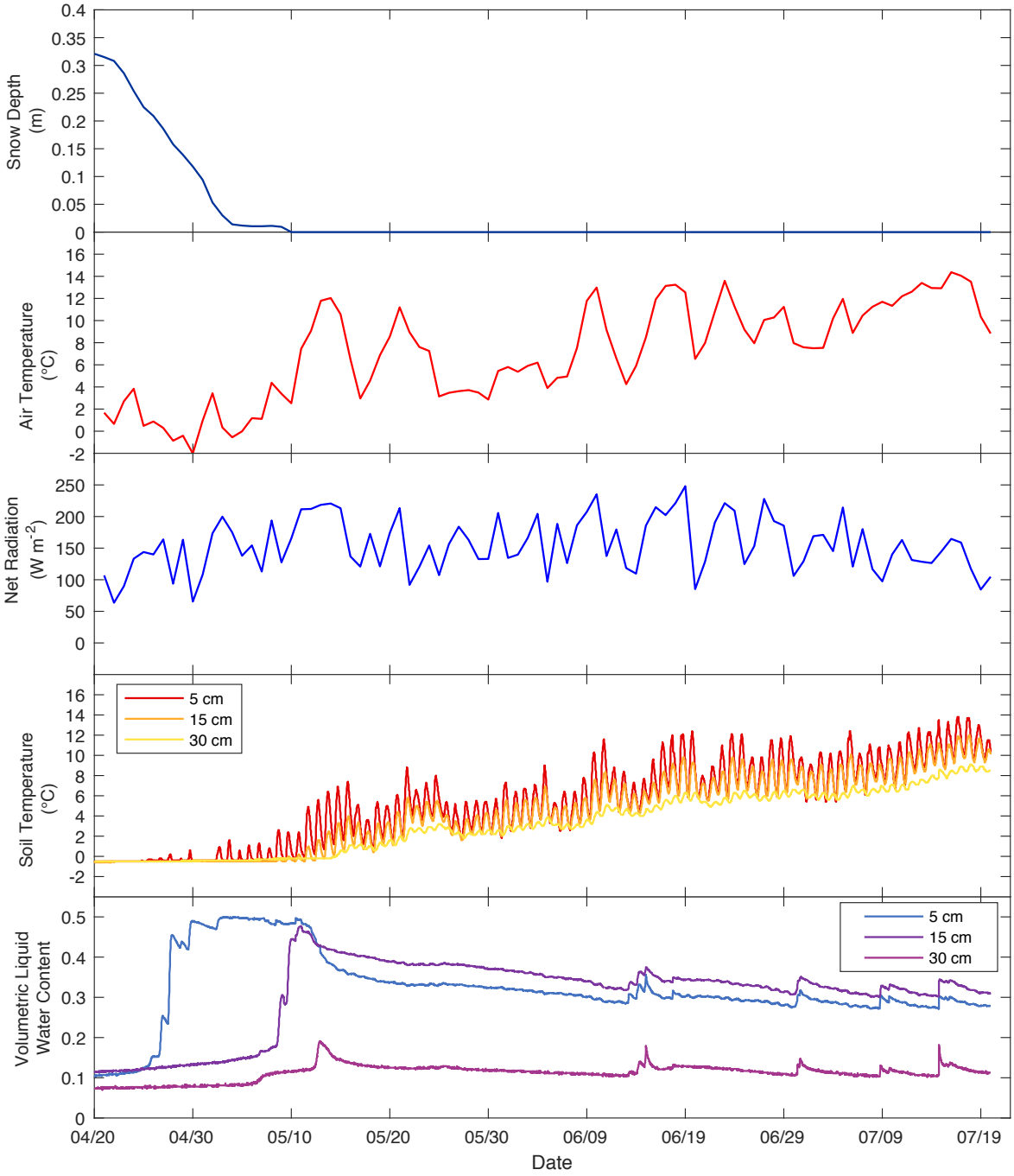

Figure 4.6: Climate data with soil temperature and volumetric liquid water content at PLT during the thawing period.

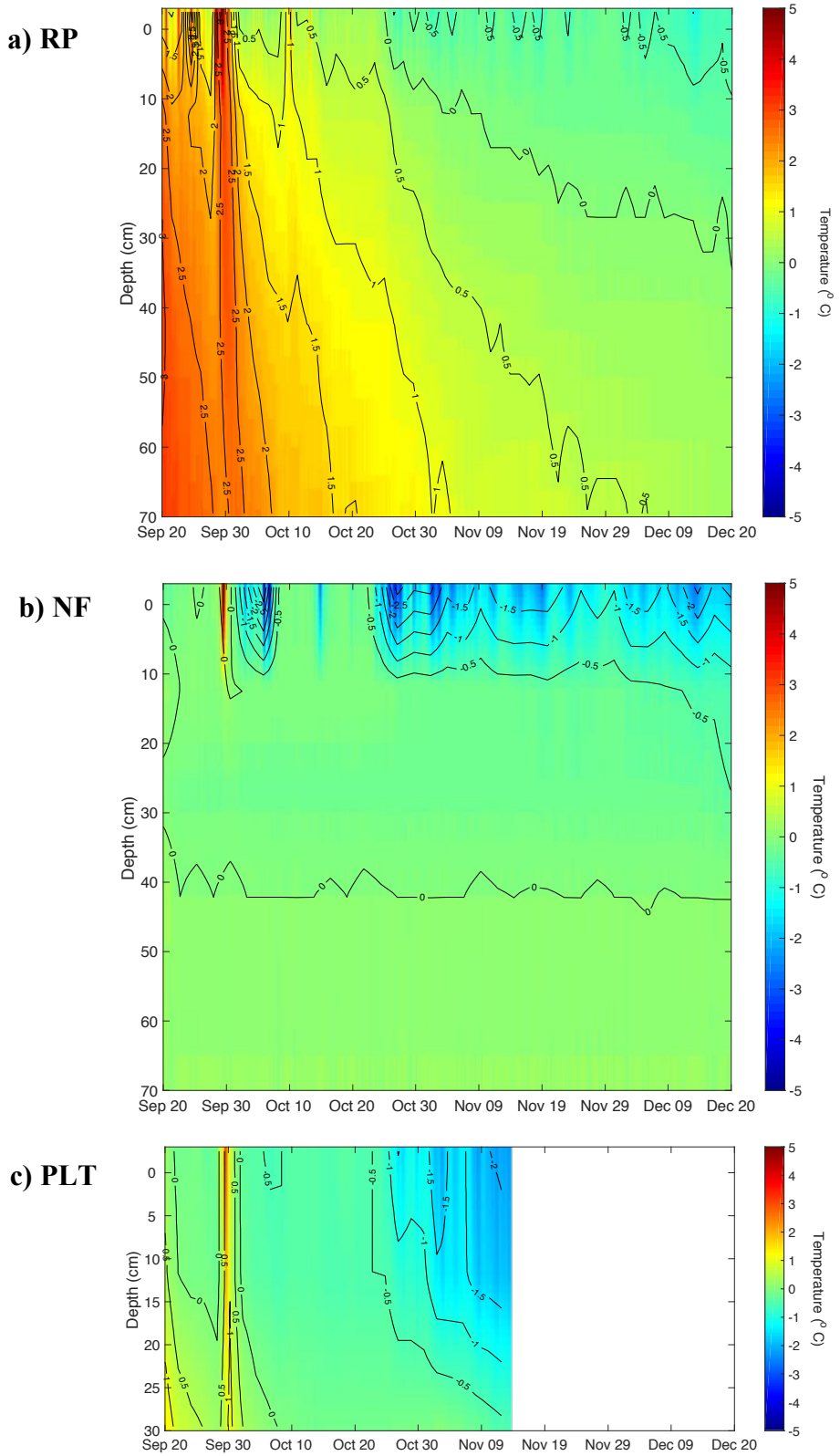

Figure 4.7: Soil temperature with depth during the freezing period at a) RP, b) NF, and c) PLT.

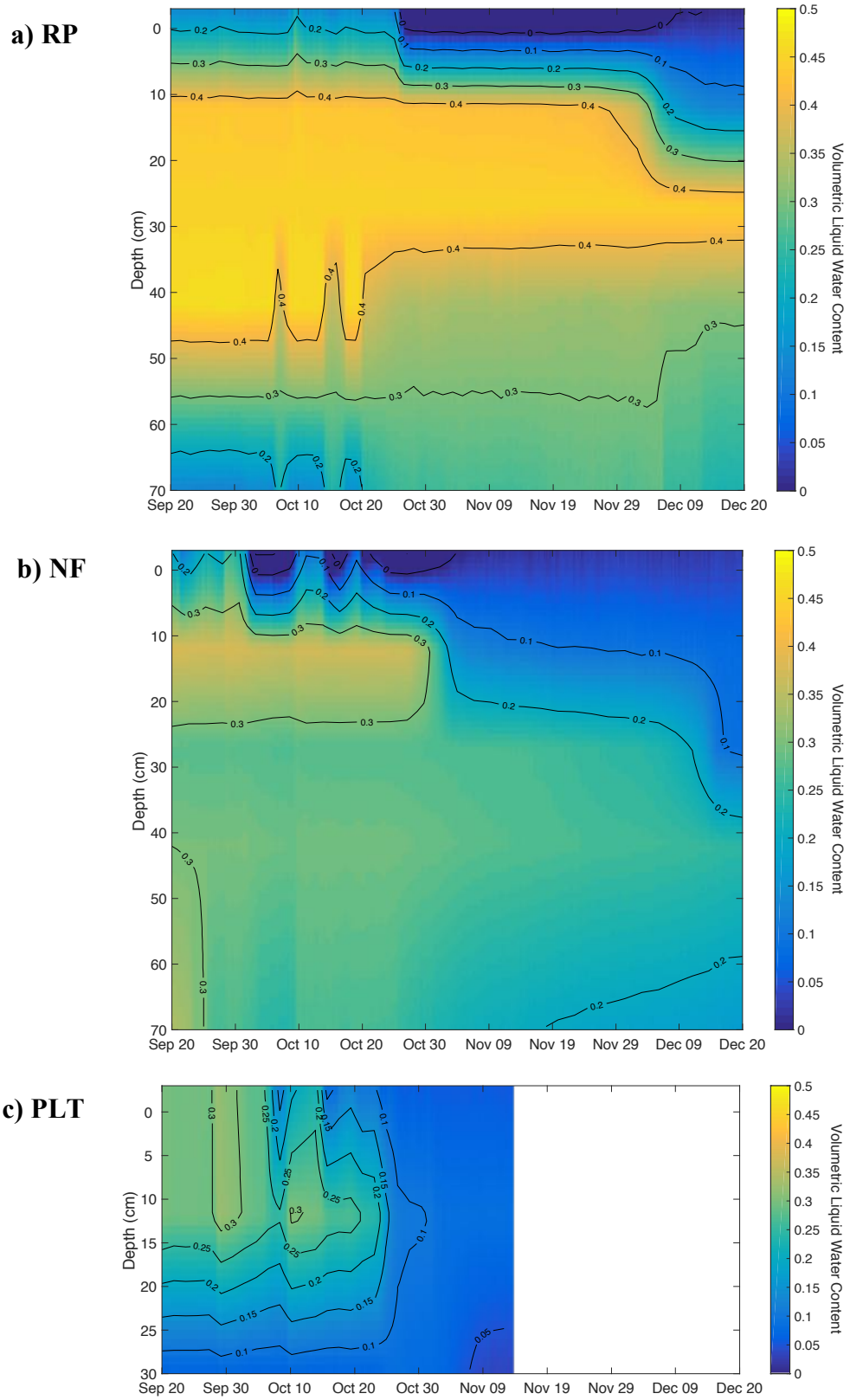

Figure 4.8: Volumetric liquid water content with depth during the freezing period at a) RP, b) NF, and c) PLT.

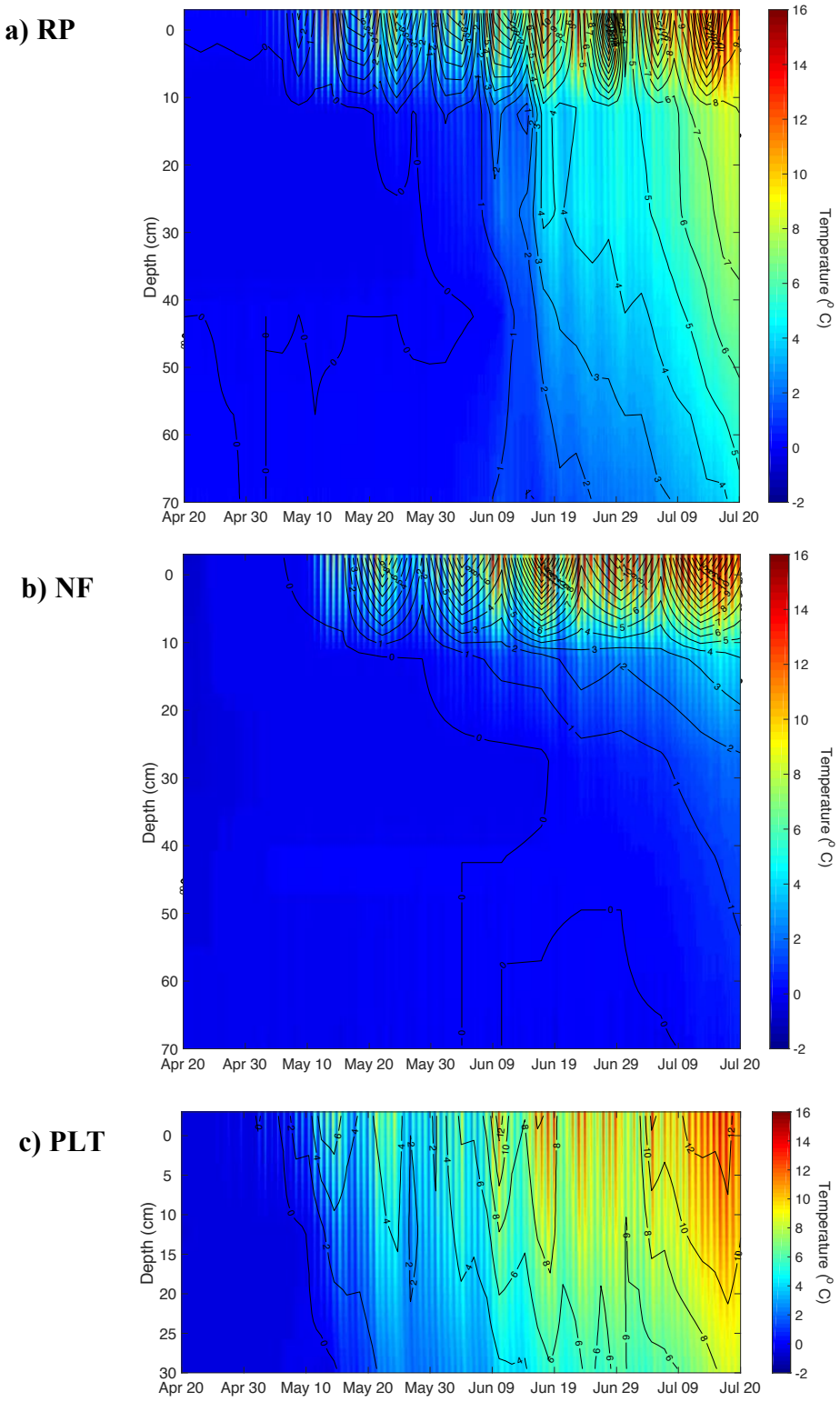

Figure 4.9: Soil temperature with depth during the thawing period at a) RP, b) NF, and c) PLT.

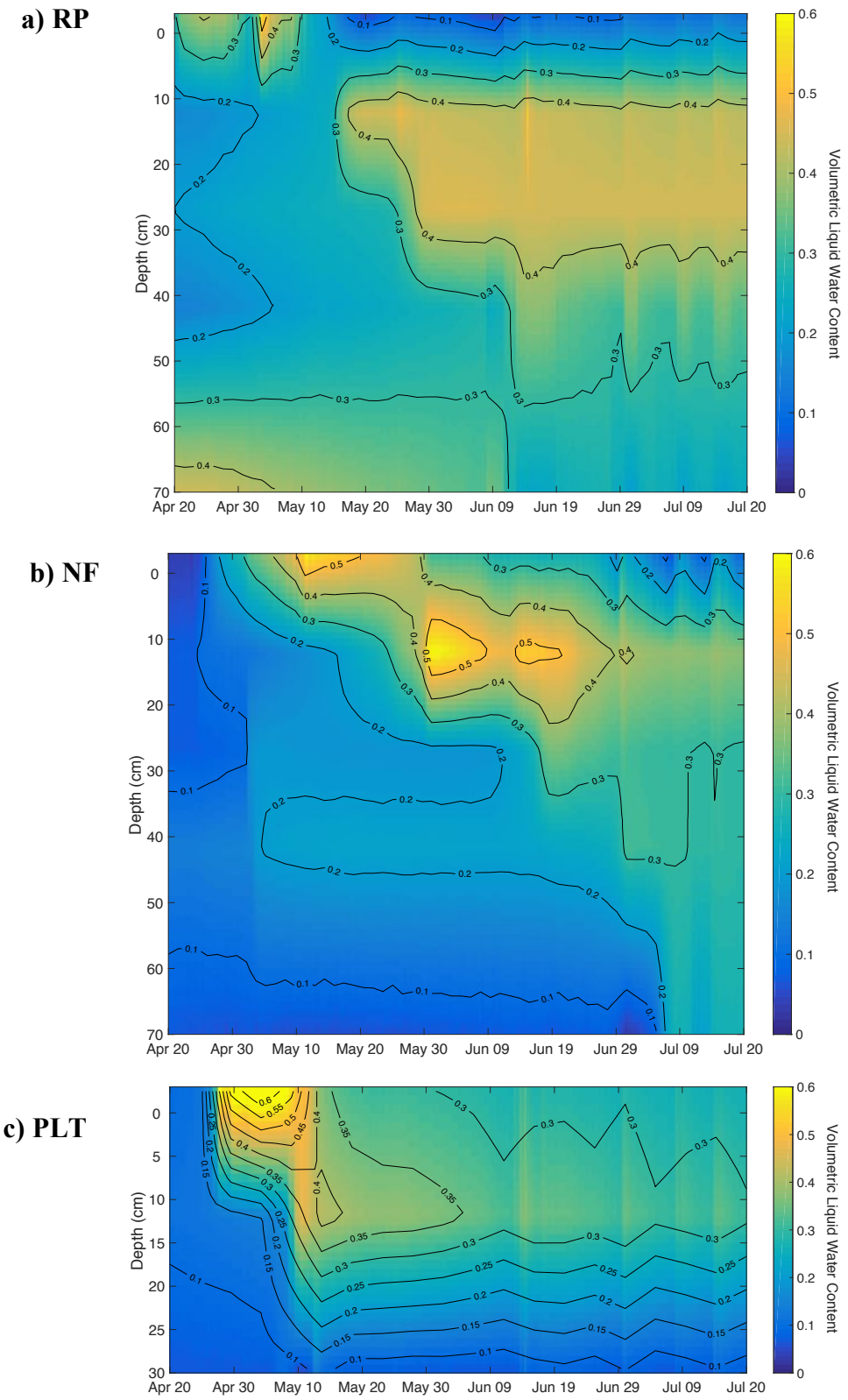

Figure 4.10: Volumetric liquid water content with depth during the thawing period at a) RP, b) NF, and c) PLT.

a)

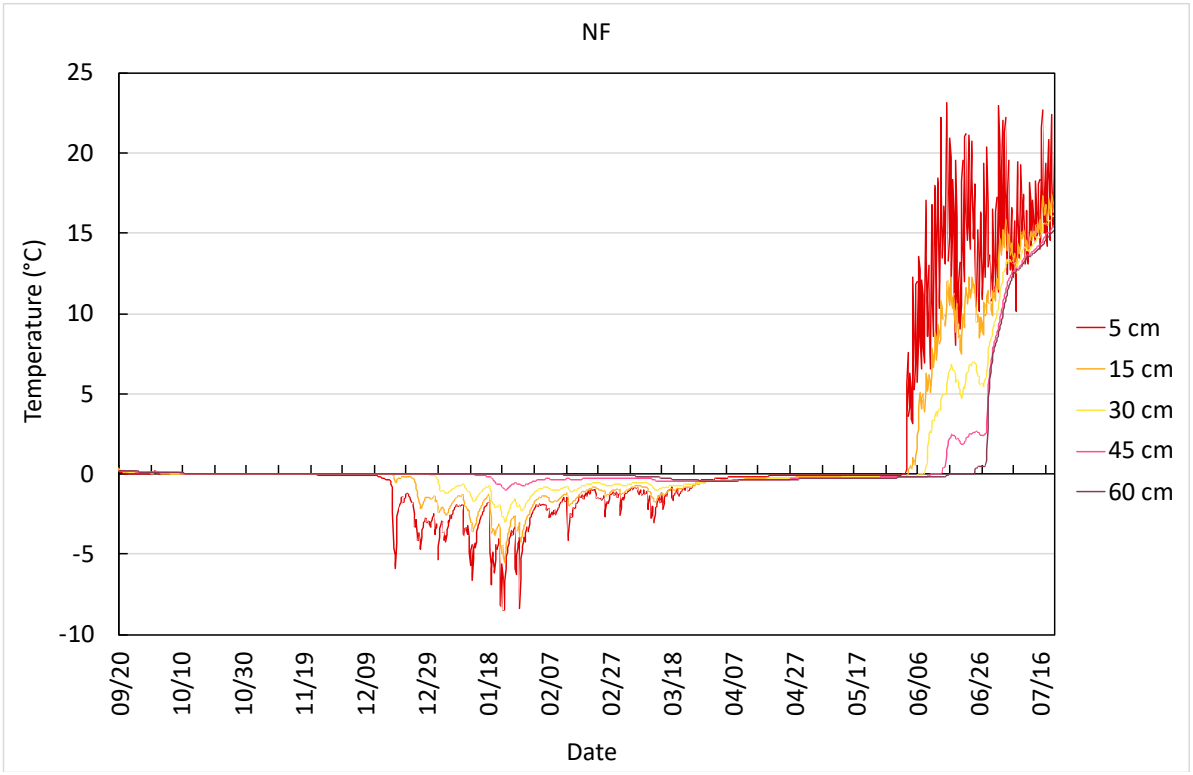

b)

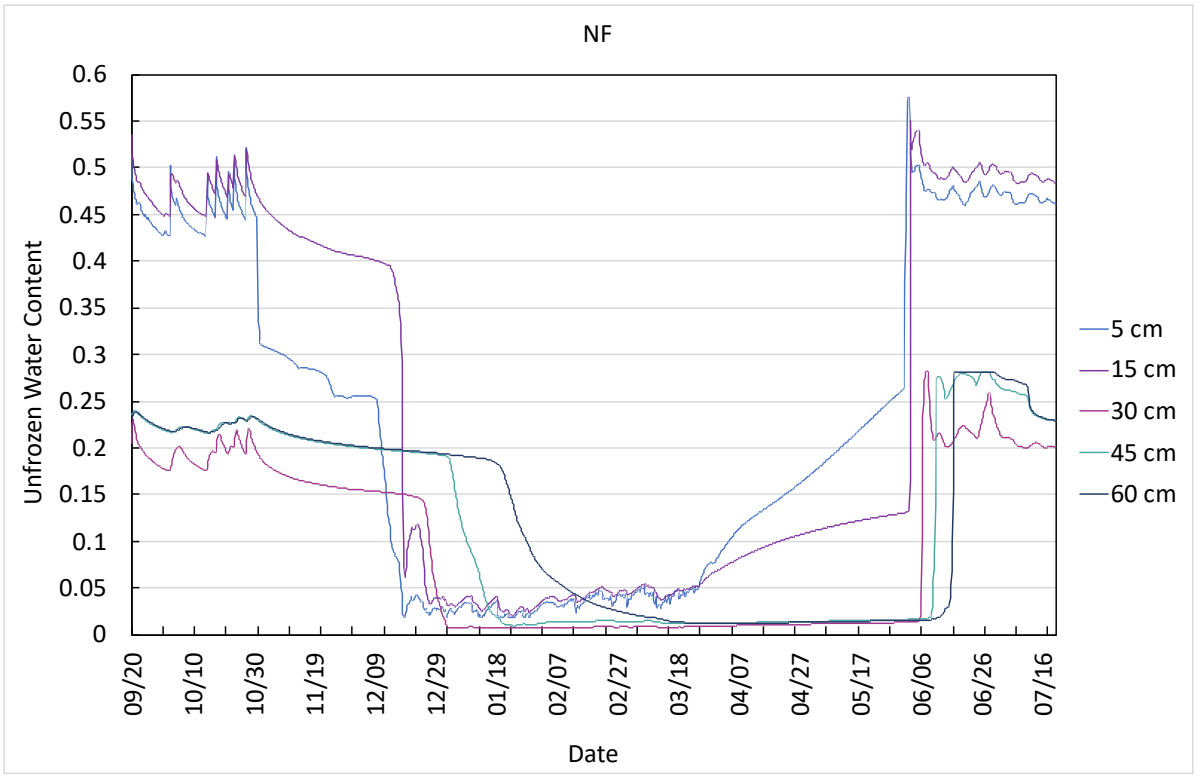

Figures 4.11: Modelled a) soil temperature and b) unfrozen volumetric water content at NF from September 2015 to July 2016.

a)

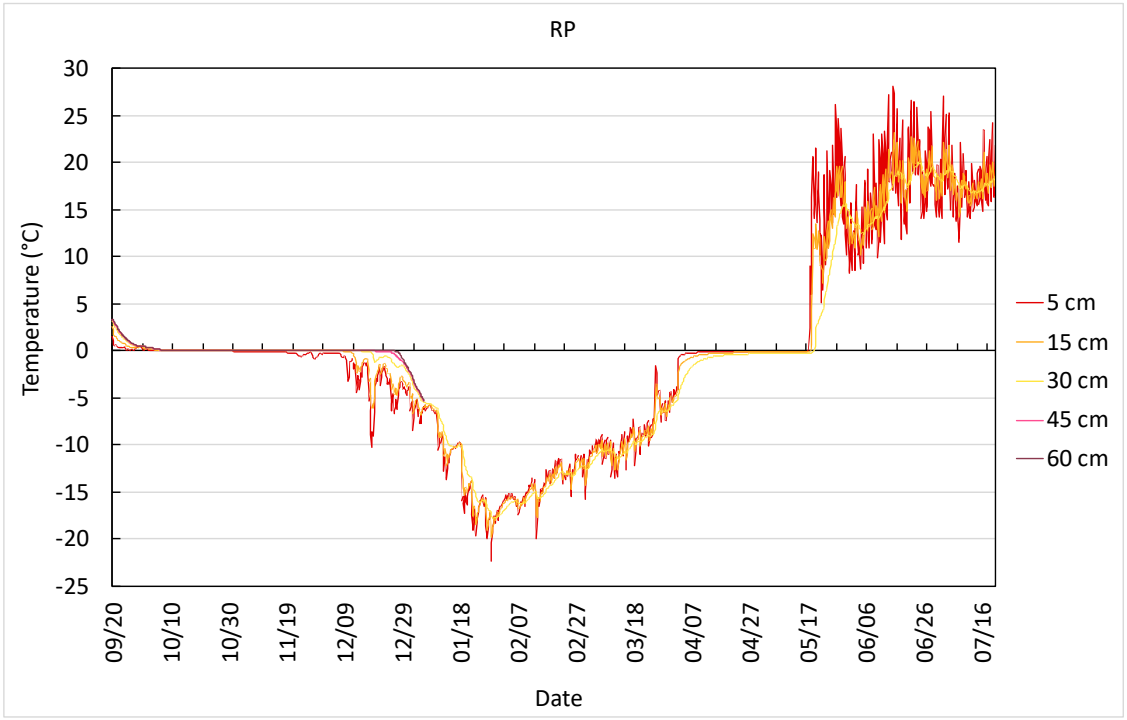

b)

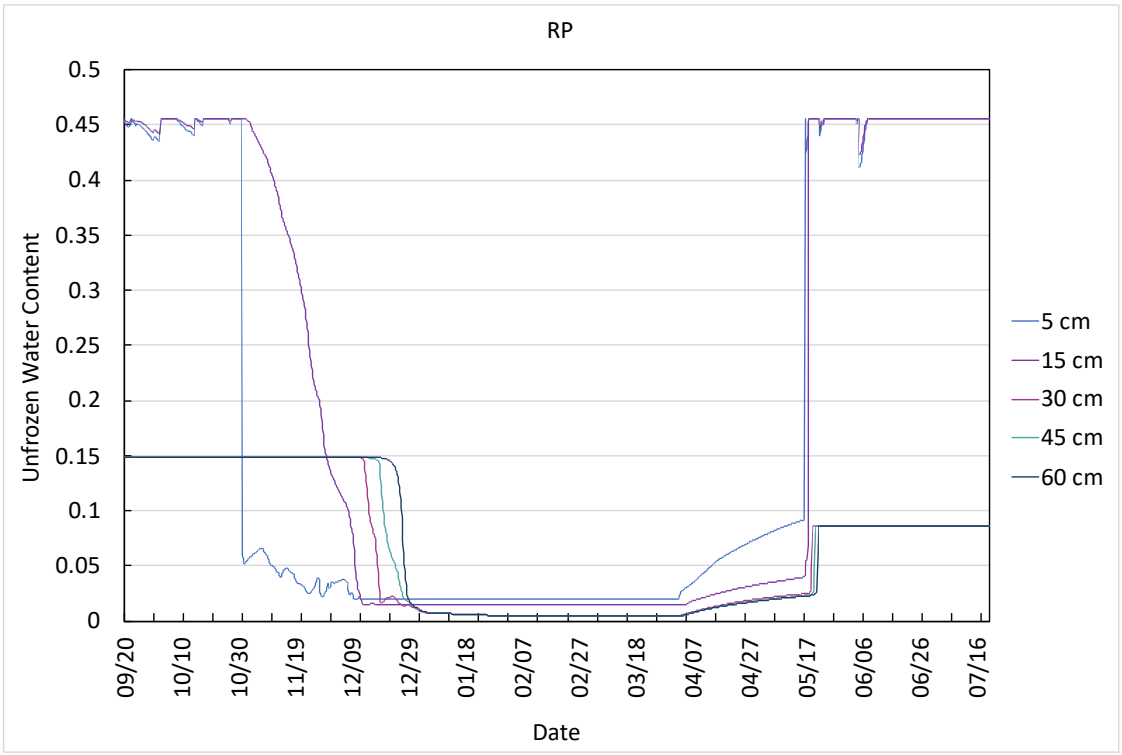

Figures 4.12: Modelled a) soil temperature and b) unfrozen volumetric water content at RP from September 2015 to July 2016.

a)

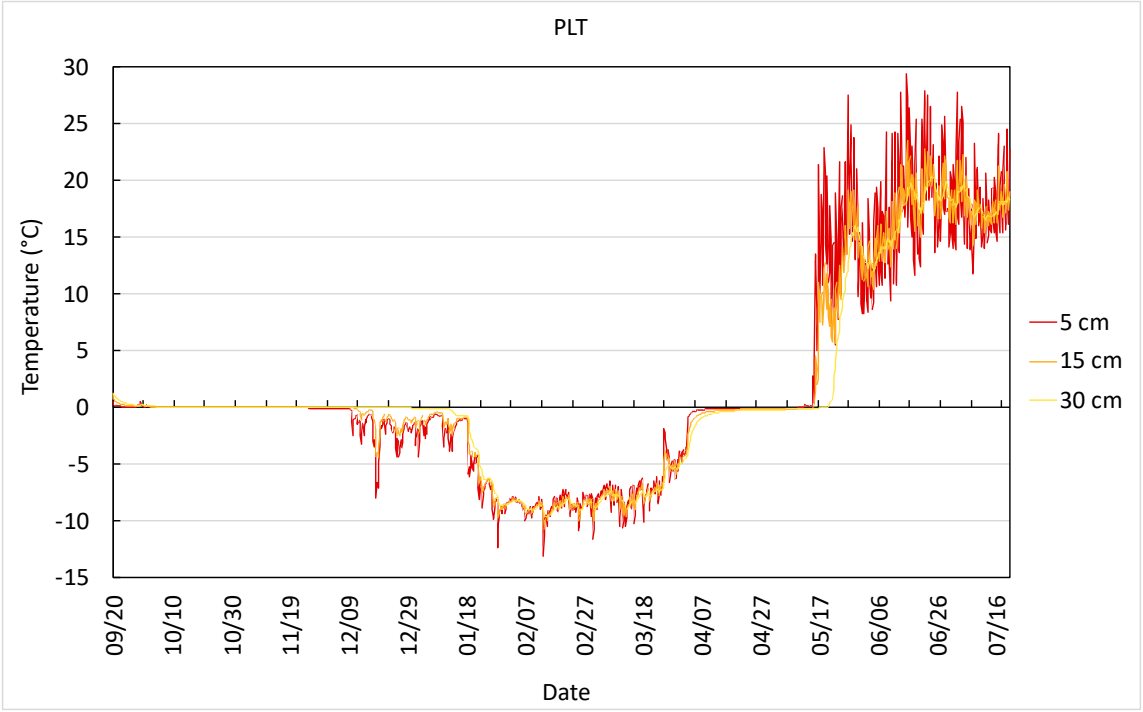

b)

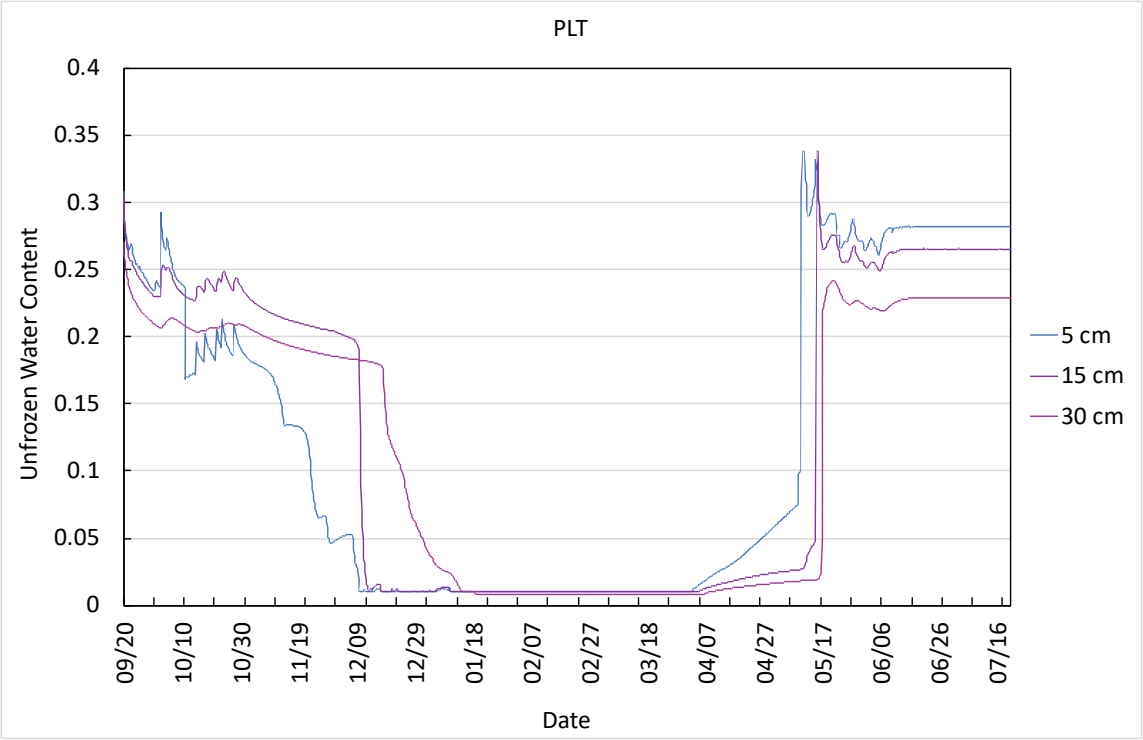

Figures 4.13: Modelled a) soil temperature and b) unfrozen volumetric water content at PLT from September 2015 to July 2016.

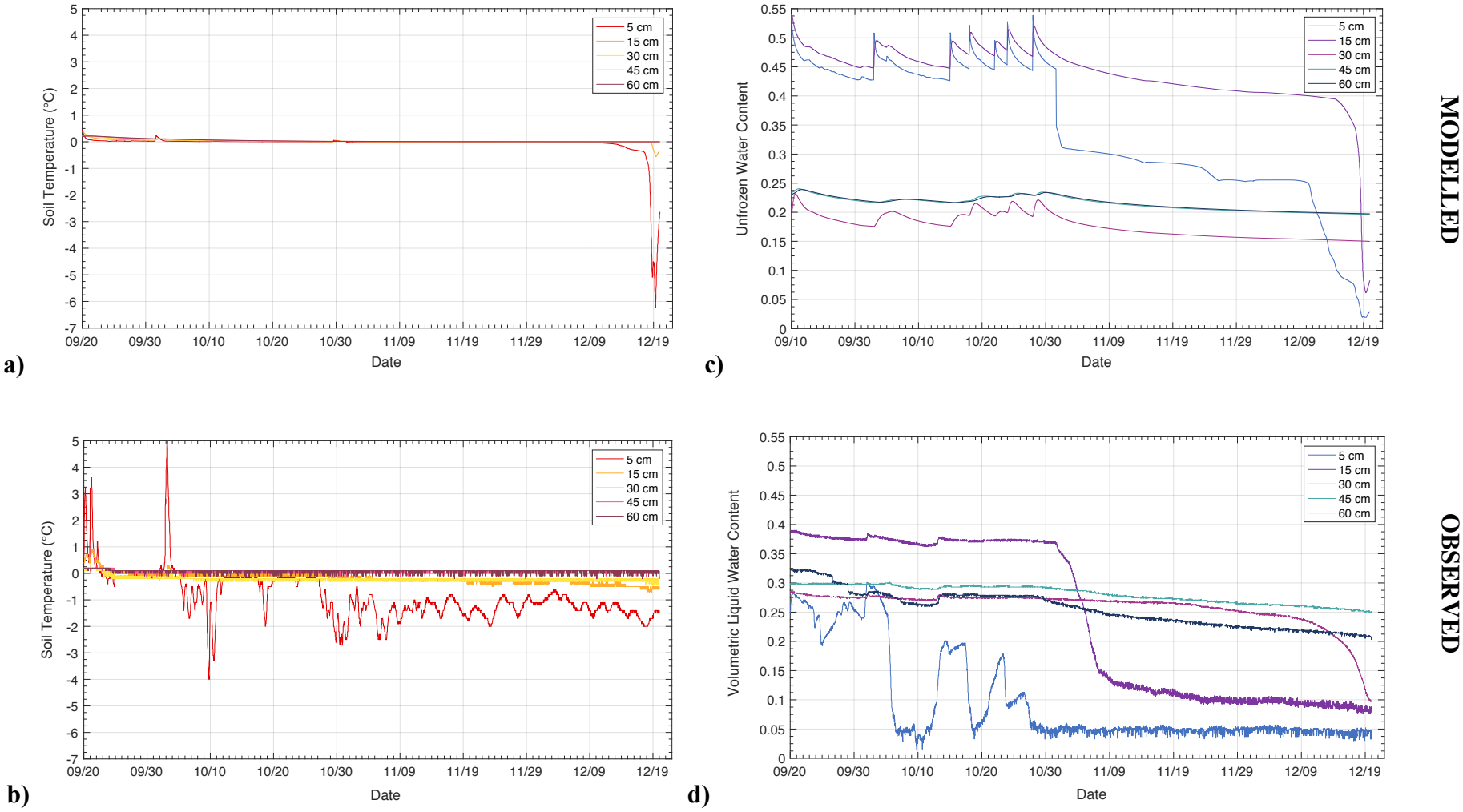

Figures 5.1: Modelled vs. observed soil temperature and unfrozen volumetric water content at NF during the freezing period.

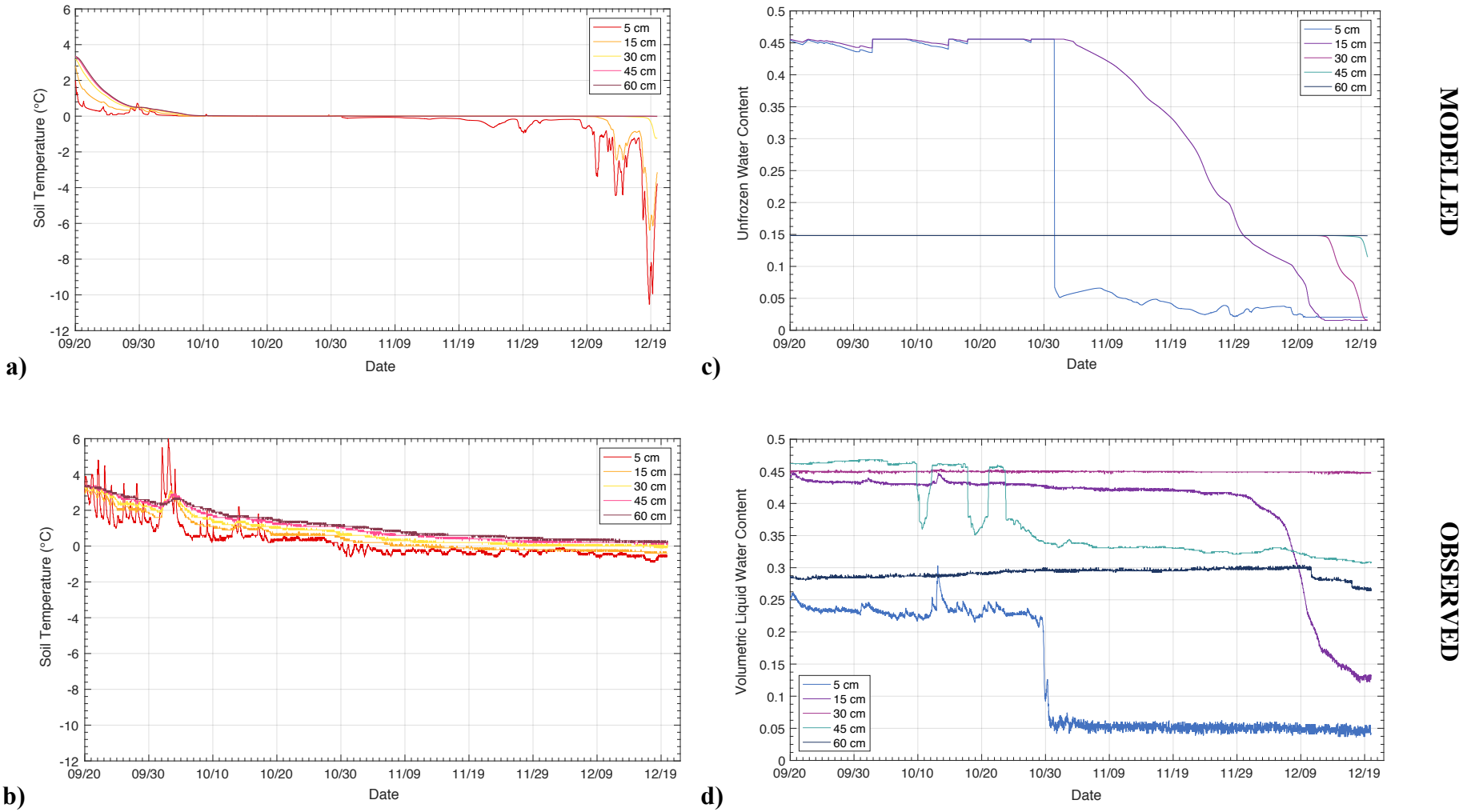

Figures 5.2: Modelled vs. observed soil temperature and unfrozen volumetric water content at RP during the freezing period.

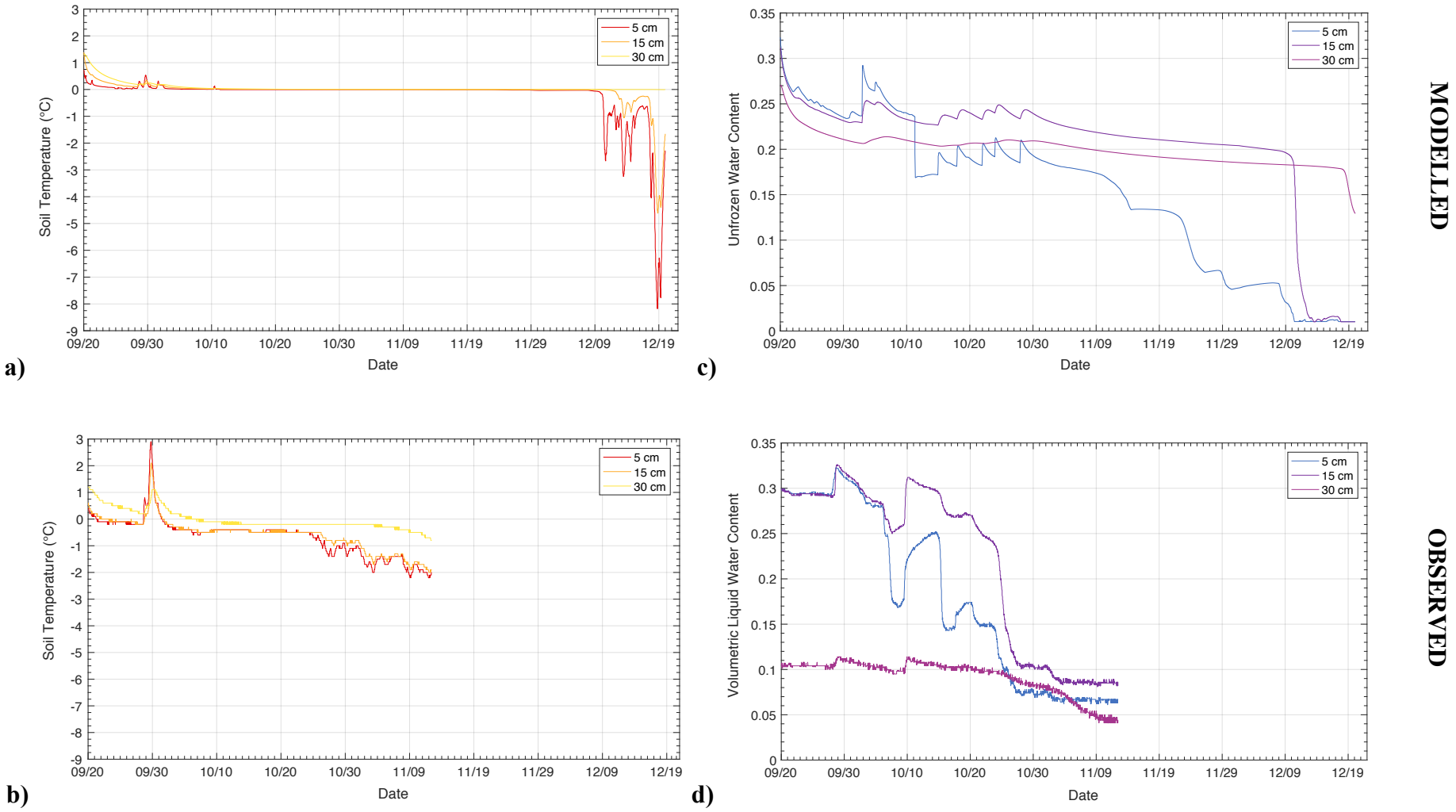

Figures 5.3: Modelled vs. observed soil temperature and unfrozen volumetric water content at PLT during the freezing period.

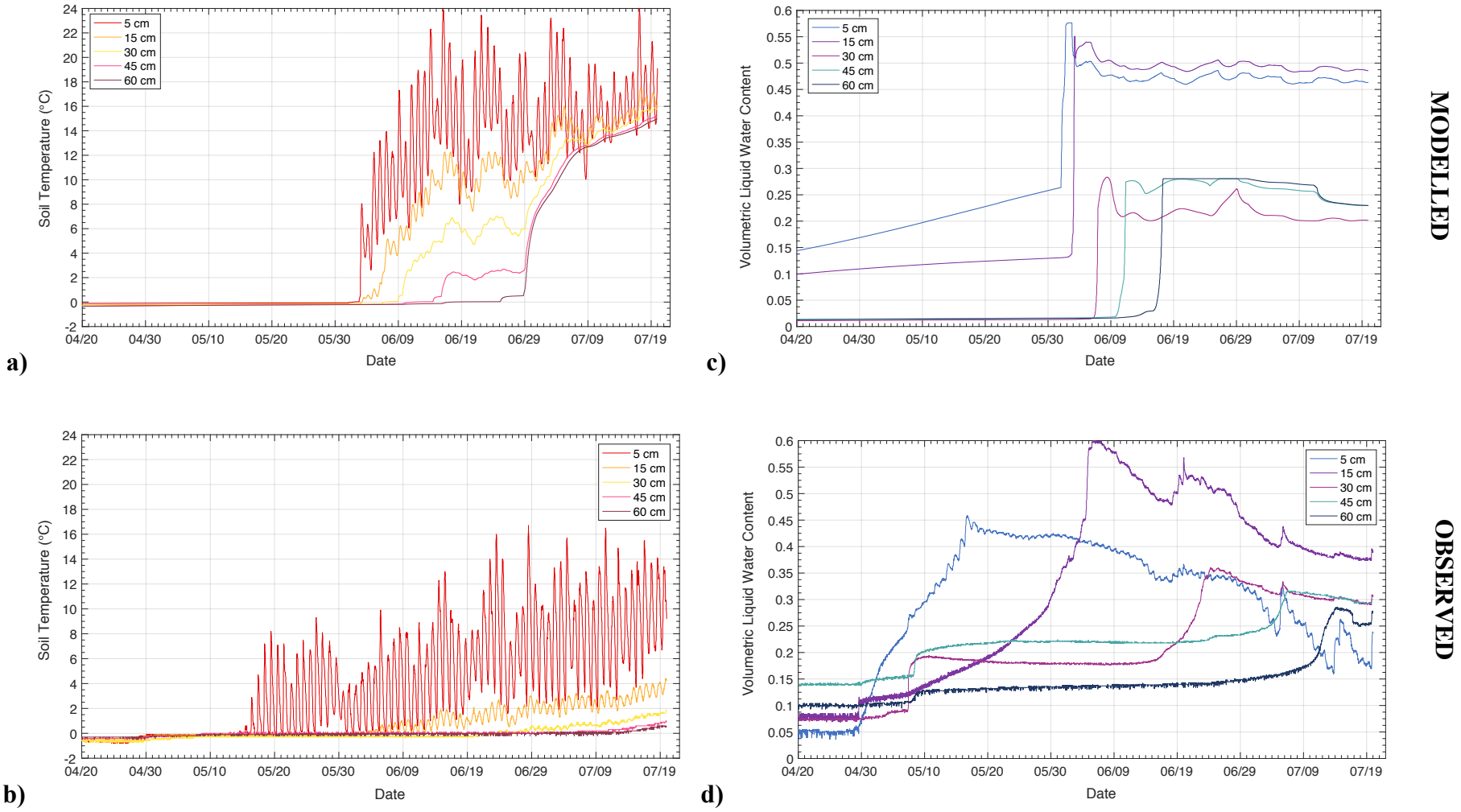

Figures 5.4: Modelled vs. observed soil temperature and unfrozen volumetric water content at NF during the thawing period.

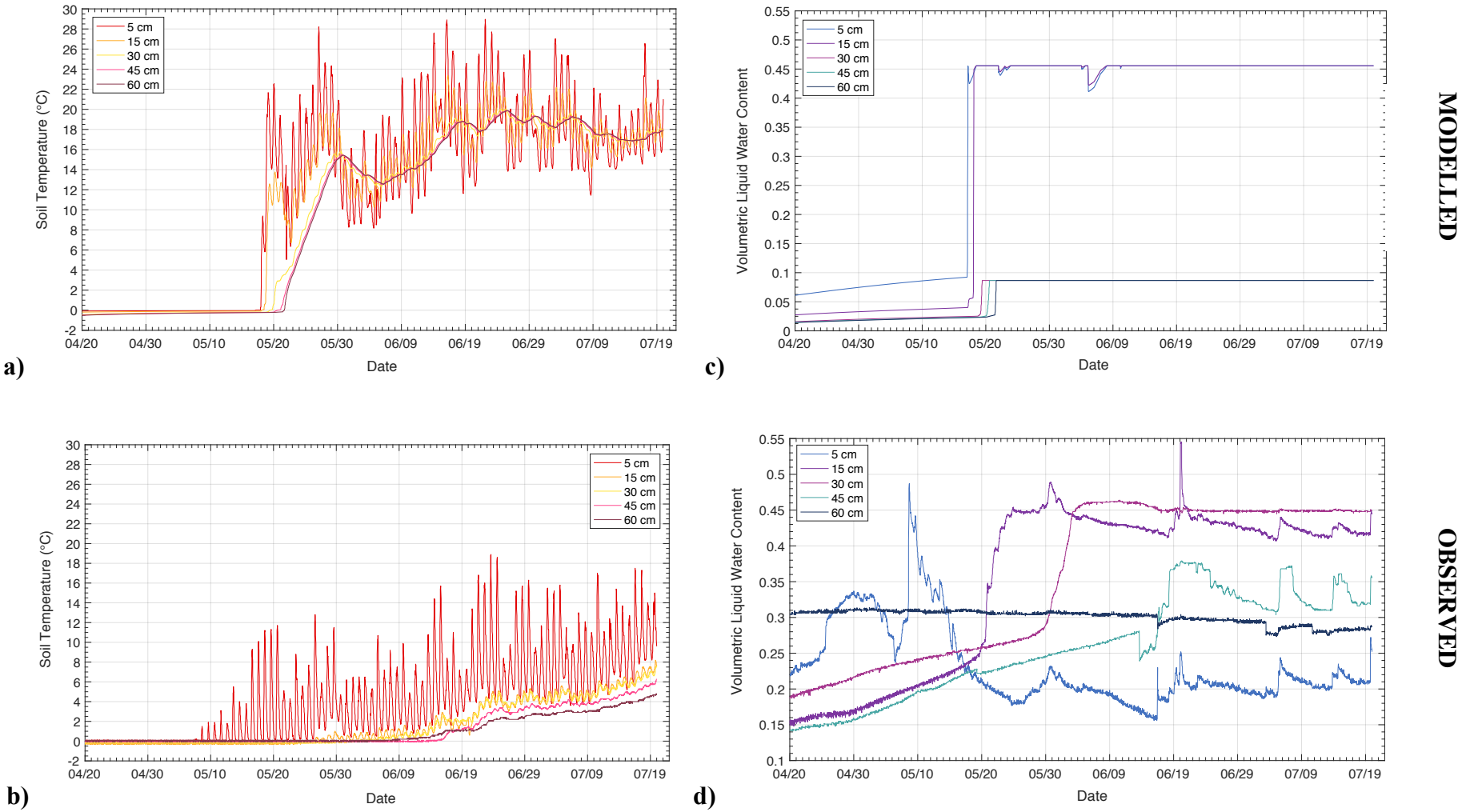

Figures 5.5: Modelled vs. observed soil temperature and unfrozen volumetric water content at RP during the thawing period.

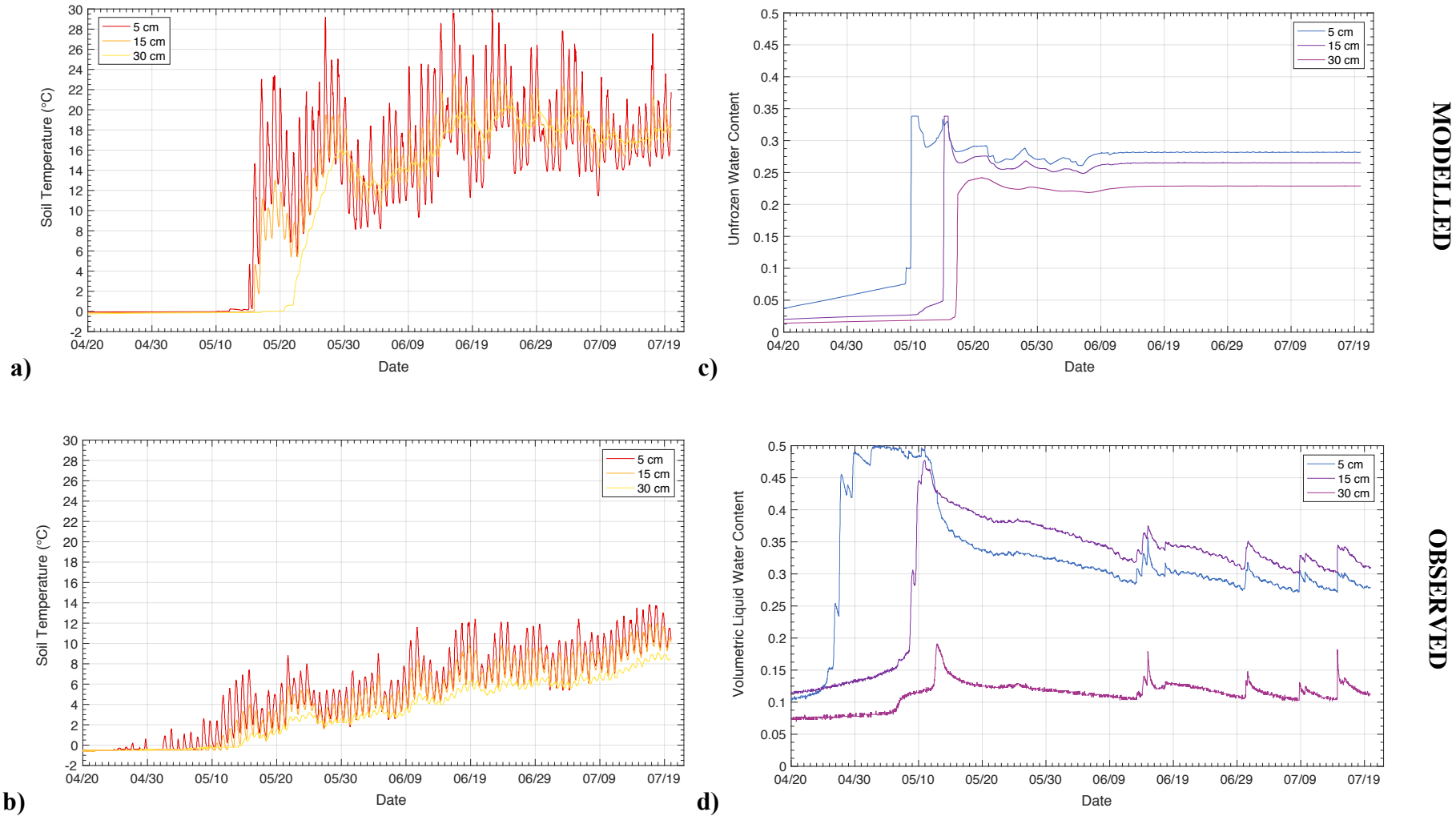

Figures 5.6: Modelled vs. observed soil temperature and unfrozen volumetric water content at PLT during the thawing period.

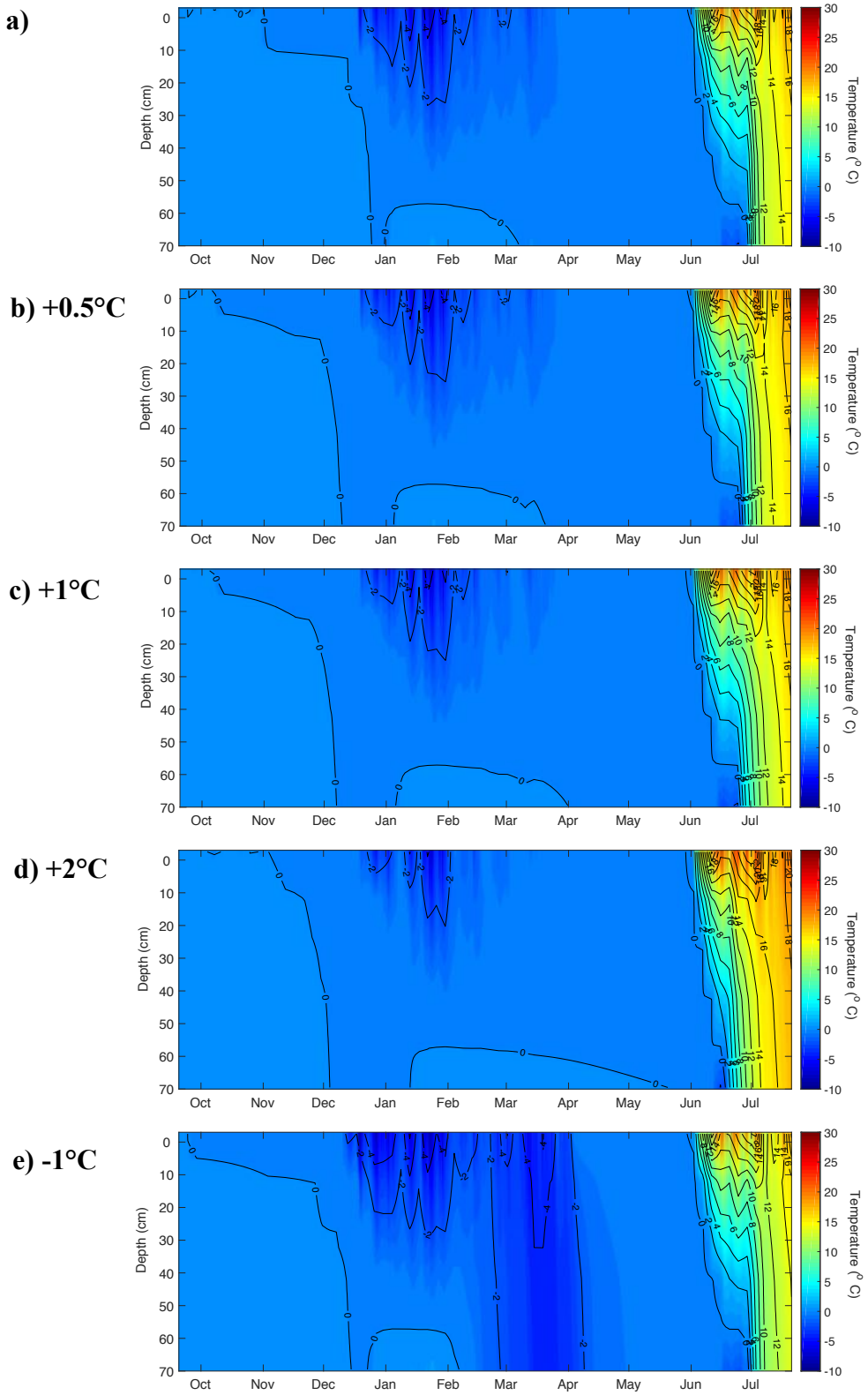

Figure 5.7: Soil temperature sensitivity to changes in air temperature from a) initial model by b) +0.5°C, c) +1°C, d) +2°C, and e) -1°C.

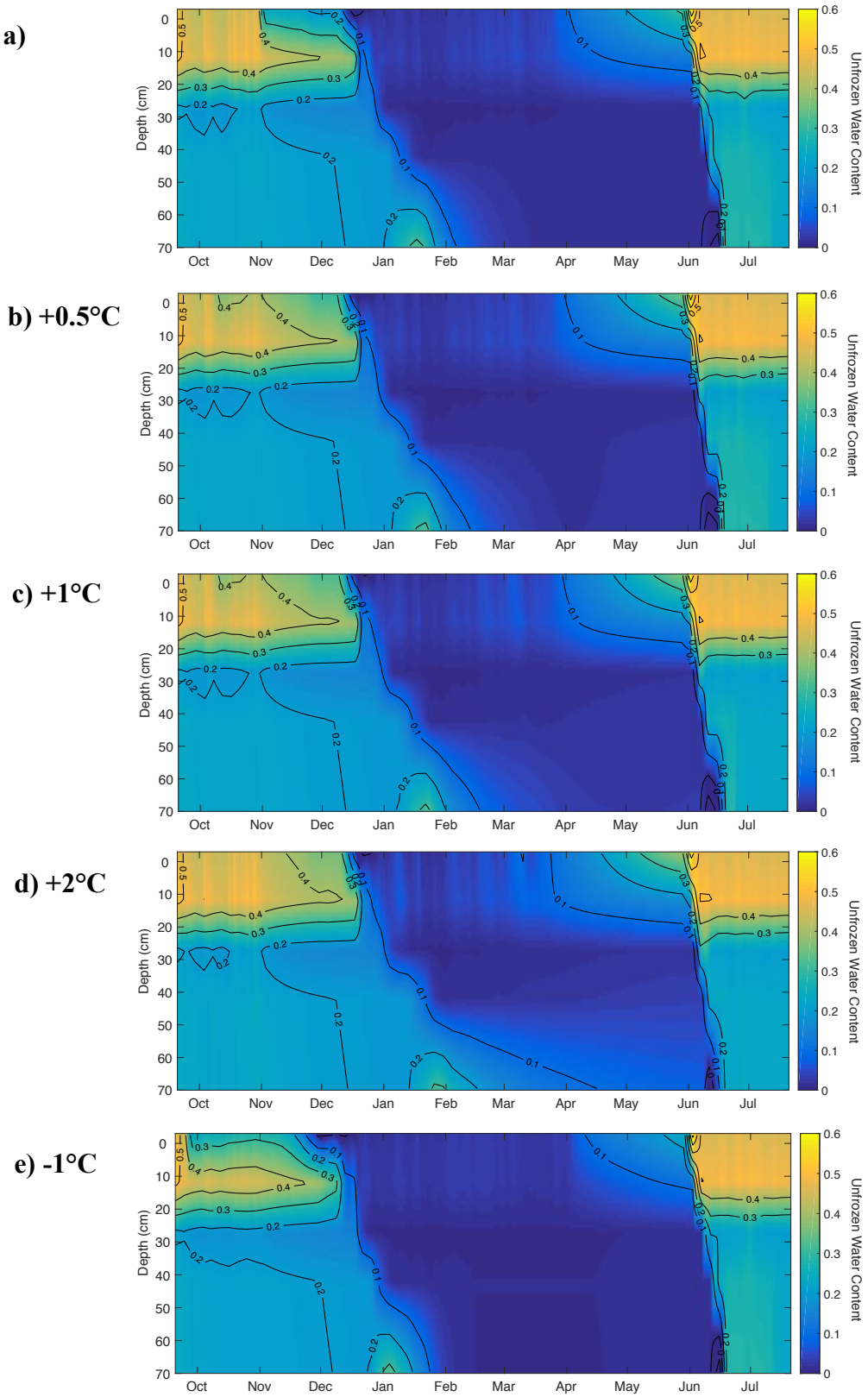

Figure 5.8: Unfrozen volumetric water content sensitivity to changes in air temperature from a) initial model by b) +0.5°C, c) +1°C, d) +2°C, and e) -1°C.

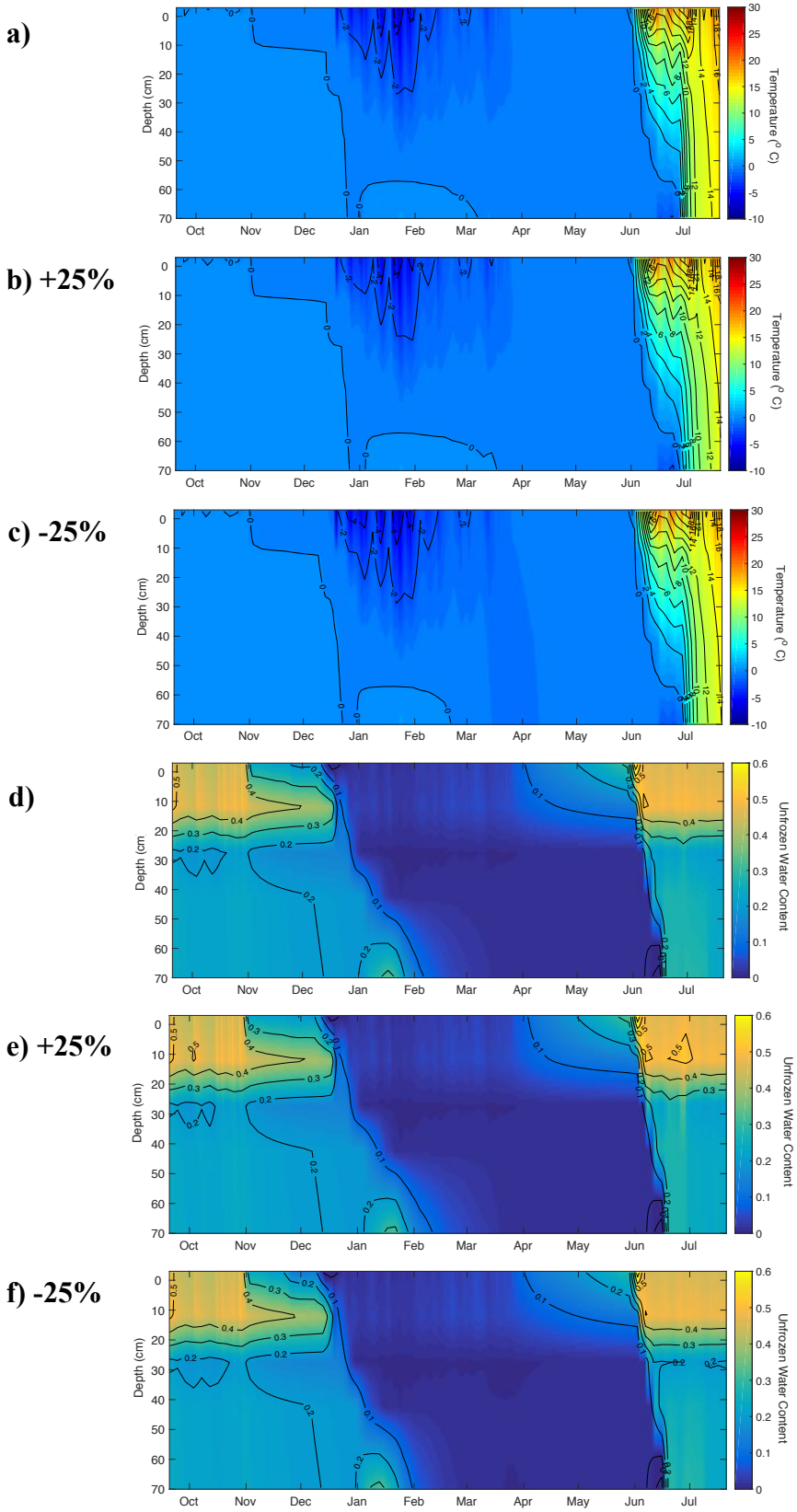

Figure 5.9: Soil temperature (a-c) and unfrozen water content (d-f) sensitivity to changes in precipitation from initial model (a, d) by +25% (b, e) and -25% (c, f).

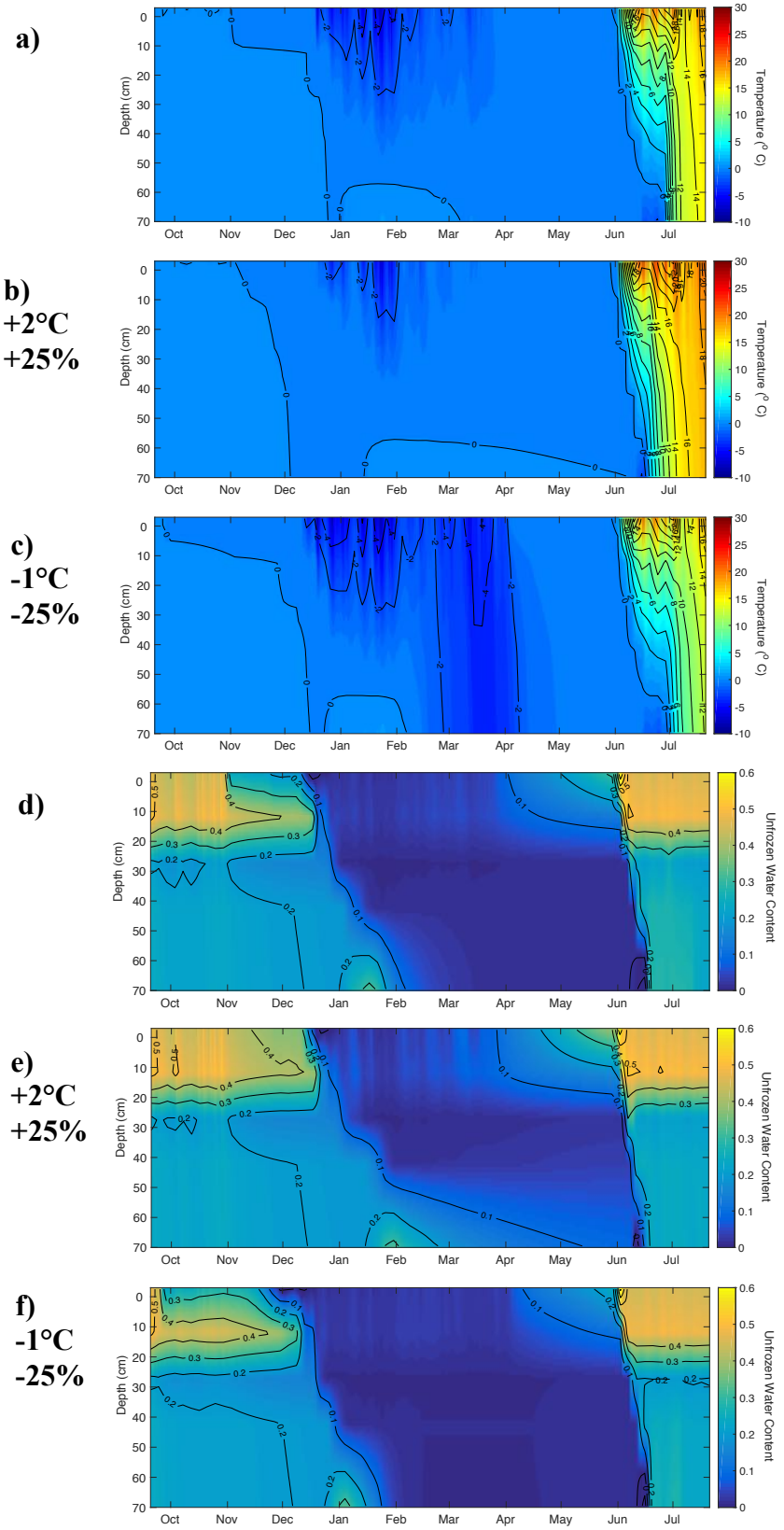

Figure 5.10: Soil temperature (a-c) and unfrozen water content (d-f) sensitivity from initial model (a, d) to warmer and wetter (b, e) and cooler and drier (c, f) climate scenarios.